

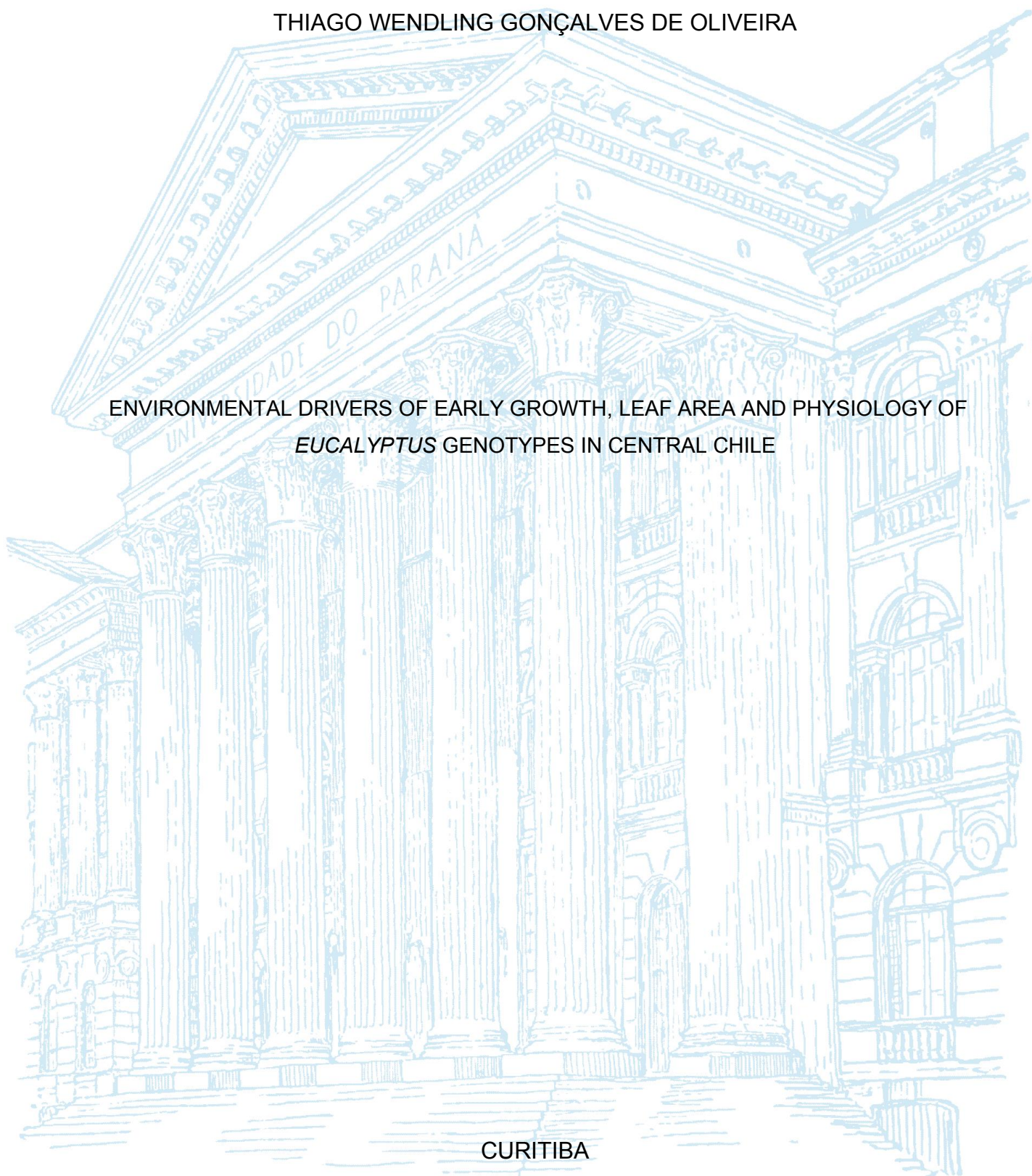
UNIVERSIDADE FEDERAL DO PARANÁ

THIAGO WENDLING GONÇALVES DE OLIVEIRA

ENVIRONMENTAL DRIVERS OF EARLY GROWTH, LEAF AREA AND PHYSIOLOGY OF  
*EUCALYPTUS* GENOTYPES IN CENTRAL CHILE

CURITIBA

2021



THIAGO WENDLING GONÇALVES DE OLIVEIRA

ENVIRONMENTAL DRIVERS OF EARLY GROWTH, LEAF AREA AND PHYSIOLOGY OF  
*EUCALYPTUS* GENOTYPES IN CENTRAL CHILE

Tese apresentada ao curso de Pós-Graduação em Engenharia Florestal, Setor de Ciências Agrárias, Universidade Federal do Paraná, como requisito parcial à obtenção do título de Doutor em Engenharia Florestal.

Orientador: Prof. Dr. Carlos Roberto Sanquetta

Coorientadores: Prof. Dr. Rafael Rubilar Pons

Prof(a). Dr(a). Ana Paula Dalla Corte

CURITIBA

2021

Ficha catalográfica elaborada pela  
Biblioteca de Ciências Florestais e da Madeira - UFPR

Oliveira, Thiago Wendling Gonçalves de

Environmental drivers of early growth, leaf area and physiology of *eucalyptus* genotypes in central Chile / Thiago Wendling Gonçalves de Oliveira. – Curitiba, 2021.  
100 f. : il.

Orientador: Prof. Dr. Carlos Roberto Sanquetta

Coorientadores: Prof. Dr. Rafael Rubilar Pons

Profa. Dra. Ana Paula Dalla Corte

Tese (Doutorado) - Universidade Federal do Paraná, Setor de Ciências Agrárias, Programa de Pós-Graduação em Engenharia Florestal. Defesa: Curitiba, 23/04/2021.

Área de concentração: Manejo Florestal.

1. Fisiologia vegetal - Chile. 2. Eucalipto - Chile. 3. Ecologia florestal. 4. Mudanças climáticas. 5. Interação genótipo-ambiente. 6. Árvores - Crescimento. 7. Teses. I. Sanquetta, Carlos Roberto. II. Pons, Rafael Rubilar. III. Dalla Corte, Ana Paula. IV. Universidade Federal do Paraná, Setor de Ciências Agrárias. V. Título.

CDD – 634.9

CDU – 634.0.161(83)



MINISTÉRIO DA EDUCAÇÃO  
SETOR DE CIÊNCIAS AGRÁRIAS  
UNIVERSIDADE FEDERAL DO PARANÁ  
PRÓ-REITORIA DE PESQUISA E PÓS-GRADUAÇÃO  
PROGRAMA DE PÓS-GRADUAÇÃO ENGENHARIA  
FLORESTAL - 40001016015P0

## TERMO DE APROVAÇÃO

Os membros da Banca Examinadora designada pelo Colegiado do Programa de Pós-Graduação em ENGENHARIA FLORESTAL da Universidade Federal do Paraná foram convocados para realizar a arguição da tese de Doutorado de **THIAGO WENDLING GONÇALVES DE OLIVEIRA** intitulada: **ENVIRONMENTAL DRIVERS OF EARLY GROWTH, LEAF AREA AND PHYSIOLOGY OF EUCALYPTUS GENOTYPES IN CENTRAL CHILE**, sob orientação do Prof. Dr. CARLOS ROBERTO SANQUETTA, que após terem inquirido o aluno e realizada a avaliação do trabalho, são de parecer pela sua APROVAÇÃO no rito de defesa.

A outorga do título de doutor está sujeita à homologação pelo colegiado, ao atendimento de todas as indicações e correções solicitadas pela banca e ao pleno atendimento das demandas regimentais do Programa de Pós-Graduação.

CURITIBA, 23 de Abril de 2021.

Assinatura Eletrônica

25/04/2021 06:21:01.0

CARLOS ROBERTO SANQUETTA  
Presidente da Banca Examinadora

Assinatura Eletrônica

26/04/2021 17:54:51.0

OTÁVIO CAMARGO CAMPOE

Avaliador Externo (UNIVERSIDADE FEDERAL DE LAVRAS)

Assinatura Eletrônica

26/04/2021 09:44:36.0

ALEXANDRE BEHLING

Avaliador Interno (UNIVERSIDADE FEDERAL DO PARANÁ)

Assinatura Eletrônica

27/04/2021 11:59:24.0

RODRIGO EIJI HAKAMADA

Avaliador Externo (UNIVERSIDADE FEDERAL RURAL DE  
PERNAMBUCO)

Assinatura Eletrônica

27/04/2021 05:59:12.0

JOSÉ LEONARDO DE MORAES GONÇALVES

Avaliador Externo (ESCOLA SUPERIOR DE AGRICULTURA - LUIZ DE  
QUEIROZ -USP)

Avenida Lothário Meissner, 632 - CURITIBA - Paraná - Brasil

CEP 80210-170 - Tel: (41) 3360-4212 - E-mail: [pgfloresta@gmail.com](mailto:pgfloresta@gmail.com)

Documento assinado eletronicamente de acordo com o disposto na legislação federal Decreto 8539 de 08 de outubro de 2015.

Gerado e autenticado pelo SIGA-UFPR, com a seguinte identificação única: 89922

Para autenticar este documento/assinatura, acesse <https://www.prppg.ufpr.br/siga/visitante/autenticacaoassinaturas.jsp> e insira o código 89922

## DEDICATION

*To my family.*

*To forest scientists (students and researchers) around the world that allow the growth of our sector.*

## ACKNOWLEDGMENTS

I gratefully acknowledge God for all love, understanding, care in my walk and above all for unconditional protection. Thanks to good spirits who help and support me in many times, where I was able to learn and believe in my work and overcome my difficulties.

Many institutions were part of this work. Thanks to Federal University of Parana (UFPR) and Graduate Program in Forest Engineering of UFPR for the opportunity to complete my studies. To University of Concepcion (UdeC) and Faculty of Forest Science at UdeC for the possibility of doctorate research. To Forest Productivity Cooperative (FPC) of Chile for assistance in data collection and field work. To CMPC and Arauco companies from Chile for the availability of resources and material for experiment to be carried out.

Thanks to the supported by the government of Chile via CONICYT FONDEF Project Number IT6I10087 and CONICYT Fondecyt Regular Project 1190835; CMPC S.A. Co.; ARAUCO S.A. Co.; Bioforest S.A. Co. and Universidad de Concepción.

Thanks to National Council for Scientific and Technological Development (CNPq) for doctorate scholarship.

Thanks to my advisors. Professor Carlos Roberto Sanquetta for his availability to guide and assist me in my professional life and guarantee good opportunities during graduate. Professor Rafael Rubilar for his example as a forestry researcher, for trusting and believing in my work. Amazing person who teaching me that good research questions are the base of good projects. Professor Ana Paula Dalla Corte for all help and dedication during these four years.

Thanks to all the members of doctorate panel, Professor José Leonardo de Moraes Gonçalves, Professor Rodrigo Eiji Hakamada, Professor Otavio Camargo Campoe, and Professor Alexandre Behling, for the availability to participate, evaluate my study and for the criticisms and improvement suggestions.

Thanks to the professors of the Graduate Program in Forest Engineering at UFPR for their teachings and contributions during my professional life.

Especially thanks to my parents Soraya and Ricardo, for the encouragement and support at many times during all my life. Thanks to my grandmother Alice, my sister Paola and my goddaughter Thaís for making my life calm and beautiful. I love you!!!

Thanks to all my friends at BIOFIX, Forest Management Laboratory and Graduate Program in Forest Engineering at UFPR: Luani Rosa de Oliveira Piva, Deivison Venicio Souza, Vinícius Morais Coutinho, Jaçanan Eloisa de Freitas Milani, Emmanoela Costa Guaraná Araújo, Maycon Thuan Saturinino da Silva, Aline Bernarda Debastiani, Iací Dandara Santos Brasil, Franciele Alba da Silva, Bruna Mulinari Cabral, Rafael Schmitz, Rudson Silva Oliveira, Cicero Jorge Fonseca Dolácio, Linéia Roberta Zen, Manoela Mendes Duarte, Jaqueline Valerius, Aurélio Lorenço Rodrigues, Amanda Koche Marcon, Melrian Schetz, and many others.

Thanks to my friend Luiz Ricardo Sobenko which high school times provided and contributed with the reading of this study.

Thanks to my friends of Forest Productive Cooperative and University of Concepcion who provide good moments during doctorate research in Concepcion, Chile: Yosselin, Daniel, Juan, Felipe, Maria Cristina and Yuri.

Finally, I am grateful to everyone who contributed directly or indirectly to this study.

*“Creia em si mesmo, aja e verá os resultados. Quando você se esforça, a vida também se esforça para te ajudar” (Chico Xavier).*



## RESUMO

Estudos sobre o comportamento ecofisiológico de plantações de *Eucalyptus* são importantes para prever as interações entre o crescimento e as variáveis climáticas. No entanto, aqueles que envolvem monitoramento fisiológico em plantações jovens e altamente adensadas, que são mais propensos a danos causados por água e estresse térmico, não são comuns. O primeiro capítulo desta tese, intitulado "*Differences in early seasonal growth efficiency and productivity of Eucalyptus genotypes*" apresenta um estudo explorando as mudanças na eficiência de crescimento de povoamento de genótipos de *Eucalyptus* mediterrâneos ao longo de diferentes estações (verão, outono, inverno e primavera) durante seu desenvolvimento inicial. Concluímos que as mudanças de classificação ocorrem no incremento de volume e o crescimento máximo foi observado no verão, independentemente do genótipo. Diferenças no volume final da madeira sugerem que o mesmo ambiente estimula diferentes respostas de alocação de carbono para o crescimento e conseqüentemente na eficiência de crescimento de cada local. O segundo capítulo intitulado "*Physiological responses and growth of Eucalyptus genotypes under cumulative water stress*" apresenta um estudo que investiga a resposta fisiológica de genótipos de *Eucalyptus* durante uma redução progressiva do teor de água no solo e sua relação com o crescimento e estresse hídrico acumulados no mesmo período. No entanto, independentemente das diferenças genotípicas, foi observada uma diminuição na taxa de fotossíntese e fechamento estomático, o que aumentou a eficiência intrínseca do uso da água ao longo do tempo. Esta redução nas variáveis de troca gasosa foliar com mudanças moderadas na água do solo foi mais pronunciada no híbrido *Eucalyptus nitens* x *Eucalyptus globulus* (E. gloni), sendo o táxon mais sensível a mudanças na disponibilidade reduzida de água no solo. O terceiro capítulo intitulado "*Temperature effects on early growth of Eucalyptus genotypes of three taxa*" apresenta um estudo sobre o efeito da temperatura na taxa de crescimento diária. Concluímos que genótipos de alta produtividade, têm sua temperatura ótima média (16 ° C) mais próxima da temperatura média do ar do local (14 ° C) do que genótipos de baixa produtividade (25 ° C) e maior amplitude de temperatura cardinal (<17 ° C) é uma vantagem para o crescimento de genótipos face às mudanças na temperatura do ar ao longo das estações, não limitando o crescimento. Por fim, observamos que a interação entre genótipo e ambiente é determinante para orientar a partição de carbono em *Eucalyptus* e o estresse hídrico e térmico operam da mesma forma para o crescimento em situações de início de estresse no desenvolvimento inicial dos plantios.

Palavras-chave: Eficiência no crescimento, Fotossíntese, Eficiência no uso da água, Temperaturas cardiais, Ecofisiologia florestal.

## ABSTRACT

Studies on ecophysiological behavior of *Eucalyptus* plantations are important to predict the interactions between growth and climatic variables. However, those involving physiological monitoring in young and highly dense plantations that are more prone to damage caused by water and thermal stress are not common. The first chapter of this thesis entitled “*Differences in early seasonal growth efficiency and productivity of Eucalyptus genotypes*” presents a study exploring changes in stand growth efficiency of Mediterranean *Eucalyptus* genotypes over different seasons (summer, autumn, winter, and spring) during their initial development. We conclude that ranking changes occur in volume increment and the maximum growth was observed in the summer regardless of genotype. Differences in the final wood volume suggest that the same environment stimulates different responses carbon allocation for growth and consequently in growth efficiency each the site. The second chapter entitled “*Physiological responses and growth of Eucalyptus genotypes under cumulative water stress*” presents a study investigating the physiological response of *Eucalyptus* genotypes during a progressive reduction of soil water content and its relationship with growth and water stress accumulated in the same period. However, regardless of genotype differences, a decrease in the rate of photosynthesis and stomatal closure was observed, and that increased the intrinsic water use efficiency over time. This reduction in leaf gas exchange variables with moderate changes in soil water was more pronounced in *Eucalyptus nitens* x *Eucalyptus globulus* hybrid (E. gloni), being the most sensitive taxon to changes in reduced soil water availability. The third chapter entitled “*Temperature effects on early growth of Eucalyptus genotypes of three taxa*” presents a study on the effect of temperature on daily growth rate. We concluded that high productivity genotypes, have its average optimum temperature (16 °C) closer to mean air temperature of the site (14 °C) than low productivity genotypes (25 °C) and higher amplitude of cardinal temperatures (< 17 °C) is an advantage for genotypes growth face air temperature changes along the seasons not limiting stem growth. Finally, we observed that the interaction between genotype and environment is determinant to guide carbon partitioning in *Eucalyptus* and water and temperature stress operate in the same manner for stem growth in situations of beginning of stress in the initial development of plantations.

Keywords: Growth efficiency, Photosynthesis, Water use efficiency, Cardinal temperatures, Forest ecophysiology.

## RESUMEN

Los estudios sobre el comportamiento ecofisiológico de las plantaciones de *Eucalyptus* son importantes para predecir las interacciones entre el crecimiento y las variables climáticas. Sin embargo, no son comunes los que involucran el monitoreo fisiológico en plantaciones jóvenes y muy densas que son más propensas a sufrir daños por estrés hídrico y térmico. El primer capítulo de esta tesis titulado “*Differences in early seasonal growth efficiency and productivity of Eucalyptus genotypes*” presenta un estudio que explora los cambios en la eficiencia de crecimiento de los rodales de los genotipos de *Eucalyptus* mediterráneos en diferentes estaciones (verano, otoño, invierno y primavera) durante su desarrollo inicial. Concluimos que los cambios de clasificación ocurren en el incremento de volumen y el crecimiento máximo se observó en el verano independientemente del genotipo. Las diferencias en el volumen final de madera sugieren que el mismo ambiente estimula diferentes respuestas de asignación de carbono para el crecimiento y, en consecuencia, en la eficiencia del crecimiento en cada sitio. El segundo capítulo titulado “*Physiological responses and growth of Eucalyptus genotypes under cumulative water stress*” presenta un estudio que investiga la respuesta fisiológica de genotipos de *Eucalyptus* durante una reducción progresiva del contenido de agua del suelo y su relación con el crecimiento y estrés hídrico acumulados en el mismo período. Sin embargo, independientemente de las diferencias de genotipo, se observó una disminución en la tasa de fotosíntesis y cierre de estomas, lo que aumentó la eficiencia intrínseca del uso del agua con el tiempo. Esta reducción en las variables de intercambio de gases en las hojas con cambios moderados en el agua del suelo fue más pronunciada en el híbrido *Eucalyptus nitens* x *Eucalyptus globulus* (*E. gloni*), siendo el taxón más sensible a los cambios en la disponibilidad reducida de agua del suelo. El tercer capítulo titulado “*Temperature effects on early growth of Eucalyptus genotypes of three taxa*” presenta un estudio sobre el efecto de la temperatura en la tasa de crecimiento diaria. Concluimos que los genotipos de alta productividad, tienen su temperatura óptima promedio (16 ° C) más cercana a la temperatura media del aire del sitio (14 ° C) que los genotipos de baja productividad (25 ° C) y mayor amplitud de temperaturas cardinales (<17 ° C) es una ventaja para el crecimiento de los genotipos ante los cambios de temperatura del aire a lo largo de las estaciones que no limitan el crecimiento. Finalmente, observamos que la interacción entre genotipo y ambiente es determinante para guiar la partición de carbono en *Eucalyptus* y el estrés hídrico y térmico operan de la misma manera para el crecimiento en situaciones de inicio de estrés en el desarrollo inicial de las plantaciones.

Palabras-clave: Eficiencia de crecimiento, Fotosíntesis, Eficiencia en el uso del agua, Temperaturas cardinales, Ecofisiología forestal.

## SYMBOL LIST

a, b, c	Empirical coefficients in growth models (dimensionless)
A	Canopy absorbance
Adj-R <sup>2</sup>	Adjusted coefficient of determination
A <sub>n</sub>	Net assimilation rate ( $\mu\text{mol CO}_2 \text{ m}^{-2} \text{ s}^{-1}$ )
A <sub>t</sub>	Tree crown area ( $\text{m}^2$ )
B	Bias
C <sub>i</sub>	Intercellular CO <sub>2</sub> ( $\mu\text{mol CO}_2 \text{ mol air}^{-1}$ )
CSI	Current seasonal increment ( $\text{m}^3 \text{ ha}^{-1} \text{ season}^{-1}$ )
D <sub>n</sub>	Tree crown diameter in the north orientation (m)
D <sub>e</sub>	Tree crown diameter in the east orientation (m)
ET	Potential evapotranspiration (mm)
$f_b$	Light beam fraction
G	Soil heat flux density ( $\text{MJ m}^2 \text{ day}^{-1}$ )
GE	Growth efficiency ( $\text{m}^3 10,000 \text{ m}_{\text{leaf}}^{-2}$ )
g <sub>s</sub>	Stomatal conductance ( $\text{mol H}_2\text{O m}^{-2} \text{ s}^{-1}$ )
h	Total tree height (cm)
iWUE	Intrinsic water use efficiency ( $\mu\text{mol CO}_2 \text{ mol}^{-1} \text{ H}_2\text{O}$ )
K <sub>c</sub>	Light extinction coefficient (dimensionless)
LAI	Leaf area index ( $\text{m}^2 \text{ m}^{-2}$ )
LAI <sub>c</sub>	Corrected leaf area index ( $\text{m}^2 \text{ m}^{-2}$ )
MAE	Mean absolute error
PAR	Photosynthetic active radiation ( $\text{MJ m}^{-2}$ )
PPT	Precipitation (mm)
R <sup>2</sup>	Coefficient of determination
R	Correlation coefficient
r <sub>n</sub>	Radius of tree crown in north orientation (m)
r <sub>e</sub>	Radius of tree crown in east orientation (m)
rcd	Root collar diameter at 0.1-m height (cm)
RH	Relative humidity (%)
RMSE	Root mean square error
R <sub>n</sub>	Net radiation ( $\text{MJ m}^2 \text{ day}^{-1}$ )

SWHC	Soil water holding capacity (%)
t	Time (years)
T	Air temperature (°C)
$T_{\text{mean}}, T_{\text{max}}, T_{\text{min}}$	Mean, maximum, and minimum air temperature (°C)
$T_{\text{optg}}, T_{\text{ming}}, T_{\text{maxg}}$	Optimum, base minimum, and base maximum growth temperatures (°C)
Tr	Transpiration ( $\text{mmol H}_2\text{O m}^{-2} \text{s}^{-1}$ )
$u_2$	Wind speed measured at 2-m height ( $\text{m s}^{-1}$ )
V	Volume per square meter ( $\text{cm}^3 \text{m}^{-2}$ )
$v_i$	Individual tree volume ( $\text{cm}^3$ )
VPD	Vapor pressure deficit (kPa)
WSI	Water stress integral ( $\text{MPa day}^{-1}$ )
$w_{\text{stem}}$	Tree stem biomass (kg)
$W_{\text{stem}}$	Stem biomass per square meter ( $\text{kg m}^{-2}$ )
Z	Zenit angle (radian)
$\gamma$	Psychrometric constant ( $\text{kPa } ^\circ\text{C}^{-1}$ )
$\Delta$	Slope of vapor pressure curve ( $\text{kPa } ^\circ\text{C}^{-1}$ )
$\Delta\%$	Relative variation (%)
$\theta$	Soil water volumetric content ( $\text{m}^3 \text{m}^{-3}$ )
$\tau$	Ratio of PAR below canopy and above canopy (dimensionless)
$\chi$	Leaf distribution parameter (dimensionless)
$\Psi_{\text{md}}$	Midday leaf water potential (MPa)
$\Psi_{\text{pd}}$	Predawn leaf water potential (MPa)
$\Omega$	Clumping index (dimensionless)

## LIST OF FIGURES

FIGURE 1 – LOCATION OF THE TRIAL SITE (RED STAR) USED FOR DETERMINING GROWTH AND PHYSIOLOGY OF <i>EUCALYPTUS</i> GENOTYPES.....	19
FIGURE 2 – MONTHLY CHANGES IN PRECIPITATION (mm) AND MEAN TEMPERATURE (°C) FOR YUMBEL CHILE DURING 1979 TO 2014. ....	20
FIGURE 3 – PHOTOGRAPH OF THE EXPERIMENT IN MARCH 2018 (a) AND MARCH 2019 (b). .	21
FIGURE 4 – DIAGRAM OF THE EXPERIMENT DESING. ....	22
FIGURE 5 – REPRESENTATION OF THE NORTH AND EAST INTERCEPTED RADIATION READINGS BELLOW CANOPY PERFORMED WITH LI-250 IN THE MEASUREMENT PLOTS. ....	27
FIGURE 6 – AIR TEMPERATURE (a) <sup>1</sup> , PRECIPITATION AND POTENTIAL EVAPOTRANSPIRATION (b) <sup>2</sup> , VAPOR PRESSURE DEFICIT (c) <sup>1</sup> , AND PHOTOSYNTHETIC ACTIVE RADIATION (d) DURING OCTOBER 2017 AND APRIL 2019. ....	31
FIGURE 7 – CURRENT SEASONAL INCREMENT (CSI) FOR EACH GENOTYPE IN SECOND SUMMER (a), SPRING (b), WINTER (c), FALL (d), AND FIRST SUMMER (e), AND THE RELATIONSHIP BETWEEN CURRENT CSI WITH CSI IN PREVIOUS SEASON (f, g, h, AND i). <sup>1</sup> .....	33
FIGURE 8 – SEASONAL AND GENOTYPE VARIATION OF LEAF AREA INDEX (LAI <sub>C</sub> ). ....	34
_Toc74293663FIGURE 9 – LINEAR MODELS ADJUSTED FOR THE LEAF AREA INDEX (LAI <sub>C</sub> ) AND CURRENT SEASONAL INCREMENT (CSI) RELATIONSHIP FOR FIRST SUMMER AND WINTER (a), FALL (b), SPRING (c), HIGH PRODUCTIVITY GENOTYPES IN SECOND SUMMER (d), AND LOW PRODUCTIVITY GENOTYPES IN SECOND SUMMER (e). ....	37
FIGURE 10 – ANNUAL GROWTH EFFICIENCY AND SEASONAL GROWTH EFFICIENCY RELATIONSHIP AMONG <i>EUCALYPTUS</i> GENOTYPES DURING FALL (a), WINTER (b), SPRING (c), AND SECOND SUMMER (d). ....	39
FIGURE 11 –RAINFALL (PPT) AND TEMPERATURE (T), DURING THE FIRST 1.5 YEAR OF STUDY DEVELOPMENT.....	47
FIGURE 12 –CHANGES IN VOLUMETRIC SOIL WATER CONTENT (m <sup>3</sup> m <sup>-3</sup> ) AND RAINFALL (mm) BETWEEN M <sub>0</sub> AND M <sub>FINAL</sub> <sup>1</sup> . ....	48
FIGURE 13 – CUMULATIVE VOLUME FOR ALL <i>EUCALYPTUS</i> GENOTYPES BETWEEN M <sub>0</sub> AND M <sub>FINAL</sub> <sup>1</sup> . ....	52
FIGURE 14 – GENOTYPE CHANGES IN PREDAWN WATER POTENTIAL AND ITS RELATIONSHIP WITH VAPOR PRESSURE DEFICIT ALONG SEASONS FOR <i>E. globulus</i> (a, b), <i>E. nitens</i> (c, d), AND <i>E. gloni</i> (e, f) IN EARLY DEVELOPMENT. <sup>1</sup> .....	53
FIGURE 15 - GENOTYPE CHANGES IN WATER STRESS INTEGRAL FOR <i>E. globulus</i> (a), <i>E. nitens</i> (b) AND <i>E. gloni</i> (c) IN EARLY DEVELOPMENT.....	55
FIGURE 16 - WATER STRESS INTEGRAL AND VOLUME INCREMENT RELATIONSHIP BETWEEN M <sub>0</sub> AND M <sub>FINAL</sub> FOR <i>EUCALYPTUS</i> GENOTYPES. ....	56

FIGURE 17 – MAXIMUM DAILY PHOTOSYNTHESIS FOR EACH TAXON (UPPER) AND DAILY PHOTOSYNTHESIS FOR EG34, EN14, AND ENG3 (BOTTOM). .....	59
FIGURE 18 – RELATIONSHIP BETWEEN STOMATAL CONDUCTANCE AND VAPOR PRESSURE DEFICIT IN $M_0$ (a) AND $M_{FINAL}$ (b), AND BETWEEN INTRINSIC WATER USE EFFICIENCY AND VAPOR PRESSURE DEFICIT IN $M_0$ (c) AND $M_{FINAL}$ (d). <sup>1</sup> .....	60
FIGURE 19 – VARIATION IN PHOTOSYNTHETIS (a AND b) AND INTRINSIC WATER USE EFFICIENCY (c AND d) BETWEEN $M_0$ AND $M_{FINAL}$ , AND ITS RELATIONSHIP WITH GROWTH (a AND c) AND WATER STRESS INTEGRAL (b AND d) FOR <i>EUCALYPTUS</i> GENOTYPES. <sup>1</sup>	62
FIGURE 20 – CHANGES IN (a) LEAF AREA INDEX AND (b) MIDDAY WATER POTENTIAL BETWEEN $M_0$ AND $M_{FINAL}$ <sup>1</sup> .....	63
FIGURE 21 – RELATIONSHIP BETWEEN VOLUME ( $\text{cm}^3 \text{ m}^{-2}$ ) AND STEM BIOMASS ( $\text{kg m}^{-2}$ ) ON FEBRUARY 2019. <sup>1</sup> .....	71
FIGURE 22 – CHANGES IN STEM BIOMASS ( $w_{STEM}$ ) OVER THE SURVEY FOR <i>EUCALYPTUS</i> GENOTYPES. <sup>1</sup> .....	75
FIGURE 23 – CHANGES IN MINIMUM, MEAN, AND MAXIMUM TEMPERATURES FOR THE STUDY SITE DURING JANUARY 2018 TO MARCH 2019. ....	76
FIGURE 24 – VARIATION IN MEASUREMENT (SYMBOLS) AND MODELLED (LINE) STEM BIOMASS FOR EG17 (ABOVE FIGURES) AND FOR ENG20 (BELLOW FIGURES) OVER THE COURSE OF THE TRIAL FOR TREES WITHOUT (a AND c) AND WITH TEMPERATURE MODIFIER (b AND d). ....	77
FIGURE 25 - RELATIONSHIP BETWEEN TEMPERATURE MODIFIER ( $m$ ) WITH OPTIMAL TEMPERATURE (a), AND WITH CARDINAL TEMPERATURE AMPLITUDE ( $T_{MAXG} - T_{MING}$ ) (b).....	79
FIGURE 26 – TEMPERATURE MODIFIER OVER THE COURSE O THE TRIAL FOR EG17 AND ENG20. ....	81
FIGURE 27 – AVERAGE TEMPERATURE MODIFIER (DOTTED LINE) FOR <i>E. globulus</i> (a), <i>E. nitens</i> (b), AND <i>E. gloni</i> (c) AND CONSIDERING THE HIGHEST (GREEN LINE) AND THE LOWEST (RED LINE) PRODUCTIVITY GENOTYPE FOR EACH TAXA. <sup>1</sup> .....	82

## LIST OF TABLES

TABLE 1 – SOIL BULK DENSITY, SOIL WATER HOLDING CAPACITY (SWHC), ORGANIC MATTER (O.M.), CLAY, SILT, SAND, TOTAL NITROGEN (N), AND TOTAL CARBON (C) AT THE EXPERIMENT SITE FROM SOIL 100-CM PROFILE DEPTH.....	19
TABLE 2 – AVERAGE MEAN ( $T_{\text{mean}}$ ), MAXIMUM ( $T_{\text{max}}$ ), AND MINIMUM ( $T_{\text{min}}$ ) AIR TEMPERATURE, PRECIPITATION (PPT), POTENTIAL EVAPOTRANSPIRATION (ET), MAXIMUM VAPOR PRESSURE DEFICIT ( $VPD_{\text{max}}$ ), AND PHOTOSYNTHETIC ACTIVE RADIATION (PAR) DURING GROWING SEASONS. ....	30
TABLE 3 – ANALYSIS OF VARIANCE TESTING SEASON, GENOTYPE, AND GENOTYPE × SEASON INTERACTION EFFECTS FOR GROUND LINE DIAMETER ( $r_{\text{cd}}$ ), TOTAL HEIGHT (h), INDIVIDUAL VOLUME ( $v_i$ ), HECTARE VOLUME (V), CURRENT SEASONAL INCREMENT (CSI), LEAF AREA INDEX ( $LAI_C$ ). ....	32
TABLE 4 – LINEAR MODELS ADJUSTED FOR THE $LAI_C$ AND CSI (GROWTH EFFICIENCY) RELATIONSHIP FOR SEASONS AND GENOTYPES GROUPS THAT SHOWED SIGNIFICANT DIFFERENCES. <sup>1</sup> .....	35
TABLE 5 – ANALYSES OF VARIANCE P-VALUES TESTING SAMPLING INSTANCES (SI – $M_0$ AND $M_{\text{FINAL}}$ ), PERIODS (P – MORNING, MIDDAY, AND AFTERNOON), GENOTYPE (G) AND INTERACTION EFFECTS EVALUATED FOR PHOTOSYNTHESIS ( $A_n$ ), STOMATAL CONDUCTANCE ( $g_s$ ), INTERCELLULAR CARBON ( $C_i$ ), TRANSPIRATION ( $T_r$ ), MIDDAY WATER POTENTIAL ( $\Psi_{\text{md}}$ ), AND LEAF AREA INDEX (LAI). ....	57
TABLE 6 – DESCRIPTIVE STATISTICS FOR PHOTOSYNTHESIS ( $A_n - \mu\text{mol CO}_2 \text{ m}^{-2} \text{ s}^{-1}$ ), STOMATAL CONDUCTANCE ( $g_s - \text{mol H}_2\text{O m}^{-2} \text{ s}^{-1}$ ), INTERCELLULAR CARBON ( $C_i - \text{MMOL CO}_2 \text{ mol air}^{-1}$ ), TRANSPIRATION ( $T_r - \text{mmol H}_2\text{O m}^{-2} \text{ s}^{-1}$ ), MIDDAY WATER POTENTIAL ( $\Psi_{\text{md}} - \text{MPa}$ ), AND LEAF AREA INDEX (LAI – $\text{m}^2 \text{ m}^{-2}$ ) FOR <i>EUCALYPTUS</i> TAXA DURING SAMPLING INSTANCES <sup>1</sup> . ....	58
TABLE 7 – ADJUSTED COEFFICIENTS, $R^2$ , AND ROOT MEAN SQUARE ERROR (RMSE) IN STEM BIOMASS MODEL FOR EACH GENOTYPE.....	71
TABLE 8 – GROWTH FUNCTION, INVERSE AND DERIVATIVES FOR GROWTH ( $f(t)$ ) IN FUNCTION OF TIME (t) WHERE a, b AND c ARE MODEL PARAMETERS. ....	72
TABLE 9 – CORRELATION (R), BIAS (B), MEAN ABSOLUTE ERROR (MAE), AND ROOT MEAN SQUARE ERROR (RMSE) FROM THE ADJUSTED GROWTH MODELS. ....	75
TABLE 10 – MEAN, STANDARD DEVIATION (SD), COEFFICIENT OF VARIATION (CV%), F-VALUES OF ANALYSIS OF VARIANCE BY THE p-CATEGORY <sup>1</sup> , MODEL PARAMETERS (a, b, c, $T_{\text{min}_g}$ , $T_{\text{opt}_g}$ , $T_{\text{max}_g}$ ), ROOT MEAN SQUARE ERROR (RMSE) FOR <i>EUCALYPTUS</i> GENOTYPES. ....	78
TABLE 11 - MEAN, STANDARD DEVIATION (SD), COEFFICIENT OF VARIATION (CV%), F-VALUES OF ANALYSIS OF VARIANCE BY THE p-CATEGORY <sup>1</sup> , AND MODEL PARAMETERS (a, b, c, $T_{\text{min}_g}$ , $T_{\text{opt}_g}$ , $T_{\text{max}_g}$ ) AT TAXA LEVEL.....	80



## SUMMARY

<b>1 GENERAL INTRODUCTION .....</b>	<b>16</b>
1.1 OBJECTIVES .....	18
1.1.1 General objective .....	18
1.1.2 Specific objectives .....	18
<b>2 GENERAL MATERIALS AND METHODS .....</b>	<b>18</b>
2.1 SITE CHARACTERISTICS.....	18
2.2 EXPERIMENTAL DESIGN .....	20
2.3 CLIMATE VARIABLES.....	23
<b>3 CHAPTER 1 - DIFFERENCES IN EARLY SEASONAL GROWTH EFFICIENCY AND PRODUCTIVITY OF <i>EUCALYPTUS</i> GENOTYPES .....</b>	<b>24</b>
3.1 INTRODUCTION.....	24
3.2 MATERIAL AND METHODS .....	26
3.2.1 Tree measurements .....	26
3.2.2 Statistical Analyses .....	29
3.3 RESULTS.....	30
3.3.1 Climate .....	30
3.3.2 Genotype and seasonal effects on growth and growth efficiency.....	31
3.4 DISCUSSION .....	39
3.5 CONCLUSIONS .....	42
<b>4 CHAPTER 2 - PHYSIOLOGICAL RESPONSES AND GROWTH OF <i>EUCALYPTUS</i> GENOTYPES UNDER CUMULATIVE PLANT WATER STRESS ..</b>	<b>43</b>
4.1 INTRODUCTION.....	44
4.2 MATERIALS AND METHODS.....	46
4.2.1 Growth.....	46
4.2.2 Seasonal measurements of predawn leaf water potential .....	46
4.2.3 Volumetric soil water content ( $\theta$ ) and sampling instances.....	47
4.2.4 Leaf gas-exchange .....	49
4.2.5 Midday water potential ( $\Psi_{md}$ ) .....	49
4.2.6 Leaf area index (LAI) .....	49
4.2.7 Statistical analyses .....	50
4.3 RESULTS.....	51
4.3.1 Growth in a period of moderately decreased soil water ( $M_0$ and $M_{final}$ ).....	51

4.3.2 Seasonal measurements of predawn leaf water potential ( $\Psi_{pd}$ ) and water stress integral (WSI) .....	52
4.3.3 Volume increment (IncVol) and water stress integral (WSI).....	56
4.3.4 Physiological and LAI measurements during the decreased soil water availability period ( $M_0$ and $M_{final}$ ).....	57
4.4 DISCUSSION .....	64
4.5 CONCLUSIONS .....	67
<b>5 CHAPTER 3 TEMPERATURE EFFECTS ON EARLY GROWTH OF <i>EUCALYPTUS</i> GENOTYPES OF THREE TAXA .....</b>	<b>68</b>
5.1 INTRODUCTION .....	68
5.2 MATERIAL AND METHODS .....	69
5.2.1 Tree measurements .....	69
5.2.2 Growth Model and data analyses .....	72
5.3 RESULTS.....	74
5.3.1 Tree growth .....	74
5.3.2 Site range in air temperature .....	76
5.3.3 Temperature model parameters and air temperature modifier .....	76
5.4 DISCUSSION .....	83
5.5 CONCLUSION .....	85
<b>6 FINAL CONCLUSIONS AND CONSIDERATIONS .....</b>	<b>86</b>
<b>REFERENCES.....</b>	<b>89</b>

## 1 GENERAL INTRODUCTION

The pressure for natural forest conservation, global population, and demand for wood products expect to largely increase until 2050, then we will face an increment in investments, research, and importance in planted forest around the world (World Wildlife Fund, 2012), especially in areas where industrial forestry is dominant such as South America (Elias and Boucher, 2014). Countries in South America were dominated by annual forest plantation, mainly *Eucalyptus* species (Payn et al., 2015) and these plantations sum up billions of dollars into world economies (Booth, 2013).

*Eucalyptus* competitiveness is high productivity compared to other species and natural forests (above 30 m<sup>3</sup> ha<sup>-1</sup> yr<sup>-1</sup>), short rotations (average 10 years), and a wide variation of wood products such as charcoal, pulp, paper, and solid products (Rockwood et al., 2008; Booth, 2013). This was possible due to advances in silvicultural practices, breeding programs, hybridization, and clonal forest production (Gonçalves et al., 2013).

Recent studies have shown that the increase in environmental changes, such as drought and extremes temperatures along *Eucalyptus* development, generate impacts in final timber production (Binkley et al., 2017; Elli et al., 2020). Global climate is undergoing changes that will impact all ecosystems and the consequences of these changes are still uncertain as well (IPCC, 2014). In this context, ecophysiological approaches are necessary to understand the influence rate of environmental variables in early forest production (Gauthier and Jacobs, 2018).

Chile is one of these countries that faced environmental constraints because most forest plantations are in areas with a Mediterranean climate, characterized by rains during winter and a drought period in summer (INIA, 1989). Since 2000, the reforestation areas increased in the country, and forest plantation areas with eucalyptus species accumulated in Chile were of 45,482 hectares. *E. globulus* and *E. nitens* species and its hybrids genotypes have been extensively planted in Chile because of high productivity, desire for fiber and pulp yield, and tolerance to drought and cold temperatures (INFLOR, 2020; Rubilar et al., 2020).

Among environmental constraints, variations in air temperature and soil water content are recognized as being key factors that control plant growth and development along the months, seasons, and years (Battaglia et al., 1996; Wang et al., 2013). These factors have a direct relation with *Eucalyptus* productivity, affecting physiological

processes such as photosynthesis (Taiz et al., 2017) and efficiency of resources use and consequently wood production (Stape et al., 2004; Binkley et al., 2017).

For instance, water supply influence carbohydrate available for wood production (Stape et al., 2008), increased net primary production by 27%, foliage production by 14%, and light use efficiency by 20% in response to irrigation in different sites in Brazil (Ryan et al., 2010), because increasing in available water increase fraction of photosynthesis used for wood growth. Furthermore, sub-optimal temperatures also affect plant metabolism due to this effect in enzymatic reactions (Taiz et al., 2017), since out of minimum and maximum temperatures for development, forest growth is interrupted (Landsberg and Sands, 2011).

Considering these environmental traits, the foresters decision of the proper *Eucalyptus* species and genotypes must be related to the susceptibility of plants to water deficit, growth, survival and adaptations during establishment, with selection of best materials for ecophysiological attributes, such as photosynthesis, leaf area index, growth efficiency, water use efficiency and leaf water potential (Albaugh et al., 2013).

For this, seeking a better understanding of the genetic, growth, and physiological process along the early *Eucalyptus* development is crucial for better understanding stress tolerance and match genotypes to a particular site, due higher susceptibility to abiotic stress by young *Eucalyptus* plantations (Drake et al., 2009). Faced with these gaps, it defined the three chapters of this thesis. In the first chapter, we discuss the changes in early growth and leaf area (growth efficiency) relationships among eucalyptus genotypes in different growing seasons. In the second chapter, we discuss changes in physiology during decreased soil water content among eucalyptus genotypes with different growth rates and accumulated water stress integral. Finally, the third chapter will deal with cardinal air temperature effects in early growth among eucalyptus genotypes. The chapters were entitled as follows:

- 1) Differences in early seasonal growth efficiency and productivity of *Eucalyptus* genotypes.
- 2) Physiological responses and growth of *Eucalyptus* genotypes under cumulative water stress.
- 3) Temperature effects on early growth of *Eucalyptus* genotypes of three taxa.

## 1.1 OBJECTIVES

### 1.1.1 General objective

The study aimed to evaluate the response of different *Eucalyptus* genotypes to environmental drivers (e.g., soil water content and temperature), in changes of early growth, leaf area and physiological behavior on 1.5-year of development in experiment in Central South Chile.

### 1.1.2 Specific objectives

- The first chapter aimed to determine the interaction between season and genotype on early growth efficiency over 1.5 year of development of different *Eucalyptus* genotypes.

- The second chapter aimed to analyze the relationship between growth and water stress integral on changes in photosynthesis, intrinsic water use efficiency, midday water potential and leaf area index of different *Eucalyptus* genotypes under a short period of decreased soil water content.

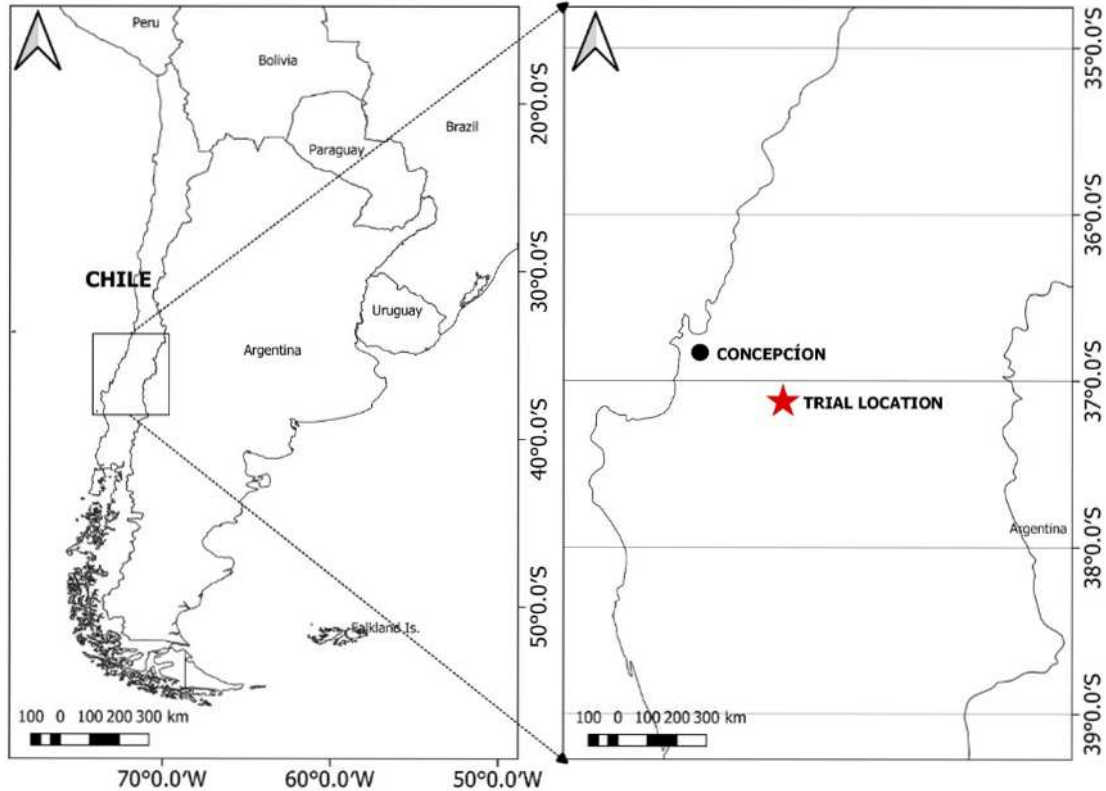
- The third chapter aimed to identify the cardinal air temperatures effects on early daily growth over 1.3 year of development of different *Eucalyptus* genotypes.

## 2 GENERAL MATERIALS AND METHODS

### 2.1 SITE CHARACTERISTICS

The study site was located 9.6 km east of Yumbel, Bio-Bio region, central South Chile (37°8'0.01" S, 72°27'34.70" W, 200 m.a.s.l.) (FIGURE 1), in the forest nursey of CMPC Forestal Mininco. The experiment was established on land previously used for a bioenergy study involving *Acacia* and *Eucalyptus* spp., where the stumps, after harvesting, were removed mechanically, and the remaining residues crushed and incorporated into the soil by harrowing. The study soil site is classified as an Entisol (Soil Survey Staff, 1999), formed by volcanic black sands of andesitic and basaltic origin with low water holding capacity. A summary of the local soil profile description is presented in TABLE 1.

FIGURE 1 – LOCATION OF THE TRIAL SITE (RED STAR) USED FOR DETERMINING GROWTH AND PHYSIOLOGY OF *EUCALYPTUS* GENOTYPES.



Source: The author (2021).

TABLE 1 – SOIL BULK DENSITY, SOIL WATER HOLDING CAPACITY (SWHC), ORGANIC MATTER (O.M.), CLAY, SILT, SAND, TOTAL NITROGEN (N), AND TOTAL CARBON (C) AT THE EXPERIMENT SITE FROM SOIL 100-cm PROFILE DEPTH.

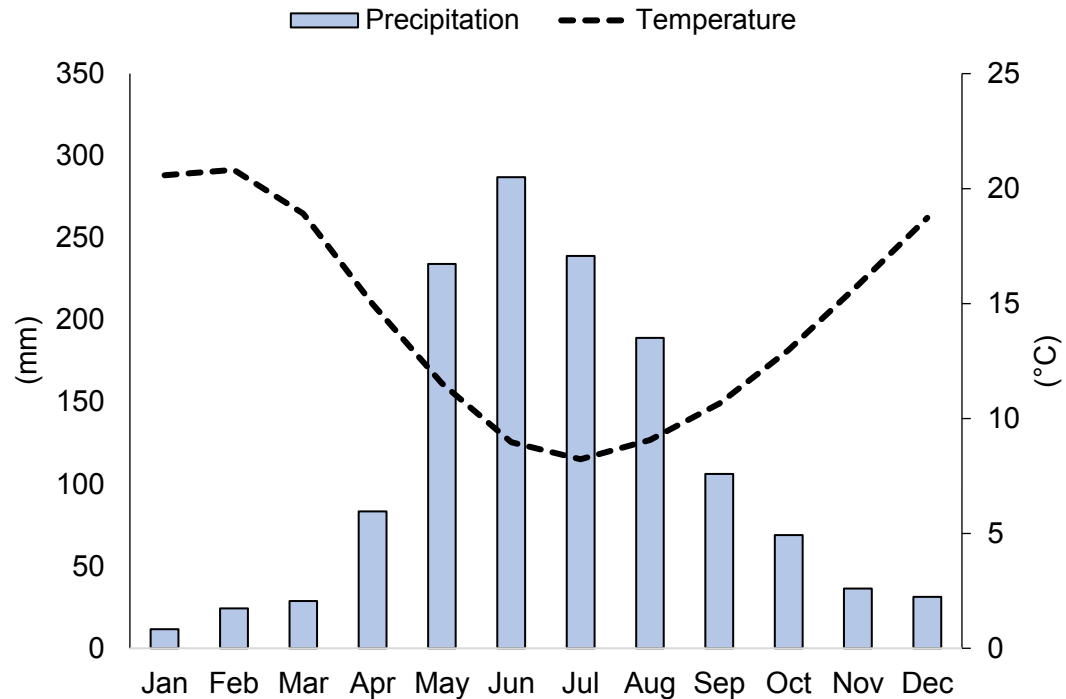
Depth (cm)	Bulk density (g cm <sup>-3</sup> )	SWHC	O.M.	Clay	Silt	Sand	Total N	Total C
					%			
0 – 20	1.50	4.46	1.28	0.99	12.3	86.6	0.13	1.54
20 – 40	1.45	4.79	0.44	1.50	5.16	93.3	0.03	0.36
40 – 60	1.43	5.07	0.30	2.06	3.53	94.3	0.01	0.21
60 – 80	1.43	4.88	0.27	2.06	4.31	93.6	0.01	0.13
80 – 100	1.43	5.15	0.22	0.90	6.80	92.2	0.01	0.10

Source: Rubilar et al. (2020).

The climate of the experimental site is characterized as Csb (i.e., warm-summer Mediterranean climate), with winter rains (Sarricolea et al., 2017). Historical climate records for a period of 35 years (1979–2014) were available (<https://globalweather.tamu.edu/>) at the time of the study. The average annual precipitation at the site is 1328 mm, occurring mainly during winter (600 mm). Summer is drier with an average annual precipitation of 60 mm. The mean annual temperature is 14.2 °C, with an absolute maximum occurring in January (38.9 °C) and an absolute

minimum in July ( $-1.7\text{ }^{\circ}\text{C}$ ). Solar radiation ranged between  $10.4\text{ MJ m}^{-2}\text{ day}^{-1}$  in July (winter) to  $29.3\text{ MJ m}^{-2}\text{ day}^{-1}$  in January (summer) (FIGURE 2).

FIGURE 2 – MONTHLY CHANGES IN PRECIPITATION (mm) AND MEAN TEMPERATURE ( $^{\circ}\text{C}$ ) FOR YUMBEL CHILE DURING 1979 TO 2014.

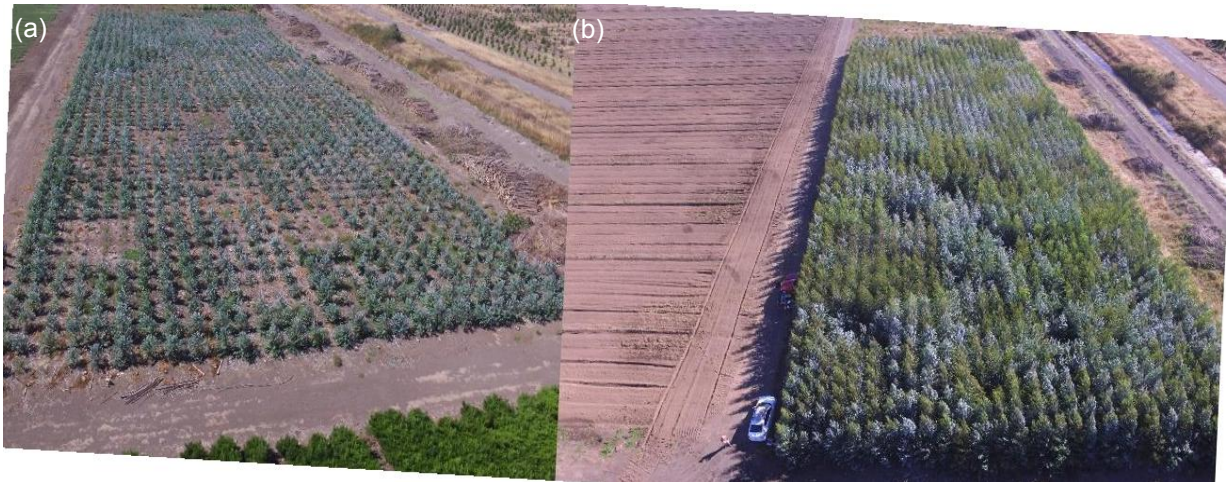


Source: The author (2021).

## 2.2 EXPERIMENTAL DESIGN

A completely randomized block design with three replicates was established on October 31, 2017, using 22 *Eucalyptus* genotypes. These genotypes are commercial and are part of the tree-improvement program of CMPC Forestal Mininco and ARAUCO forest companies. These tree-improvement programs aimed the selection of genotypes with desirable fiber and pulp yield, higher growth rate and resistance to drought and cold temperatures as well. Plant genetic material consisted in ten cuttings of *E. globulus* (EG1, EG17, EG18, EG19, EG21, EG28, EG30, EG31, EG33, and EG34), three seedlings of *E. nitens* (EN12, EN13, and EN14), and nine cuttings of *E. nitens*  $\times$  *E. globulus* (*E. gloni*) hybrids (ENG2, ENG3, ENG4, ENG5, ENG7, ENG8, ENG20, ENG22, and ENG25) (FIGURE 3).

FIGURE 3 – PHOTOGRAPH OF THE EXPERIMENT IN MARCH 2018 (a) AND MARCH 2019 (b).

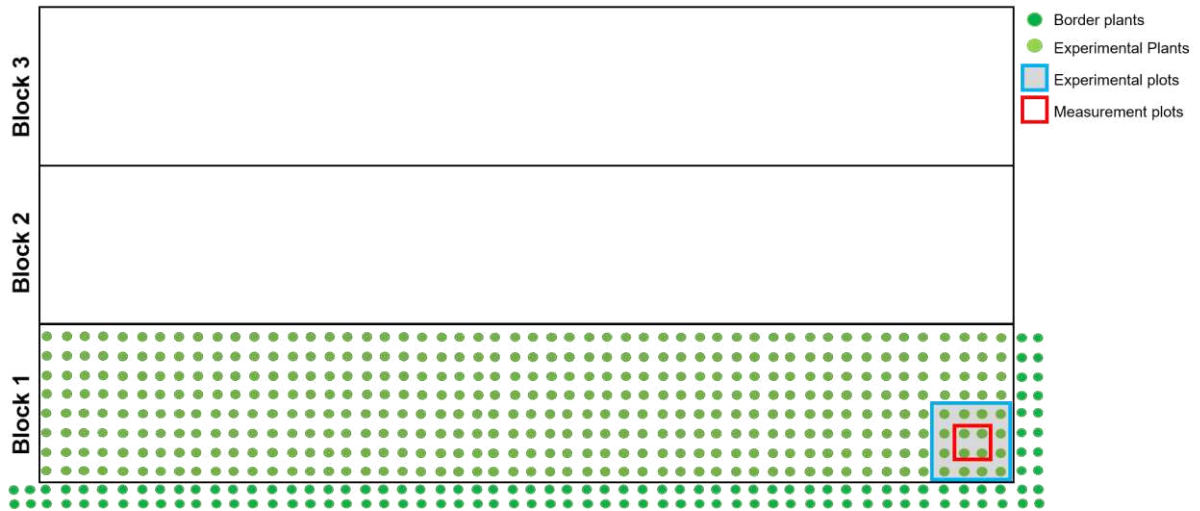


Source: The author (2021).

Plants of homogeneous size (3-mm root collar diameter and 30-cm height) for each genotype and with no visual disease symptoms or damage were selected from nursery material. Plants were established at 1 x 1.5 m spacing (6667 trees ha<sup>-1</sup>), and experimental plots consisted of 4 x 4 trees with 2 x 2 trees internal measurement plots (FIGURE 4). Small dimensions plots were used to ensure maximum homogeneous conditions of plant growth, to accelerate early canopy closure, intraspecific competition by greater site occupancy, genotype response on use of site available resources, and increase stress and risks in response to droughts (Hakamada et al., 2020a). Replanting occurred one month after establishment and proportion of replanted individuals was 2% (8 seedlings).



FIGURE 4 – DIAGRAM OF THE EXPERIMENT DESIGN.



Source: The author (2021).

Weed control using glyphosate ( $2.5 \text{ l ha}^{-1}$ ) was done before planting in December 2017 and again in September 2018 to maintain weed-free conditions. Nutrient additions were applied to eliminate any potential nutritional deficits. During planting, individual trees were fertilized with 30 g commercial controlled-release fertilizer (Basacote® Plus 12M; COMPO EXPERT, Münster, Germany) containing 15% N, 8%  $\text{P}_2\text{O}_5$ , 12%  $\text{K}_2\text{O}$ , 2%  $\text{MgO}$ , and 5% S which was applied into the planting holes. Plants were properly irrigated from the time of planting until March 2018 (first dry summer season) to ensure survival, and again from the end of November 2018 until mid-February 2019 (second dry summer season). The irrigation was performed by dripper lines, with 50-cm emission point spacing along the planting line. The accumulated water provided by irrigation during the first and second dry summer periods was 664 and 158 mm, respectively. Furthermore, the irrigation management was performed based on a daily water balance, with evaporation records from a Class-A evaporation pan, located near the experimental area (McMahon et al., 2013). The irrigation was always carried out until the soil reached field capacity. It is emphasized that from mid-February 2019 until late March 2019 the irrigation treatment was turned off to evaluate plant physiological responses as soil water decreased.

### 2.3 CLIMATE VARIABLES

Daily values of minimum, mean, and maximum air temperature ( $^{\circ}\text{C}$ ), precipitation (mm), relative humidity (%), wind speed ( $\text{m s}^{-1}$ ), and photosynthetic active radiation ( $\text{MJ m}^{-2} \text{ day}^{-1}$ ) were collected from a weather station located 600 m near the experiment site. Also, minimum, mean, and maximum vapor pressure deficit (VPD; kPa) was calculated as follows:

$$\text{VPD} = \left(1 - \frac{\text{RH}}{100}\right) \cdot \left[ \frac{610.7 \times 10^{\left(\frac{7.5T}{237.7+T}\right)}}{1000} \right] \quad (1)$$

where, VPD is the vapor pressure deficit (kPa), RH is the relative humidity (%), and T is the air temperature ( $^{\circ}\text{C}$ ).

Daily potential evapotranspiration (ET) was calculated using the Penman-Monteith equation (Allen et al., 1989):

$$\text{ET} = \frac{0.408 \cdot \Delta \cdot (R_n - G) + \gamma \cdot \frac{900}{T + 273} \cdot u_2 \cdot \text{VPD}}{\Delta + \gamma \cdot (1 + 0.34 \cdot u_2)} \quad (2)$$

where, ET is the potential evapotranspiration (mm),  $R_n$  is the net radiation of crop surface ( $\text{MJ m}^{-2} \text{ day}^{-1}$ ), G is the soil heat flux density ( $\text{MJ m}^{-2} \text{ day}^{-1}$ ),  $\gamma$  is the psychrometric constant ( $\text{kPa } ^{\circ}\text{C}^{-1}$ ),  $u_2$  is the wind speed measured at 2-m height ( $\text{m s}^{-1}$ ), and  $\Delta$  is the slope of the vapor pressure curve ( $\text{kPa } ^{\circ}\text{C}^{-1}$ ).

### 3 CHAPTER 1 - DIFFERENCES IN EARLY SEASONAL GROWTH EFFICIENCY AND PRODUCTIVITY OF *EUCALYPTUS* GENOTYPES

#### ABSTRACT

Understanding the changes in early growth efficiency (GE, growth / leaf area) may improve forest production through selection of specific genotypes at early stages. We investigated the early growth response of different genotypes of *Eucalyptus globulus* (10), *E. nitens* (3), and *E. nitens* × *E. globulus* (*E. gloni*) (9) in south central Chile. To evaluate seasonal growth, seedlings of each genotype were established in a complete randomized block design in a coarse sandy soil (i.e., low water holding capacity) with irrigation during spring and summer. A current seasonal increment (CSI) in wood volume (cm<sup>3</sup> m<sup>-2</sup>) and leaf area index (LAI) were estimated to calculate GE (CSI/LAI) at 4.1, 7.5, 10.4, 13.4, and 17.1 months of age, corresponding to five sequential growing seasons (first summer, fall, winter, spring, and second summer). The interaction of genotype and season had a significant effect ( $p < 0.001$ ) on CSI, but not on LAI causing large changes in seasonal GE. In general, CSI values declined in winter but increased greatly in second summer. LAI values were stable during the first three seasons, increased in spring, and peaked in the second summer. During the season of maximum growth rate, a strong relationship between growth and LAI was not observed. The highest growth efficiencies were observed mainly for *E. nitens* and *E. gloni* genotypes, which were able to growth with small values of LAI. Our findings showed that eucalyptus genotypes with higher annual GE did not present higher seasonal GE, except in the second summer season. Changes in seasonal and annual growth efficiency performance, suggest that the same environment drive a large response in genotypes early growth, as consequence of climate influences in carbon allocation in *Eucalyptus* genotypes.

Keywords: Leaf area index, Wood growth, Forest production, Growing season.

#### 3.1 INTRODUCTION

*Eucalyptus* plantations are increasingly exposed to drought, fires, heat, and pests that could reduce productivity under climate change (Booth, 2013). However, there is potential to mitigate these adverse factors by planting adapted genetic materials (Binkley et al., 2017; Binkley and Stape, 2004). The interaction of genotype and environment has strong implications regarding the selection of the best genetic material for a specific site (Oliveira et al., 2018), particularly during the early ages where the potential for genotype selection for growth and adaptation in *Eucalyptus* breeding programs has been observed (Harrand et al., 2009; Luo et al., 2010). Relative growth responses, matched with appropriate genotype selection and an adequate site

potentially, enable increased *Eucalyptus* productivity and facilitate high stocking at full rotation (Binkley et al., 2004; Boreham and Pallett, 2009).

A key driver of forest growth rates is leaf area, and its interaction with environmental conditions largely determines stem growth (Du Toit and Dovey, 2005; Laclau et al., 2008; Smethurst et al., 2003). Leaf area represented an important variable for ecophysiological studies, since higher values of leaf area indicated higher plant photosynthetic area, however higher plant transpiration (Hakamada et al., 2020b), which are influenced by water balance and climate variations over the months and years of forest growth (Khoury and Coomes, 2020).

The ratio of annual or periodic growth to leaf area is called growth efficiency (GE) (Waring et al., 1980), and it defines canopy efficiency in terms of net assimilation rates of carbon dioxide (CO<sub>2</sub>) (Waring et al., 2016). When *Eucalyptus* is grown under conditions of adequate resource supply (i.e., water and nutrients) or in managed plantations at favorable sites, GE is known to increase because plant increase the leave efficiency in assimilate and allocate CO<sub>2</sub> to stem growth (Whitehead and Beadle, 2004). However, since *Eucalyptus* genotypes did not show a similar growth rate in the same environment, these changes are also possible related to the dynamics of the leaf area over the same period.

*Eucalyptus* forest areas placed in subtropical regions faced seasonal changes in air temperature and radiation, also in regions with Mediterranean climate, such as Central South Chile, they present the dry summer period with high atmospheric demand (Rubilar et al., 2020), resulting in interaction of season and genotype in growth rate and leaf area. However, little is known about whether the driver of early GE changes is seasonal growth or seasonal change in leaf area index (LAI), especially during early forest development when stress effects, such as drought, are most pronounced (Drake et al., 2009). Our understanding is that, if a seasonal increment in leaf area leads to the same proportional seasonal increment in growth, there is no change in seasonal GE.

Considering the gap in knowledge about eucalyptus GE during early development, this study aimed to determine the interaction between season and genetic on early growth efficiency (growth/LAI) over 1.5 years of development of different *Eucalyptus* genotypes. We tested the hypothesis that during the early development the interaction of season and genetic are potential effect of changing in ranking of early growth and leaf area index among different *Eucalyptus* genotypes and

higher growth efficiencies during the seasons are expected for genotypes with higher annual growth efficiencies.

## 3.2 MATERIAL AND METHODS

### 3.2.1 Tree measurements

Total tree height ( $h$ ; cm) and root collar diameter ( $rdc$ ; cm) were measured monthly for each tree of the measurement plots (2 x 2 trees). Seasonal cumulative values of  $rdc$  and  $h$  were measured to match the dates when the leaf area index (LAI) was measured. Monthly tree growth measurements were taken from January 2018 to March 2019 (67 and 513 days after planting, respectively). For seasonal growth comparisons, five growing seasons were considered: first summer (January 2018 to March 2018), fall (April 2018 to June 2018), winter (July 2018 to September 2018), spring (October 2018 to December 2018), and second summer (January 2019 to March 2019). These five seasons present different average values of air temperature ( $T$ ), precipitation (PPT), radiation ( $R_n$ ) and vapor pressure deficit (VPD) for experiment site. We estimated individual tree volume ( $v_i$ ; cm<sup>3</sup>) as:

$$v_i = 0.33\pi \cdot \frac{rdc^2}{4} \cdot h \quad (3.1)$$

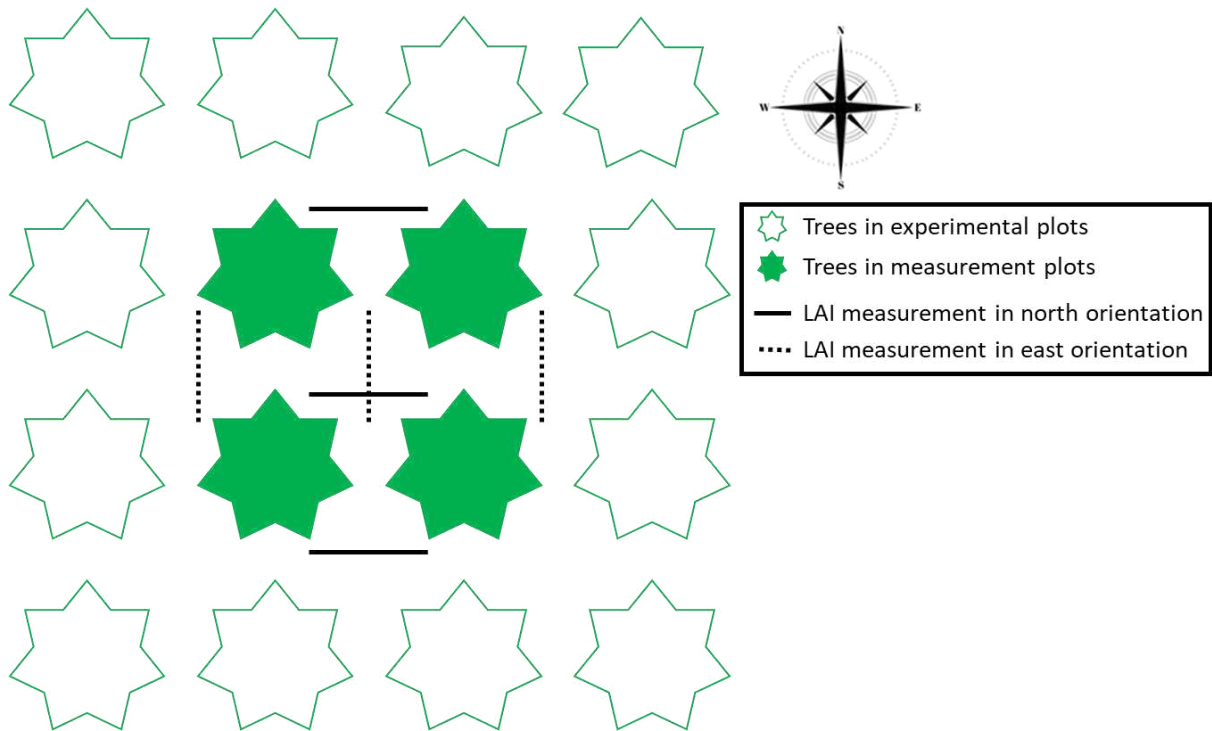
where,  $v_i$  is the individual tree volume (cm<sup>3</sup>),  $rdc$  is the root collar diameter measured at 10 cm above ground (cm), and  $h$  is the total tree height (cm).

Volume was scaled up to square meter ( $V$ ; cm<sup>3</sup> m<sup>-2</sup>) by summing  $v_i$  in measurement plots and divided by measurement plot area (6 m<sup>2</sup>). The form factor value (0.33) was according to others studies with similar genotypes on the same location (Rubilar et al., 2020; Watt et al., 2014). The current seasonal increment (CSI; cm<sup>3</sup> m<sup>-2</sup> season<sup>-1</sup>) for each of the five growing seasons was estimated as the difference between  $V$  at the beginning and end of each season. Also, we evaluate tree survival and there was no mortality during the experiment.

LAI was estimated for each plot (66 measurements plots). Estimates were obtained using midday (11:00h to 14:00h) photosynthetically active radiation (PAR) interception, by measures below the tree canopy PAR in the north and east orientation

(n = 6) avoiding empty spaces in between tree canopy that did not contribute to light interception (FIGURE 5), and outside the experimental area (n =1) using a ceptometer (Li-191R & Li-250; LICOR Scientific, Lincoln, Nebraska, USA).

FIGURE 5 – REPRESENTATION OF THE NORTH AND EAST INTERCEPTED RADIATION READINGS BELLOW CANOPY PERFORMED WITH LI-250 IN THE MEASUREMENT PLOTS.



Source: The author (2021).

Estimates were obtained under clear-sky conditions in March 2018 (S1), June 2018 (S2), August 2018 (S3), December 2018 (S4), and February 2019 (S5). The LAI is derived from the model proposed by Norman and Jarvis (1975) which computes the sky conditions at data acquisition, effects of canopy architecture, optical properties of the leaves, in addition of the time of year and hour of day under sun angle, assuming that leaves are randomly distributed in the canopy.

$$\text{LAI} = \frac{\left[ \left( 1 - \frac{1}{2K_c} \right) f_b - 1 \right] \ln(\tau)}{A(1 - 0.47f_b)} \quad (3.2)$$

where, LAI is tree leaf area index ( $\text{m}^2 \text{m}^{-2}$ ),  $K_c$  is tree extinction coefficient (Campbell, 1986),  $f_b$  is the light beam fraction, assumed to be 0.881,  $\ln(\tau)$  is the logarithmic of

ratio of PAR bellow tree canopy and outside of experimental area, and  $A$  is canopy absorbance in PAR, assumed to be 0.86.

$$K_c = \frac{\sqrt{\chi^2 + \tan(Z)^2}}{\chi + 1.744(\chi + 1.182)^{-0.733}} \quad (3.3)$$

where,  $Z$  is zenit angle in radians and  $\chi$  is leaf distribution parameter, assumed to be 1.

Since LAI measurements were performed before canopy closure, we corrected LAI values base on average trees crown area ( $A_t$ ;  $m^2$ ) in measurement plots, using measurements of trees crown diameter in the north ( $D_n$ ; m) and east ( $D_e$ ; m) orientation, assuming a geometric shape equivalent to ellipsoid with horizontal axes formed by the crown projection radius.

$$r_n; r_e = \frac{(D_n; D_e)}{2} \quad (3.4)$$

$$A_t = \pi \cdot r_n r_e \quad (3.5)$$

where,  $r_n$  is the radius of tree crown in north orientation (m),  $r_e$  is the radius of tree crown in east orientation (m) for horizontal plane,  $D_n$  is the tree crown diameter in the north orientation (m),  $D_e$  is the tree crown diameter in the east orientation (m),  $\pi$  is  $\pi$  constant (3.1415926), and  $A_t$  is the tree crown area ( $m^2$ ).

It was used the relationship between  $A_t$  and plot area ( $6 m^2$ ) to estimated clumping index ( $\Omega$ ) and calculated the corrected LAI ( $LAI_c$ ) for each genotype.

$$\Omega = \frac{A_t}{6} \quad (3.6)$$

$$LAI_c = LAI \cdot \Omega \quad (3.7)$$

where,  $\Omega$  is the clumping index (dimensionless) and  $LAI_c$  is the corrected leaf area index ( $m^2 m^{-2}$ ).

Finally, GE was estimated as the ratio of CSI to LAI<sub>c</sub> calculated at the corresponding season (le Maire et al., 2019; Waring et al., 2016). We also calculated the annual GE as the difference between V measured in January 2018 and March 2019 divided by the LAI<sub>c</sub> estimated in February 2019.

### 3.2.2 Statistical Analyses

Analyses of variance (ANOVA) were used to analyze season and genotype differences in cumulative and seasonal growth and LAI<sub>c</sub>. Season was considered fixed effects, because climate variables in seasons (e.g., temperature, PPT, VPD, and PAR) changes systematically along the years and also genotype was considered fixed effect because in this study we evaluated only a few numbers of genotypes of interest. Blocks were considered random effects because in this study was assumed that soil characteristics varied aleatory among blocks. All ANOVA analyses were performed using the MIXED procedure. Seasons and genotypes differences in rcd, h, vi, V, CSI, and LAI<sub>c</sub>, were determined with the LSMEANS statement using the Tukey-Kramer adjustment ( $p < 0.05$ ) in MIXED procedure.

Linear regression was used to evaluated changes in CSI responses during each season with the previous season considering all genotypes. We used regression analysis in the GLM procedure to assess the relationship between CSI and LAI<sub>c</sub>, considering full versus reduced models for season and genotypes, using contrast options in GLM procedure. For the relationship among annual GE and seasonal GE, we used regression analyses for all evaluated genotypes.

Models were compared using significance of coefficients ( $p < 0.05$ ) adjusted coefficient of determination (Adj-R<sup>2</sup>; Eq. 3.8) and root mean square error (RMSE; Eq. 3.9). Analyses were performed using SAS®Studio ([https://www.sas.com/en\\_us/software/studio.html](https://www.sas.com/en_us/software/studio.html)). When required, variables were log transformed to meet the assumptions of normality and homoscedasticity. All graphical analyses were performed in R software using the ggplot2 package (Wickham et al., 2020).

$$\text{Adj}_R^2 = 1 - (1 - R^2) \left( \frac{n - 1}{n - p - 1} \right) \quad (3.8)$$



$$\text{RMSE} = \sqrt{\frac{1}{n} \sum_{i=1}^n (O_i - E_i)^2} \quad (3.9)$$

where,  $\text{Adj}_R^2$  is the adjusted coefficient of determination,  $R^2$  is the coefficient of determination,  $p$  is the number of coefficients in the model, RMSE is the root mean square error,  $n$  is the number of observations,  $O_i$  is the  $i$ th observed value, and  $E_i$  is the  $i$ th estimated value.

### 3.3 RESULTS

#### 3.3.1 Climate

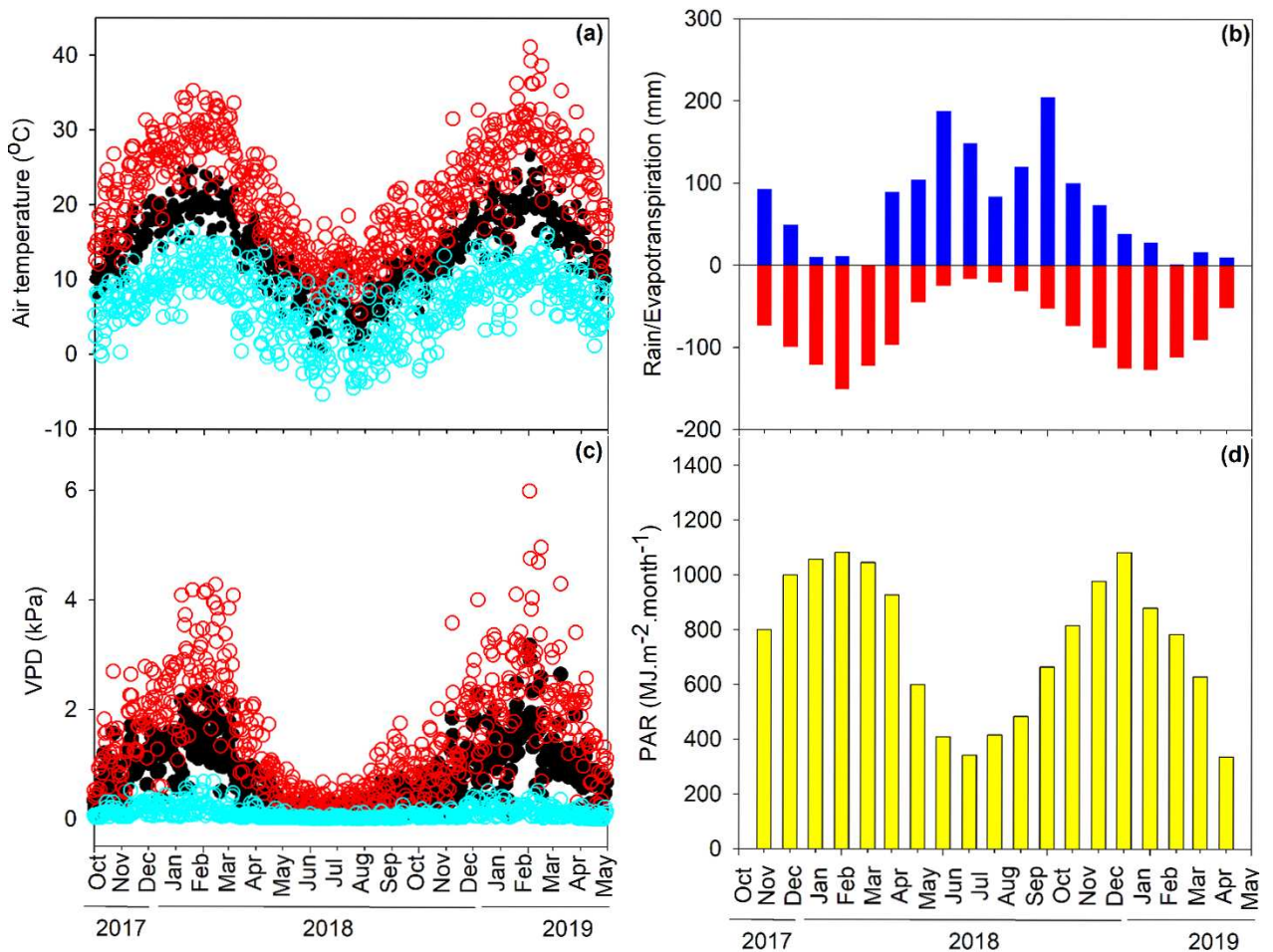
Average T, VPD, sum of PPT, and ET across seasons are presented in TABLE 2. During the experiment, the average temperature was 14 °C. The maximum and minimum absolute air temperatures were recorded in February 2019 (41.2 °C) and June 2018 (-5.4 °C), respectively. Seasonal VPD showed a similar trend to temperature. During summer (January to March), maximum VPD ranged between 2.0 and 5.0 kPa, whereas during winter (July to September) VPD ranged from 0.03 to 0.51 kPa. During the experiment, total PPT and ET were 1212 and 1217 mm, respectively. Precipitation occurred mainly in winter (July to September; 414 mm) with 60 mm falling during the summer months. Total PAR in summer was almost the double of total PAR in winter (FIGURE 6).

TABLE 2 – AVERAGE MEAN ( $T_{\text{mean}}$ ), MAXIMUM ( $T_{\text{max}}$ ), AND MINIMUM ( $T_{\text{min}}$ ) AIR TEMPERATURE, PRECIPITATION (PPT), POTENTIAL EVAPOTRANSPIRATION (ET), MAXIMUM VAPOR PRESSURE DEFICIT ( $\text{VPD}_{\text{max}}$ ), AND PHOTOSYNTHETIC ACTIVE RADIATION (PAR) DURING GROWING SEASONS.

Season	Months	Year	$T_{\text{mean}}$ (°C)	$T_{\text{max}}$ (°C)	$T_{\text{min}}$ (°C)	PPT (mm)	ET (mm)	$\text{VPD}_{\text{max}}$ (kPa)	PAR (MJ season <sup>-1</sup> )
First summer	Jan–Mar	2018	19.1	27.5	10.6	63	387	2.54	1720
Fall	Apr–Jun		9.9	16.1	4.5	420	115	0.66	775
Winter	Jul–Sep		7.8	13.7	2.7	414	97	0.52	889
Spring	Oct–Dec		14.2	21.2	7.4	262	273	1.39	1556
Second summer	Jan–Mar	2019	18.8	29.0	10.2	53	345	2.50	1396

Source: The author (2021).

FIGURE 6 – AIR TEMPERATURE (a) <sup>1</sup>, PRECIPITATION AND POTENTIAL EVAPOTRANSPIRATION (b) <sup>2</sup>, VAPOR PRESSURE DEFICIT (c) <sup>1</sup>, AND PHOTOSYNTHETIC ACTIVE RADIATION (d) DURING OCTOBER 2017 AND APRIL 2019.



Source: The author (2021).

<sup>1</sup> Minimum temperature and VPD are represented by open blue circles, mean temperature and VPD by closed black circles, and maximum temperature and VPD by open red circles.

<sup>2</sup> Blue bars represent cumulative monthly precipitation and red bars cumulative monthly potential evapotranspiration.

### 3.3.2 Genotype and seasonal effects on growth and growth efficiency

All growth variables showed effects of season and genotype (TABLE 3); however, significant interactions for genotype × season were observed only for CSI. The differences CSI among genotypes at the end of the 1.5-year survey were very large and highly significant in the last season (second summer). In the second summer, CSI ranged from 1766 to 3642 cm<sup>3</sup> m<sup>-2</sup> season<sup>-1</sup> and we observed that all genotypes presented a large growth increment between the spring and second summer.

TABLE 3 – ANALYSIS OF VARIANCE TESTING SEASON, GENOTYPE, AND GENOTYPE × SEASON INTERACTION EFFECTS FOR GROUND LINE DIAMETER (*rcd*), TOTAL HEIGHT (*h*), INDIVIDUAL VOLUME (*vi*), HECTARE VOLUME (*V*), CURRENT SEASONAL INCREMENT (*CSI*), LEAF AREA INDEX (*LAI<sub>c</sub>*).

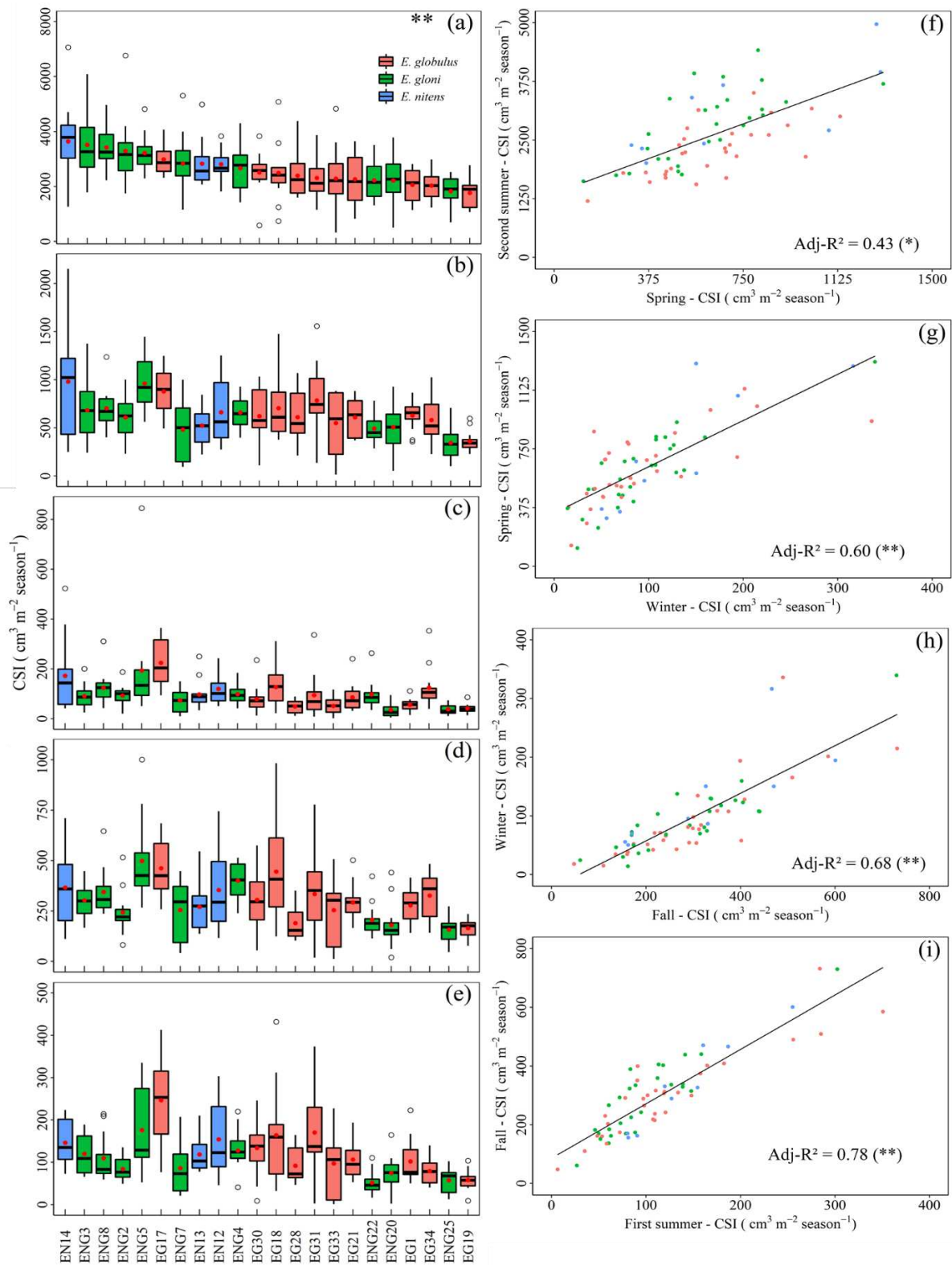
Effects	<i>rcd</i>	<i>h</i>	<i>vi</i>	<i>V</i>	<i>CSI</i>	<i>LAI<sub>c</sub></i>
Season	< 0.001	< 0.001	< 0.001	< 0.001	< 0.001	< 0.001
Genotype	< 0.001	< 0.001	< 0.001	< 0.001	< 0.001	< 0.001
Genotype × Season	0.9999	0.9921	0.0862	0.1168	0.0021	0.9258

Source: The author (2021).

According to Tukey-Kramer adjustment in ANOVA, we observed two genotype groups which showed significantly different *CSI* values ( $p < 0.05$ ) in the second summer (S5): high productivity ( $3172 \pm 318 \text{ cm}^3 \text{ m}^{-2} \text{ season}^{-1}$  – EN14, ENG3, ENG8, ENG2, ENG5, EG17, ENG7, EN13, EN12) and low productivity ( $2235 \pm 262 \text{ cm}^3 \text{ m}^{-2} \text{ season}^{-1}$  – ENG4, EG30, EG18, EG28, EG33, EG21, ENG22, ENG20, EG31, EG1, EG34, ENG25, EG19).

Genotype ranking changed through the study period. Some genotypes (e.g., EG18 or EG31) started with strong growth for the first three seasons, but then slowed down, while others (e.g., EN14 and ENG3) improved growth over time (FIGURE 7). In general, *E. globulus* genotypes presented the lowest growth rate at the end of the 1.5-year period compared to *E. nitens* and *E. gloni* genotypes. As a rule, we observed a similar growth pattern in each season, e.g., in winter the growth rate of all genotypes decreased and improved again in spring.

FIGURE 7 – CURRENT SEASONAL INCREMENT (CSI) FOR EACH GENOTYPE IN SECOND SUMMER (a), SPRING (b), WINTER (c), FALL (d), AND FIRST SUMMER (e), AND THE RELATIONSHIP BETWEEN CURRENT CSI WITH CSI IN PREVIOUS SEASON (f, g, h, AND i).<sup>1</sup>



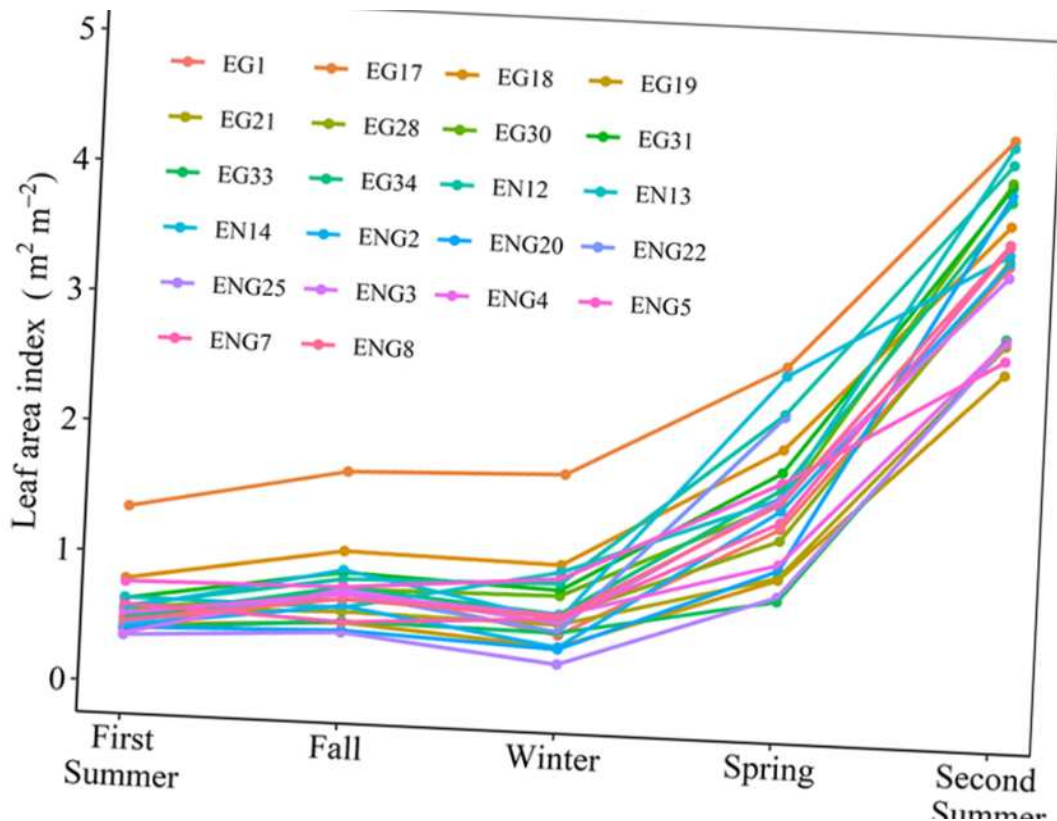
Source: The author (2021).

<sup>1</sup>Mean value is the red point and box plots rankings are based on volume growth at second summer. asterisks indicate significance (\*\* p < 0.001, \*p < 0.05, " " = not significant).

The relationship between a particular season CSI with the previous season CSI values decreased over time. Genotypes with the highest CSI in the first summer also presented higher CSI in the fall, and the highest CSI values observed in fall also presented higher CSI in winter. However, genotypes that presented  $200 \text{ cm}^3 \text{ m}^{-2} \text{ season}^{-1}$  in winter reached a large range of CSI in spring ( $500$  to  $1500 \text{ cm}^3 \text{ m}^{-2} \text{ season}^{-1}$ ), the same was observed for CSI in spring and second summer, where a large range of second summer CSI ( $1500$  to  $4000 \text{ cm}^3 \text{ m}^{-2} \text{ season}^{-1}$ ) occurred for the same CSI in spring ( $500 \text{ cm}^3 \text{ m}^{-2} \text{ season}^{-1}$ ). These results suggest that as trees get older, they responded differently to environmental constraints (season) even in a short early development period (1.5 years).

The average  $\text{LAI}_c$  showed little change during the first summer ( $0.56 \text{ m}^2 \text{ m}^{-2}$ ), fall ( $0.76 \text{ m}^2 \text{ m}^{-2}$ ), and winter ( $0.70 \text{ m}^2 \text{ m}^{-2}$ ). Across all genotypes,  $\text{LAI}_c$  increased after winter and reached the highest values during the second summer ( $3.64 \text{ m}^2 \text{ m}^{-2}$ ). It was also observed that seasonal changes in  $\text{LAI}_c$  followed seasonal changes in growth during early development (FIGURE 8), especially after winter.

FIGURE 8 – SEASONAL AND GENOTYPE VARIATION OF LEAF AREA INDEX ( $\text{LAI}_c$ ).



Source: The author (2021).

Comparisons of the full versus the reduced linear models between CSI and  $LAI_c$  showed that season effects were significant ( $F = 515.1$ ,  $p < 0.0001$ ) (TABLE 4). Interestingly, there were no differences in models tested for first summer and for winter ( $F=0.78$ ,  $p=0.4383$ ). In fact, similar growth rates among genotypes were observed for these first summer and for winter. The slope of the linear models represents the relationship between CSI and  $LAI_c$ , in other words, the GE. For the first summer, fall, winter and spring, all genotypes followed a single line (TABLE 4; FIGURE 9).

Lower GE was observed in the first summer and winter with a growth rate of  $112.5 \text{ cm}^3 \text{ m}^{-2}_{\text{leaf}}$ . A significant improvement in GE ( $267.9 \text{ cm}^3 \text{ m}^{-2}_{\text{leaf}}$ ) was observed in fall, since we found an increase in growth with small changes in  $LAI_c$ . A similar increment in GE ( $211.9 \text{ cm}^3 \text{ m}^{-2}_{\text{leaf}}$ ) was observed in spring. A single regression for the second summer did not show any significant relationship between CSI and  $LAI_c$  (Adj- $R^2=0.10$ ,  $p=0.02$ ) unlike other seasons. Therefore, we adjusted linear models considering ANOVA genotype groups (high productivity and low productivity).

TABLE 4 – LINEAR MODELS ADJUSTED FOR THE  $LAI_c$  AND CSI (GROWTH EFFICIENCY) RELATIONSHIP FOR SEASONS AND GENOTYPES GROUPS THAT SHOWED SIGNIFICANT DIFFERENCES.<sup>1</sup>

Groups		$\hat{\beta}_0$	$\hat{\beta}_1$	Adj – $R^2$	RMSE
First summer and Winter		35.72 **	112.5 **	0.51	48.26
Fall		95.43 **	267.9 **	0.61	87.92
Spring		291.9 **	211.9 **	0.59	167.3
Second summer – High productivity	EN14, ENG2, ENG3, ENG7, ENG8	258.5 ns	865.8 *	0.51	630.3
	ENG5, EG17, EN12, EN13	2703 **	64.95 ns	0.04	485.2
Second summer – Low productivity	ENG4, EG30, EG33, EG21	1224 *	365.9 *	0.27	550.6
	EG1, EG18, EG19, EG31, EG34, ENG20, ENG22, ENG25	1670 **	121.9 ns	0.10	419.7

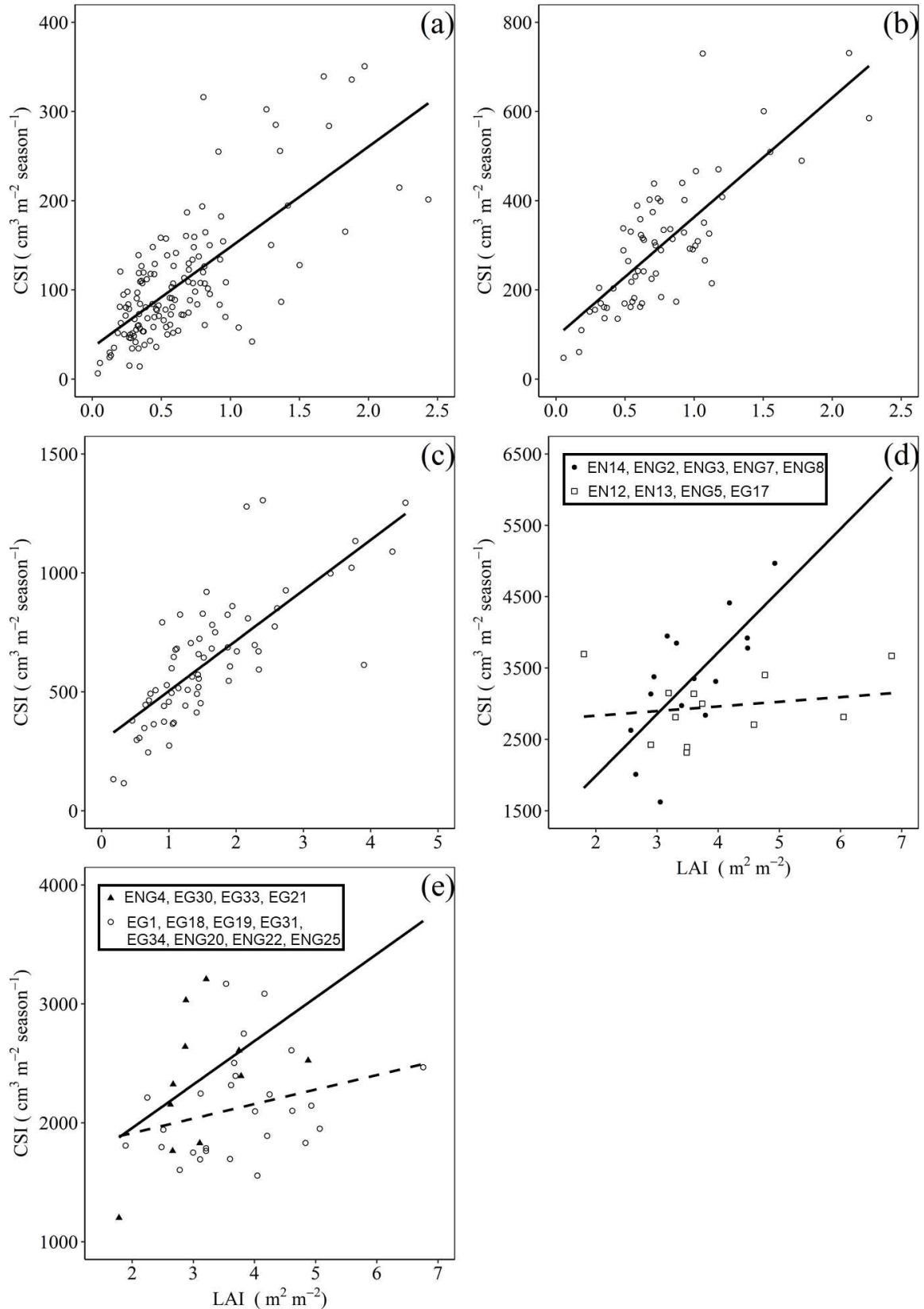
Source: The author (2021).

<sup>1</sup> Linear models are represented by the expression  $CSI = \hat{\beta}_0 + \hat{\beta}_1 \cdot LAI_c$  and goodness of fit of models was evaluated by coefficient significance (ns = not significance, \* =  $p < 0.05$ , and \*\* =  $p < 0.001$ ), adjust coefficient of determination (Adj- $R^2$ ), and root mean square error (RMSE).

For high productivity genotypes, a first group (EN14, ENG2, ENG3, ENG7, and ENG8) presented the highest GE values ( $865.8 \text{ cm}^3 \text{ m}^{-2}_{\text{leaf}}$ ). A second group (ENG5, EG17, EN12, and EN13) that showed high LAI values did not show proportional increases in growth and growth rate could be considered as a single line ( $2703 \text{ cm}^3 \text{ m}^{-2}_{\text{leaf}}$ ) for all observed LAI values. For low productivity genotypes, we also observed a

third group (ENG4, EG30, EG33, and EG21) which increased their growth with  $LAI_c$  ( $365.9 \text{ cm}^3 \text{ m}^{-2}_{\text{leaf}}$ ), although this response was not as strong as in the high productivity group ( $Adj - R^2 = 0.27$ ). Also, a fourth low productivity group (EG1, EG18, EG19, EG31, EG34, ENG20, ENG22, and ENG25) also did not present a significative relationship between growth and LAI (FIGURE 9).

FIGURE 9 – LINEAR MODELS ADJUSTED FOR THE LEAF AREA INDEX ( $LAI_c$ ) AND CURRENT SEASONAL INCREMENT (CSI) RELATIONSHIP FOR FIRST SUMMER AND WINTER (a), FALL (b), SPRING (c), HIGH PRODUCTIVITY GENOTYPES IN SECOND SUMMER (d), AND LOW PRODUCTIVITY GENOTYPES IN SECOND SUMMER (e).

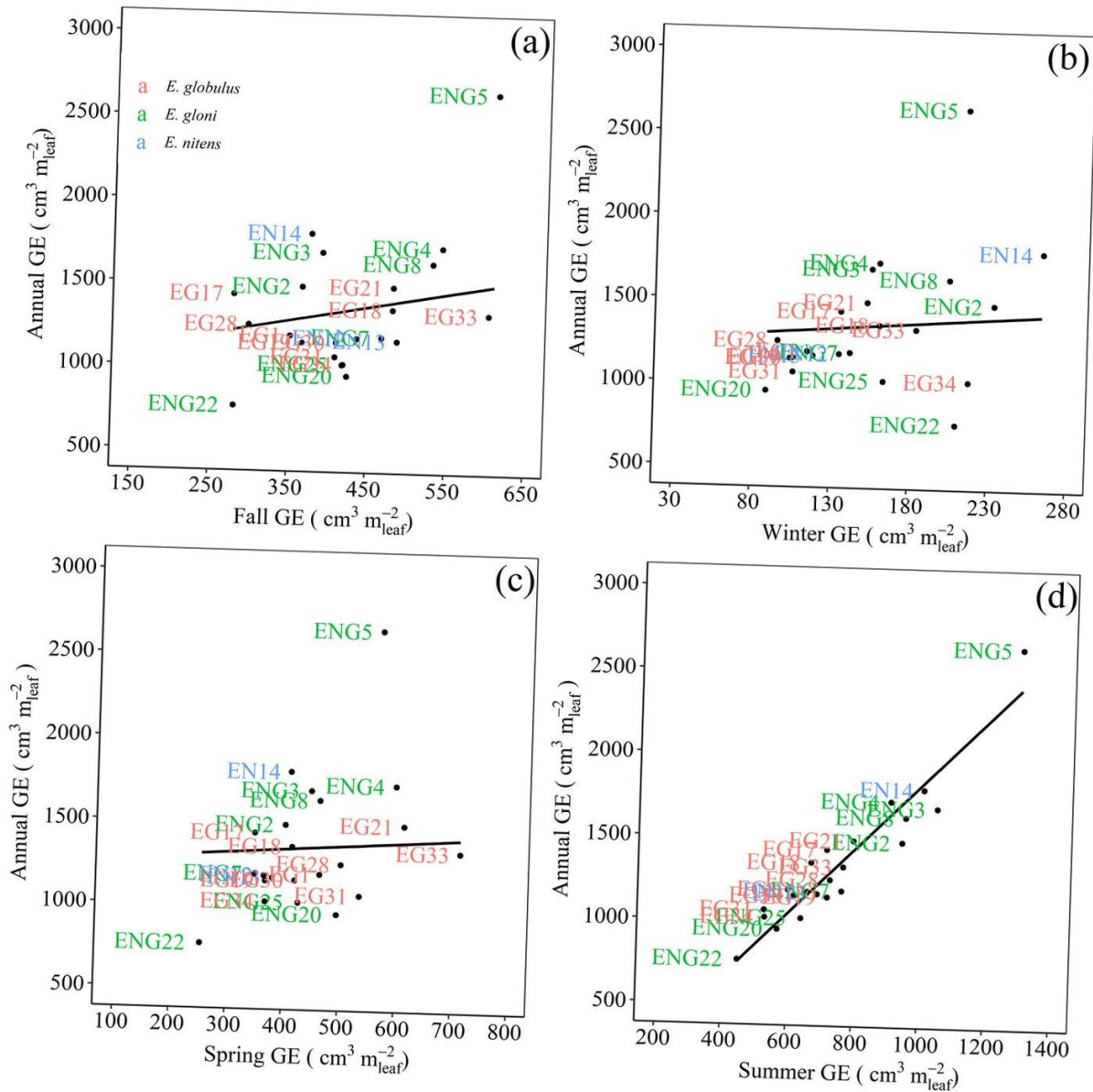


Source: The author (2021).



When we compared seasonal GE with annual GE, we observed that the second summer GE was the only season significantly related to annual GE ( $F = 436.53$ ,  $p < 0.001$ ,  $\text{Adj} - R^2 = 0.87$ ), while fall ( $F=3.11$ ,  $p=0.08$ ,  $\text{Adj} - R^2 = 0.05$ ), winter ( $F=0.56$ ,  $p=0.46$ ,  $\text{Adj} - R^2 = 0.01$ ), and spring ( $F=0.63$ ,  $p=0.63$ ,  $\text{Adj} - R^2 = 0.01$ ) were not significant (FIGURE 10). The main reason for this were the differences in growth rates among genotypes through the seasons. Genotypes that presented higher annual growth were the ones that grew more during the second summer. However, we observed that a single *E. gloni* genotype (ENG5) had the highest annual GE and it was able to maintain higher seasonal GE over time, showing a strong regulation in growth without changes leaf area values. We did not use data from the first summer GE in seasonal and annual GE analysis, because that season was similar to winter GE.

FIGURE 10 – ANNUAL GROWTH EFFICIENCY AND SEASONAL GROWTH EFFICIENCY RELATIONSHIP AMONG EUCALYPTUS GENOTYPES DURING FALL (a), WINTER (b), SPRING (c), AND SECOND SUMMER (d).



Source: The author (2021).

### 3.4 DISCUSSION

This study evaluated the early growth, LAI<sub>c</sub> and GE responses of *Eucalyptus* genotypes across different seasons during their 1.5-year of development. To date, few studies have investigated the performance of genotypes during early growth under different seasonal conditions in the same environment. We observed that the increment in growth across seasons improved early GE, even with greater changes in

LAI. Higher productivity was observed mainly for *E. nitens* and *E. gloni* genotypes, possibly because *E. nitens* and some of its hybrids were capable of using the available resource (soil water and temperature) efficiently during early development and properly partition the photosynthetic compounds for wood production, even with the lack of *E. nitens* ability to acclimate under warmer temperatures (spring and summer) (Battaglia et al., 1998).

The reduction of CSI in winter resulted in a decrease in GE during the same period for all genotypes, even with small changes in LAI<sub>c</sub>, when compared to the previous seasons (first summer and fall). According to Whitehead and Beadle (2004), the dominant factor causing a reduction in growth during winter is lower available radiation, especially at higher latitudes, and we also observed lower PAR values in that season. As radiation is an essential resource for photosynthesis, its low availability results in decreased plant metabolism, affecting growth (Whitehead and Beadle, 2004). In addition, lower winter temperatures (sometimes below 0 °C in our study) are known to affect forest productivity (McMurtrie et al., 1994; Watt et al., 2014). Differences in *Eucalyptus* growth along the plantations get older showed constating strategies of resource acquisition dynamics and allocation among genotypes (le Maire et al., 2019). This was confirmed by the decrease in season CSI relationships along the survey, where genotypes with maximum growth in second summer were not the same during the previous season.

Several studies have shown that volume increment is strongly dependent on leaf area and its variation during tree growth (Stape et al., 2004; Binkey et al., 2017; Rubilar et al., 2020). Although the relationship between LAI<sub>c</sub> and growth in *Eucalyptus* has been evaluated (Smethurst et al., 2003; Whitehead and Beadle, 2004), few studies have investigated how this relationship changes, especially during the early development of *Eucalyptus*. Such information will facilitate improved genotype selection and the achievement of better genetic gain in eucalyptus breeding programs since the peak stress in *Eucalyptus* stands occur after complete crown closure what occurs earlier in high density stands allowing that stress effect be visualized earlier between genotypes (Luo et al., 2010). In our season with the maximum growth rate (second summer), we did not observe a stronger relationship between growth and LAI<sub>c</sub>. This response may suggest a different efficiency behavior in some genotypes, which achieved a higher growth rate without an increase in leaf area, this makes them more efficient in wood volume production and possible changes in early growth efficiency

was related to changes in genotype growth rates since there was a non-significant interaction for  $LAI_c$ .

We observed a 128% increase in average  $LAI_c$  values between the spring and the second summer and a 313% increment in CSI values during the same seasons. This low LAI-CSI correlation in the second summer could be linked to higher atmospheric demand in the summer months (i.e., VPD), potentially leading to increased water deficits and resulting in the partitioning of carbon assimilates to other plant organs, such as roots, which would reduce the relative stem growth in some *Eucalyptus* genotypes (Ryan et al., 2010). Another possible explanation is that canopy closure, as reflected by an increment in  $LAI_c$  between spring and second summer, increased intraspecific competition between genotypes which affected stem biomass increment (Gonçalves et al., 2013; Tomé et al., 1994), consequently changing the GE response. This explanation is supported by the non-strong relationship observed between leaf area and growth in the second summer compared to other seasons.

One group of high productivity genotypes in the second summer did respond with a larger increment in growth with leaf area increment, compared with the other high productivity group which presented an average growth values regardless of  $LAI_c$ . Although leaf area is very important for *Eucalyptus* growth, it is not the only parameter which affects growth (Wang et al. 2019), and sometimes genotypes with lower  $LAI_c$  can present higher photosynthetic rates (Mu et al., 2010). Changes in GE across the seasons were more strongly related to CSI than to  $LAI_c$ . Consequently, the second summer, which had the highest CSI of all seasons during early development, also showed higher GE (300 to 2000  $\text{cm}^3 \text{m}^{-2}_{\text{leaf}}$ ). This accounted for our observation of significant differences in GE only in the second summer, because during this season we observed a greater range in CSI between genotypes (1200 to 4900  $\text{cm}^3 \text{m}^{-2} \text{season}^{-1}$ ).

Different seasonal GE compared to annual GE resulted from changes in genotype growth increments through the seasons. Our findings showed that eucalyptus genotypes with higher GE at the end of early development did not presented higher seasonal GE, excepted in the second summer. This supports the suggestion that the season with maximum growth should be used for the selection of genotypes with higher annual GE and allowing forest managers to make decisions about the productivity of *Eucalyptus* plantations (Silva et al., 2016).

*Eucalyptus globulus* genotypes showed the highest GE in the first summer; however, we observed a decrease in the GE of these genotypes in subsequent seasons. This was most likely related to a reduction in relative growth compared to the maximum possible growth during each season, and may indicate that most *E. globulus* genotypes did not exhibit their full growth potential at this site. The GE results of this study suggest that *E. globulus* genotypes may be highly sensitive to environmental differences during early development because they largely changed growth and GE across the seasons, compare to *E. nitens* and *E. gloni* (Rubilar et al., 2020; White et al., 1996; White et al., 2009).

Since environmental differences (seasons) affect early growth and leaf area in eucalypts, a lower GE could indicate poor species and/or genotype adaptation to the experimental location. Our results showed that the growth ranking of genotypes was not stable among seasons, which implies an interaction between genotypes × season (environment). Furthermore, we observed that leaf area affected growth for the first year of development, after which there was a genotype interaction in the growth / leaf area relationship (GE). However, physiological comparisons among *Eucalyptus* genotypes in controlled studies are needed to ensure a deeper understanding of genotype differences and possible strategies under drought and heat risks throughout their development.

### 3.5 CONCLUSIONS

Seasons and genetic interaction presented a large effect on early growth relationships among *Eucalyptus* genotypes, however non-significant changes in leaf area index. Changes in seasonal and annual growth efficiency performance, suggest that the same environment drive a large response in genotypes early growth, as consequence of climate influences in carbon allocation in *Eucalyptus* plantations. This information should be taken in consideration for specific genotypes plantation in each site, allowing them to achieve their full growth potential.

## 4 CHAPTER 2 - PHYSIOLOGICAL RESPONSES AND GROWTH OF *EUCALYPTUS* GENOTYPES UNDER CUMULATIVE PLANT WATER STRESS

### ABSTRACT

Understanding how changes in soil water availability affects *Eucalyptus* physiology and growth is critical under the current climate change scenario. However, reduced information exist on how even small changes in soil water may affect physiological responses of *Eucalyptus* genotypes and their relationship with early productivity. Our experiment evaluated changes in physiological traits during a short period of decreased soil water availability and compared growth and cumulative water stress of 1.5-year-old 22 Mediterranean eucalyptus genotypes established at high initial planting density (6666 trees ha<sup>-1</sup>). The experiment was established over a coarse sandy soil with low water holding capacity in central South Chile under high summer vapor pressure deficits (VPD). Selected genotypes considered 10 *Eucalyptus globulus*, 3 *E. nitens* and 9 *E. nitens* x *E. globulus* hybrids. Seasonal predawn leaf water potential ( $\Psi_{pd}$ ) was evaluated at 114, 224, 281, 379, and 475 days after planting under well irrigated conditions. Afterwards and until 510 days after planting (40 days without irrigation) two sampling instances were considered: a first sampling instance at the end of well irrigated conditions  $M_0$  (475 days after planting) and second instance after 40 days without irrigation  $M_{final}$  (508 days after planting). During that period, we measured midday water potential ( $\Psi_{md}$ ), diurnal changes in net photosynthesis ( $A_n$ ), stomatal conductance ( $g_s$ ) and leaf area index (LAI). Using ANOVA and linear regression, we evaluated genotype differential responses at each sampling instance. Results indicated a broad range of water stress integral (WSI) values among genotypes showing contrasting levels of accumulated water stress during the early development. Interestingly, *E. globulus* presented 30% more water stress than *E. nitens*, and genotypes with the highest WSI showed the lowest volume growth during decreased soil water. In general, there was a reduction in  $A_n$  and  $g_s$  for genotypes in the morning and midday between  $M_0$  and  $M_{final}$ , but small changes in mid-afternoon values. Average values of intrinsic water use efficiency (iWUE) increased between  $M_0$  and  $M_{final}$ . Midday water potential presented small changes, however there was a large increment in LAI for almost all genotypes. We observed that there was no relationship between growth and WSI with  $A_n$ , while changes in iWUE were more pronounced for genotypes with lower WSI, which suggested that genotypes showing high changes of iWUE they were more sensible to changes in soil water, such as ENG2, ENG5 and EN14. Our results suggest that *E. gloni* genotypes were more sensible to small changes in soil water availability, allowing them to maintain average high productivity. Observed response patterns of genotypes physiology may allow for advanced in understanding possible drought risk for eucalyptus genotypes.

Key-words: Water stress integral, photosynthesis, intrinsic water use efficiency, forest growth, water potential.

## 4.1 INTRODUCTION

*Eucalyptus* species dominate ecosystems across Australia and nearby islands and many species have been introduced in other countries for forest production, occupying a broad range of environmental conditions (Whitehead and Beadle, 2004; Binkley et al., 2017). However, climate change scenarios predict increasing droughts duration and intensity in tropical and subtropical areas (IPCC, 2014). Lower water availability in regions with a Mediterranean climate that include severe summer droughts may affect severely *eucalyptus* growth, survival, and physiology under limiting water stress conditions and understanding the genetic response of improved materials is required (Hérault et al., 2013; Correia et al., 2014; Rubilar et al., 2020).

Water availability is one of the principal factors controlling the productivity of ecosystems and drought is the most critical threat for agriculture and tree mortality (Stape et al., 2010; Allen et al., 2010; Lévesque et al., 2013; Allen et al., 2015). The severity and temporal scale of water deficits affect tree physiology and growth. Identifying water deficit responses is critical for early detection of tree mortality and productivity, and these response patterns may determine the tolerance of tree species to lower water availability (Waring and Landsberg, 2011; Vicente-Serrano et al., 2013; Hérault et al., 2013). Breeding of trees that are tolerant to water deficits may be a promising approach, but it requires knowledge of plant genetics and physiological mechanisms during plant development (Landsberg and Waring, 2017).

Water deficits have short and long terms effects on plants. Short terms are linked with physiological responses and long terms with morphological and growth responses. Thus, the relationship between plant water status (e.g., leaf water potential) and forest yield was necessary to integrate effects of water status over of plant development, called water stress integral (WSI) (Myers, 1988). The water stress integral consists of the summation of plant water potential at defined intervals over the measurement periods. A larger absolute values of water stress integral represented larger amounts of accumulated water stress and causes a reduction in forest growth. The ability of plants to develop and succeed under expect limited soil water conditions is the manifestation of one or more adaptative changes at all these different levels (Chaves et al., 2003).

Water deficits limit cell division and elongation because of the reduction in turgor pressure (Taiz et al., 2017). Short-term responses to avoid water stress include

the maintenance of higher water potentials, reduction of carbon assimilation, stomatal closure, root signal recognition (Chaves et al., 2003; Silva et al., 2016; Silva et al., 2017), and reduction of leaf area by shedding or diminishing leaf sizes (Gauthier and Jacobs, 2018). Leaf water potential, stomatal conductance, and transpiration are key important factors that influence the plant water status (Farooq et al., 2009; Martorell et al., 2014). Higher water-use efficiency is usually linked with stomatal closure to reduce transpiration when the soil dries, but it is also sometimes positively correlated with productivity (Saravanan, 2018). Water use efficiency has been identified as a key parameter for evaluating *Eucalyptus* adaptation to water deficits and shows a wide variation among *Eucalyptus* species and genotypes (Navarrete-Campos et al., 2013). However, stomatal closure limits CO<sub>2</sub> uptake by leaves reducing photosynthetic rates (Myers and Landsberg, 1989; Santos et al., 2019; Saravanan, 2018), which in turn reduces productivity.

Stomata respond to chemical signals while the leaf water potential is kept constant and a negative carbon balance can occur as a result of the reduction in photosynthesis; these responses tend to increase during periods of water stress (Kolb and Stone, 2000). However, some *Eucalyptus* genotypes show different responses accumulated water stress (White et al., 2000; Silva et al., 2017). Plants with higher osmotic adjustment are capable of tolerating drought periods by allowing the cell to maintain turgor (Chaves et al., 2003), and this is very common among *Eucalyptus* species (Merchant et al., 2007). According to Merchant et al. (2007), *Eucalyptus* show a clear coordination of physiological and structural adaptations to soil water availability.

Many physiological studies have been performed in greenhouses to avoid the complication of access to different water sources in the field; however, the behavior of greenhouse plants does not necessarily reflect how trees behave in the field (Szota et al., 2011; Adams et al., 2017). The study aimed to analyze the relationship between growth and water stress integral on changes in photosynthesis, intrinsic water use efficiency, midday water potential and leaf area index of different eucalyptus genotypes under a short period of decreased soil water. We tested the hypothesis that *Eucalyptus* genotypes subjected to higher accumulated water stress integral would show lower growth during changes in soil water, resulting in higher decrease on net photosynthesis, intrinsic water use efficiency, midday water potential and leaf area index.



## 4.2 MATERIALS AND METHODS

### 4.2.1 Growth

In February 2019 and March 2019, individual tree height ( $h$ ), and root collar diameter at 0.1 m height ( $rdc$ ) were measured on four central plants in each measurement plot ( $6 \text{ m}^2$ ). According to Eq. (4.1) individual tree volume index ( $vi$ ) was determined from these measurements:

$$vi = 0.33\pi \cdot \frac{rdc^2}{4} \cdot h \quad (4.1)$$

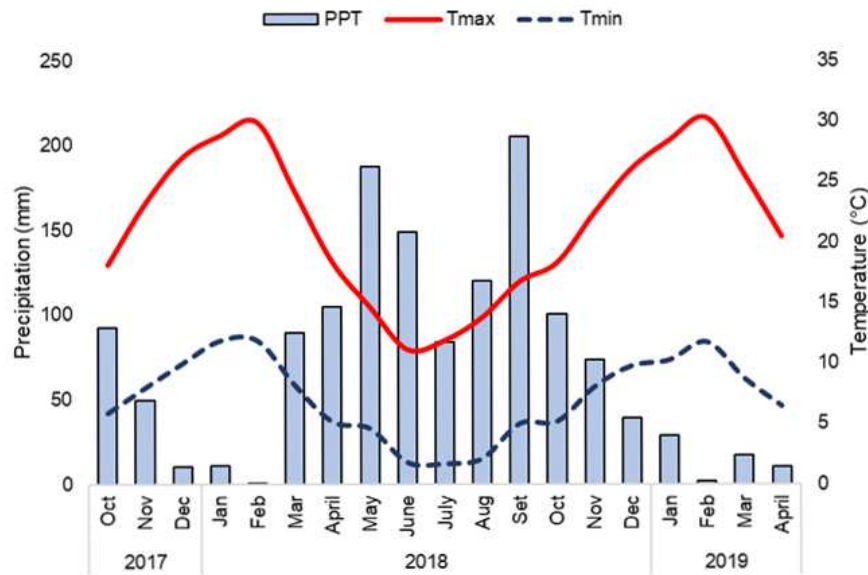
where,  $vi$  is the individual tree volume ( $\text{cm}^3$ ),  $rdc$  is the root collar diameter measured at 0.1-m height (cm), and  $h$  is the total tree height (cm).

The form factor value (0.33) was according to others studies with similar genotypes on the same location (Rubilar et al., 2020; Watt et al., 2014). Volume was scaled up to square meter ( $V$ ;  $\text{cm}^3 \text{ m}^{-2}$ ) by summing  $vi$  in measurement plots and divided by measurement plot area ( $6 \text{ m}^2$ ). Volume increment ( $IncVol$ ) was determined as the difference between  $V$  in March 2019 and  $V$  in February 2019.

### 4.2.2 Seasonal measurements of predawn leaf water potential

Predawn leaf water potential ( $\Psi_{pd}$ ) was measured at different times during the early growth with a Scholander pressure chamber (PMS Instruments, Corvallis, OR USA). Measurements were made in mature, fully expanded, and sun-exposed leaves of the upper canopy between 4:30 to 7:00 h. Seasonal measurements considered first mid-summer 2018 (February 22), early winter 2018 (June 12), mid-winter 2018 (August 8), mid-spring 2018 (November 14), second mid-summer 2019 (February 19), and early fall (March 27). These dates coincided with different periods of precipitation (PPT), evapotranspiration (ET), temperature (T), and vapor pressure deficit (VPD) at the experiment site (FIGURE 11).

FIGURE 11 –RAINFALL (PPT) and TEMPERATURE (T), DURING THE FIRST 1.5 YEAR OF STUDY DEVELOPMENT.



Source: The author (2021).

Following Myers (1988), we calculated the cumulative water stress integral (WSI) which integrating effects of plant water status over time considering the cumulative integral of  $\Psi_{pd}$  (Mitchell et al, 1999; Galindo et al., 2017) over the entire period of growth (Eq. 4.2).

$$WSI = \sum_{i=0}^t (\bar{\Psi}_{i,i+1} - c) \cdot n \quad (4.2)$$

where, WSI is the cumulative water stress integral ( $\text{MPa day}^{-1}$ ),  $\bar{\Psi}_{i,i+1}$  is the mean of predawn leaf water potential for interval  $i, i + 1$  (MPa),  $c$  is the maximum or less negative value of predawn leaf water potential during the measurements (MPa), and  $n$  is the number of days at interval  $i, i + 1$ .

#### 4.2.3 Volumetric soil water content ( $\theta$ ) and sampling instances

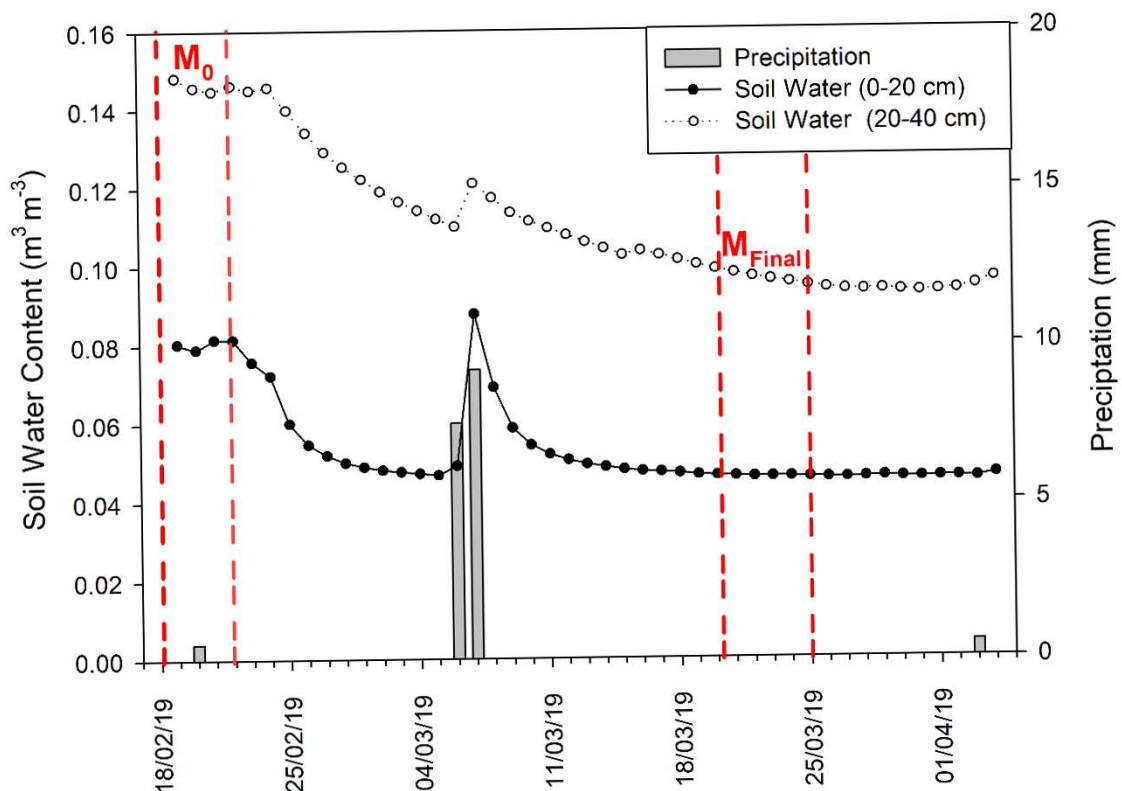
Monitoring of volumetric soil water content ( $\theta$ ) was carried out by installing three soil moisture sensors (CS655, Campbell Scientific) at two depths (i.e. 0-20 cm and 20-40 cm) in each block. Sensors were inserted to monitor water content at 5 min-intervals from February 19 until April 4 in 2019 (45 days). Sensors were connected to a CR1000 datalogger (Campbell Scientific) to record  $\theta_V$  data. From  $\theta$  measurements,

two sampling instances were determined and used to analyze genotype response differences in physiological behavior during this period of decreased soil water availability (FIGURE 12).  $M_0$  represented the final point under irrigation and the starting point under no irrigation, and  $M_{final}$  represented the final period after nearly 40 days without irrigation before increment the numbers of daily precipitation. During this period, it rained approximately 20 mm between March 6 and March 7. The final difference in  $\theta$  from  $M_0$  to  $M_{final}$  was approximately 40% for each soil depth.

1)  $M_0$  – initial measurement instance – February 18 to February 22, 2019 ( $\theta_{0-20cm} = 0.081 \text{ m}^3 \cdot \text{m}^{-3} \pm 0.02$  and  $\theta_{20-40cm} = 0.146 \text{ m}^3 \cdot \text{m}^{-3} \pm 0.03$ );

2)  $M_{final}$  – final measurement instance – March 21 to March 25, 2019 ( $\theta_{0-20cm} = 0.046 \text{ m}^3 \cdot \text{m}^{-3} \pm 0.01$  and  $\theta_{20-40cm} = 0.095 \text{ m}^3 \cdot \text{m}^{-3} \pm 0.02$ ).

FIGURE 12 –CHANGES IN VOLUMETRIC SOIL WATER CONTENT ( $\text{m}^3 \text{ m}^{-3}$ ) AND RAINFALL (mm) BETWEEN  $M_0$  and  $M_{final}$ <sup>1</sup>.



Source: The author (2021).

<sup>1</sup> Red dash lines represented the measurements intervals for  $M_0$  and  $M_{final}$ .

#### 4.2.4 Leaf gas-exchange

Leaf gas exchange measurements occurred every two days during  $M_0$  and  $M_{\text{final}}$  sampling instances and considered net  $\text{CO}_2$  assimilation rate ( $A_n$ ;  $\mu\text{mol CO}_2 \text{ m}^{-2} \text{ s}^{-1}$ ), stomatal conductance ( $g_s$ ;  $\text{mol H}_2\text{O m}^{-2} \text{ s}^{-1}$ ), transpiration ( $T_r$ ;  $\text{mmol H}_2\text{O m}^{-2} \text{ s}^{-1}$ ), and intercellular  $\text{CO}_2$  ( $C_i$ ;  $\mu\text{mol CO}_2 \text{ mol air}^{-1}$ ). Measurements were made in one plant of each genotype for each plot (block) assessing mature, fully expanded and sun-exposed leaves at 10:00h and 11:00h, 12:30h and 13:30h and 14:30h and 15:30h, using a portable infrared gas analyzer LICOR-6400 (Li-Cor, Inc., Lincoln, NE, USA). All measurements were made setting reference  $\text{CO}_2$  at  $400 \mu\text{mol.mol}^{-1}$ , light intensity (PAR) in the leaf chamber at  $1500 \mu\text{mol m}^{-2} \text{ s}^{-1}$ , a constant flow rate of  $500 \mu\text{mol s}^{-1}$  and leaf temperature ( $T_{\text{leaf}}$ ) as close possible to ambient air temperature ( $T$ ) on each measurement instance. Intrinsic water use efficiency ( $i\text{WUE}$ ;  $\mu\text{mol CO}_2 \text{ mol}^{-1} \text{ H}_2\text{O}$ ) was calculated by the ratio of  $A_n$  and  $g_s$ .

#### 4.2.5 Midday water potential ( $\Psi_{\text{md}}$ )

Midday leaf water potential ( $\Psi_{\text{md}}$ ) was measured with a Scholander pressure chamber (PMS Instruments, Corvallis, OR USA). Measurements were made in mature, fully expanded, and sun-exposed leaves of the upper canopy between 11:30 to 14:00, and occurred every two days between in  $M_0$  and  $M_{\text{final}}$  sampling instances.

#### 4.2.6 Leaf area index (LAI)

LAI was estimated for each plot in February 23 and March 25 2019 under clear-sky conditions. Estimates were obtained using midday (11:00h to 14:00h) photosynthetically active radiation (PAR) interception, by measuring below the canopy ( $n = 3$ ) PAR in the north and east orientation, and outside the experimental area ( $n = 1$ ) using a ceptometer (Li-191R & Li-250; LICOR Scientific, Lincoln, Nebraska, USA). For PAR below canopy measurements the sensor was placed in the center of the plot and among trees in the interrow. In order to estimate LAI from PAR measurements, we considered uniform leaf distribution parameter ( $\chi = 1$ ) for calculations of light extinction coefficient ( $K_c$ ) (Norman and Jarvis, 1975; Campbell, 1986):

$$K_c = \frac{\sqrt{\chi^2 + \tan(Z)^2}}{\chi + 1.744(\chi + 1.182)^{-0.733}} \quad (4.3)$$

where,  $Z$  is zenith angle in radians and  $\chi$  is leaf distribution parameter.

$$\text{LAI} = \frac{\left[ \left( 1 - \frac{1}{2K_c} \right) f_b - 1 \right] \ln(\tau)}{A(1 - 0.47f_b)} \quad (4.4)$$

where, LAI is tree leaf area index ( $\text{m}^2 \text{m}^{-2}$ ),  $K_c$  is tree extinction coefficient (Campbell, 1986),  $f_b$  is the light beam fraction, assumed to be 0.881,  $\ln(\tau)$  is the logarithmic of ratio of PAR below tree canopy and outside of experimental area, and  $A$  is canopy absorbance in PAR, assumed to be 0.86.

#### 4.2.7 Statistical analyses

The relationship between volume growth (IncVol) during soil water reduced availability (between  $M_0$  and  $M_{\text{final}}$ ) with cumulative WSI during early development was evaluated using linear regression using GLM procedure considering all taxa. We used the relationship between IncVol and WSI to check genotypes behavior for growth (high and low productivity) and for absolute WSI (high and low water stress).

Analyses of variance (ANOVA) were used to evaluate response differences among genotypes and interactions in  $A_n$ ,  $g_s$ ,  $Tr$ ,  $C_i$ ,  $\Psi_{\text{md}}$  and LAI between sampling instances ( $M_0$  and  $M_{\text{final}}$ ) considering morning, midday and afternoon assessment periods. Sampling instances, periods and genotypes were considered fixed effects and blocks were considered random effects. All ANOVA analyses were performed using the SAS PROC MIXED. Differences in  $A_n$ ,  $g_s$ ,  $Tr$ ,  $C_i$ ,  $\Psi_{\text{md}}$  and LAI were determined with the LSMEANS statement using the Tukey-Kramer adjustment ( $p < 0.05$ ). Graphical analyses were performed to evaluate changes in  $A_n$  throughout the day using the maximum values for each taxon (*E. globulus*, *E. nitens*, and *E. gloni*) and key genotypes considering the relationship between IncVol and WSI.

The percentage mean increases or reduction value ( $\Delta\%$ ) of each physiological variable and LAI between  $M_0$  and  $M_{\text{final}}$  was used to check genotype responses between measurement (Eq. 4.5). Linear regression and graphical analyses were used

to evaluate the relationship between An and iWUE with IncVol and also with WSI for all genotypes:

$$\Delta\% = \left( \frac{X_{M_{final}} - X_{M_0}}{X_{M_0}} \right) \cdot 100 \quad (4.5)$$

where,  $\Delta\%$  is the variation in physiological variables (%),  $X_{M_{final}}$  is the measurement value at  $M_{final}$  and  $X_{M_0}$  is the measurement value at  $M_0$ .

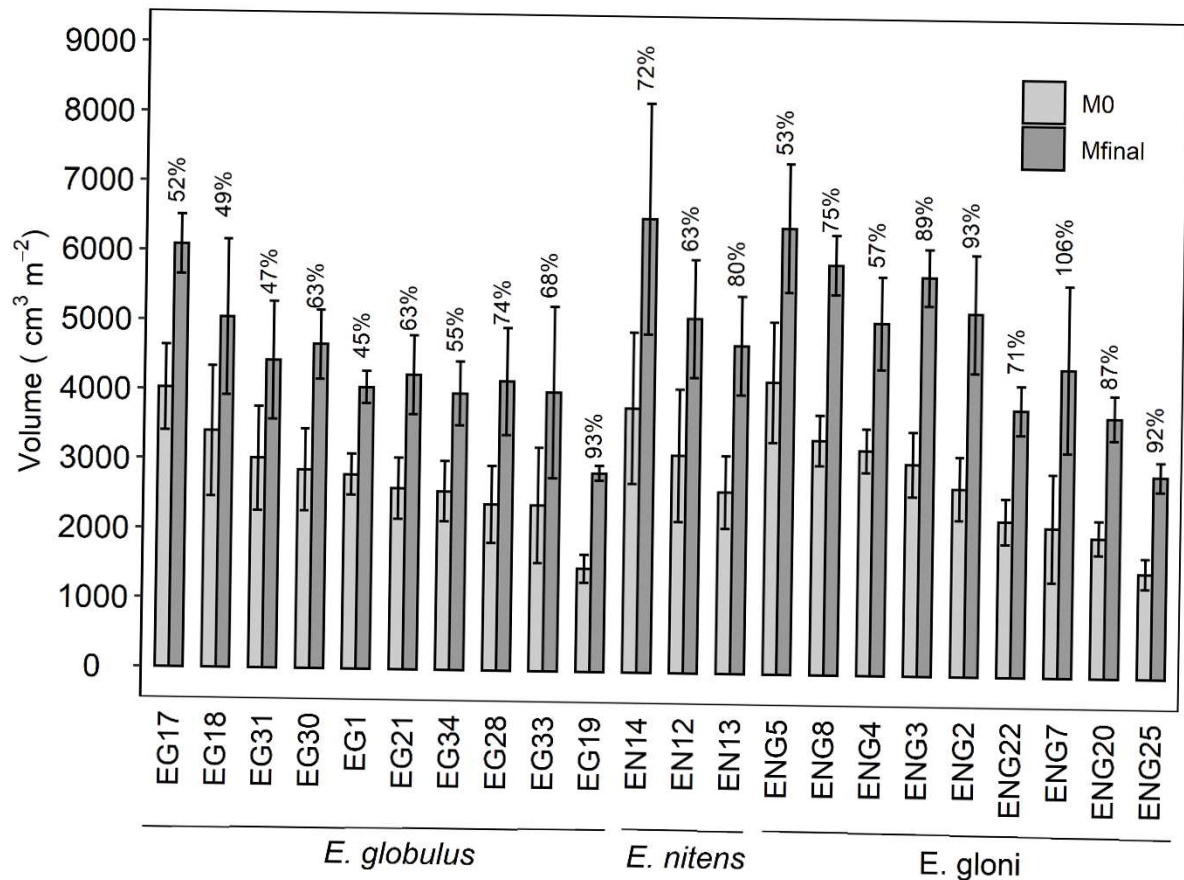
Variables were transformed as required to meet the assumptions of normality and homogeneity of variance using a Box-Cox transformation (Gaudry and Dagenais, 1979). All analyses were performed using SAS®Studio ([https://www.sas.com/en\\_us/software/studio.html](https://www.sas.com/en_us/software/studio.html)) and graphs were built using the package ggplot (Wickham, 2020) in R software (R Core Team, 2019).

## 4.3 RESULTS

### 4.3.1 Growth in a period of moderately decreased soil water ( $M_0$ and $M_{final}$ )

A larger IncVol was observed between  $M_0$  and  $M_{final}$ . Across all genotypes mean IncVol was  $1890 \pm 446 \text{ cm}^3 \text{ m}^{-2}$  in 40 days. At  $M_{final}$ , average V ranged from 2859 to  $6086 \text{ cm}^3 \text{ m}^{-2}$  for *E. globulus* with IncVol of  $1599 \text{ cm}^3 \text{ m}^{-2}$  in 40 days, while for *E. nitens* average V ranged from 4718 to  $6526 \text{ cm}^3 \text{ m}^{-2}$  with IncVol of  $2238 \text{ cm}^3 \text{ m}^{-2}$  in 40 days. For *E. gloni*, V ranged from 2900 to  $6418 \text{ cm}^3 \text{ m}^{-2}$  with an average increment, similar to *E. nitens*, of  $2086 \text{ cm}^3 \text{ m}^{-2}$  in 40 days. As similar percentage increments were obtained for all genotypes, the ranking in wood volume did not present great changes between  $M_0$  and  $M_{final}$  (FIGURE 13).

FIGURE 13 – CUMULATIVE VOLUME FOR ALL *EUCALYPTUS* GENOTYPES BETWEEN  $M_0$  and  $M_{final}$ <sup>1</sup>.



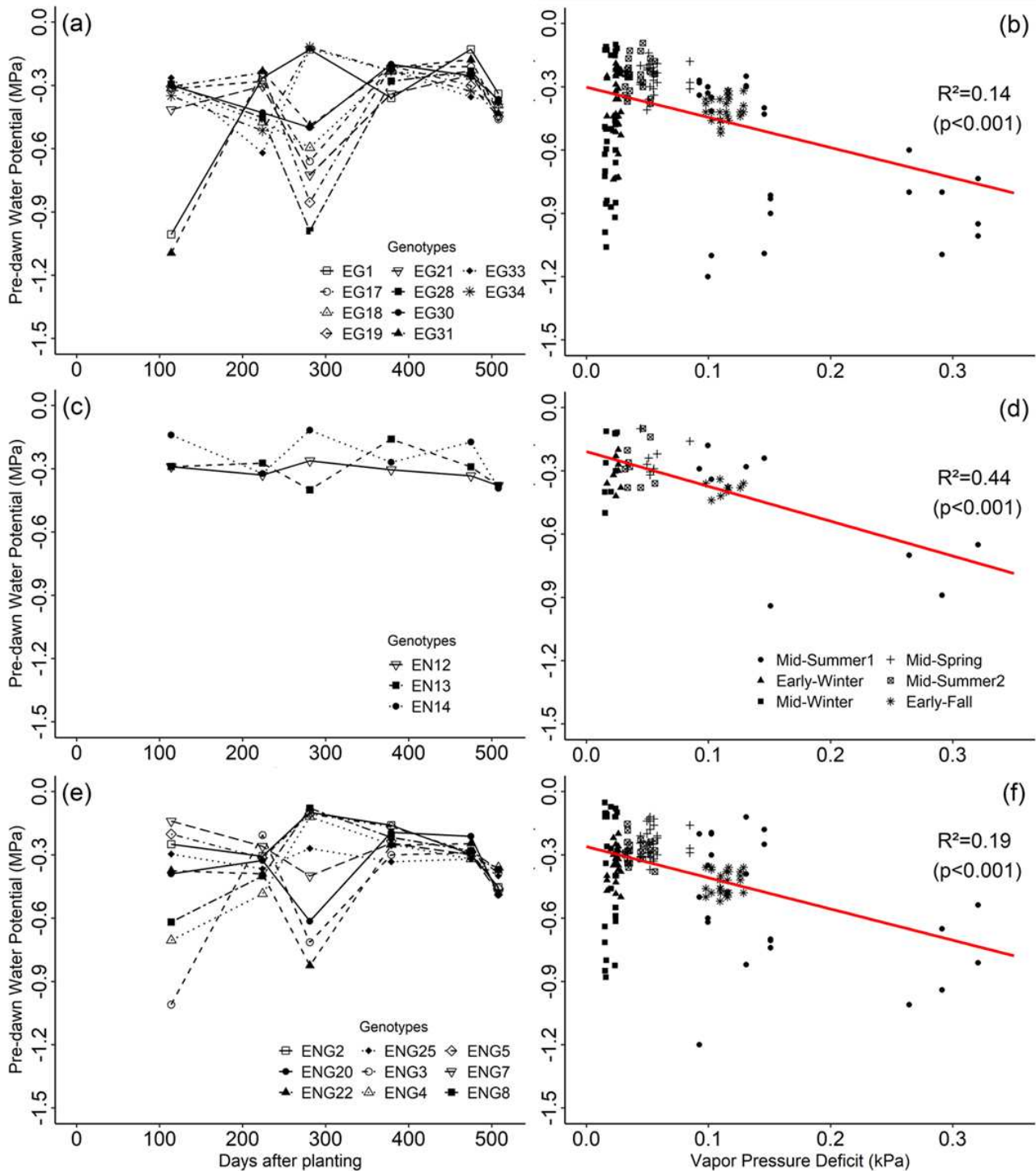
Source: The author (2021).

<sup>1</sup> Percentage represents the variation of average values between the two sampling instances. The genotype order represents the largest to the smallest cumulative volume at  $M_0$  for each taxon. Vertical bars represent the plot mean standard error ( $n = 3$ ).

#### 4.3.2 Seasonal measurements of predawn leaf water potential ( $\Psi_{pd}$ ) and water stress integral (WSI)

Magnitude of seasonal changes in  $\Psi_{pd}$  was different for each taxon during the study period (FIGURE 14 a, c, and e). Genotypes EG17, EG18, EG19, EG21, EG28, ENG3, ENG20, and ENG22 reached  $\Psi_{pd}$  values below -0.5 MPa in mid-winter (August 2018 – 281 days after planting). During the second mid-summer (February 2019 – 475 days after planting)  $\Psi_{pd}$  ranged from -0.2 to -0.4 MPa. The less negative  $\Psi_{pd}$  was -0.05 MPa (c parameter in WSI). In general, we observed a significant reduction of the  $\Psi_{pd}$  when VPD increased over the seasons for all taxa (FIGURE 14 b, d, and f).

FIGURE 14 – GENOTYPE CHANGES IN PREDAWN WATER POTENTIAL AND ITS RELATIONSHIP WITH VAPOR PRESSURE DEFICIT ALONG SEASONS FOR *E. globulus* (a, b), *E. nitens* (c, d), AND *E. gloni* (e, f) IN EARLY DEVELOPMENT.<sup>1</sup>



Source: The author (2021).

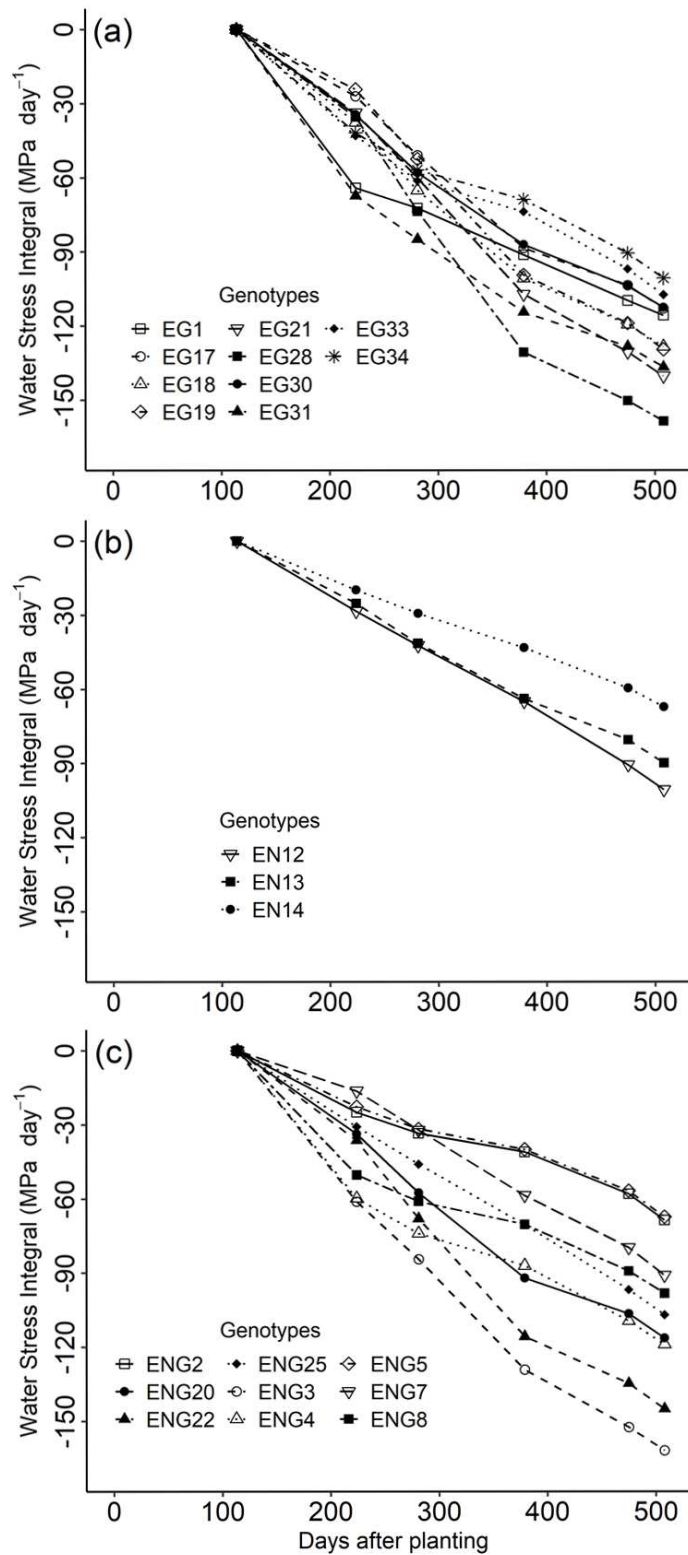
<sup>1</sup> Red lines are the linear models represented by the expression  $\Psi_{pd} = \beta_0 + \beta_1 \cdot \text{VPD}$ .

The absolute cumulative WSI for the whole period of mensuration (508 days after planting) ranged from 100 to 158 MPa day<sup>-1</sup> for *E. globulus*, from 67 to 100 MPa



day<sup>-1</sup> for *E. nitens*, and 67 to 161 MPa day<sup>-1</sup> for *E. gloni*. Larger absolute values of WSI indicated larger amounts of accumulated water stress reflected in more negative values of  $\Psi_{pd}$ . *E. globulus* showed the largest absolute average WSI (124 MPa day<sup>-1</sup>) compared to *E. nitens* (-31%) and *E. gloni* (-12%), however the largest range in WSI was observed in the *E. gloni* genotypes (FIGURE 15 a, b, and c).

FIGURE 15 - GENOTYPE CHANGES IN WATER STRESS INTEGRAL FOR *E. globulus* (a), *E. nitens* (b) AND *E. gloni* (c) IN EARLY DEVELOPMENT.

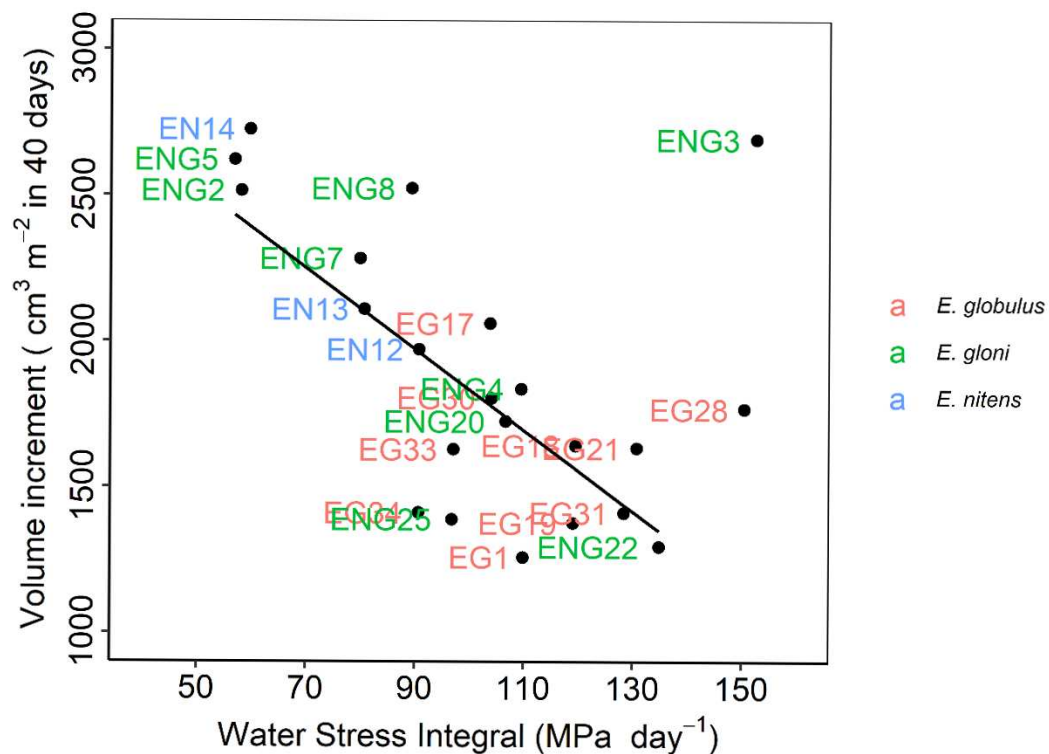


Source: The author (2021).

#### 4.3.3 Volume increment (IncVol) and water stress integral (WSI)

A significant and negative relationship was observed between IncVol, during  $M_0$  and  $M_{final}$ , and the absolute WSI during early development ( $F = 23.19$ ,  $p < 0.0001$ ). The slope of the regression model showed a decrease of IncVol of  $13.9 \text{ cm}^3 \text{ m}^{-2}$  for each  $1 \text{ MPa day}^{-1}$ . In other words, genotypes that presented larger amounts of accumulated water stress along early development reduced growth during decrease soil water availability (between  $M_0$  and  $M_{final}$ ), except for ENG3 (*E. gloni*), which showed the highest absolute WSI and the higher IncVol when compared to our regression model. All *E. nitens* genotypes (EN12, EN13, and EN14) presented high productivity (above  $1900 \text{ cm}^3 \text{ m}^{-2}$  between  $M_0$  and  $M_{final}$ ) with low water stress (below  $90 \text{ MPa day}^{-1}$ ), unlike almost all *E. globulus* genotypes (EG18, EG19, EG21, EG28, EG31, and EG34) which showed the opposite behavior. Interestingly, some *E. gloni* genotypes showed similar values to *E. nitens* (ENG2, ENG5, ENG7, and ENG8), while others followed *E. globulus* (ENG22 and ENG25) (FIGURE 16).

FIGURE 16 - WATER STRESS INTEGRAL AND VOLUME INCREMENT RELATIONSHIP BETWEEN  $M_0$  and  $M_{final}$  FOR *EUCALYPTUS* GENOTYPES.



Source: The author (2021).

#### 4.3.4 Physiological and LAI measurements during the decreased soil water availability period ( $M_0$ and $M_{final}$ )

Physiology and LAI measurements showed contrasting results (TABLE 5). For *E. globulus*, there were significant interaction for sampling instance  $\times$  period for An, Ci, and Tr, and for sampling instance  $\times$  genotype for LAI. Genotype was significant only for gs and Ci, and sampling instance only for  $\Psi_{md}$ . For *E. nitens*, a significant effect of sampling instance and genotype for gs and Tr was observed, and a significant interaction was only observed for An for sampling instance  $\times$  period. Sampling instances was significant only for LAI. *E. gloni* showed the most significant effects among taxa. The interaction between sampling instances  $\times$  period  $\times$  genotype was significant for gs and Tr, and sampling instances  $\times$  period for An and Ci. Also genotype effects was significant for all physiological variables and LAI.

TABLE 5 – ANALYSES OF VARIANCE P-VALUES TESTING SAMPLING INSTANCES (SI –  $M_0$  and  $M_{final}$ ), PERIODS (P – MORNING, MIDDAY, AND AFTERNOON), GENOTYPE (G) AND INTERACTION EFFECTS EVALUATED FOR PHOTOSYNTHESIS (An), STOMATAL CONDUCTANCE (gs), INTERCELLULAR CARBON (Ci), TRANSPIRATION (Tr), MIDDAY WATER POTENTIAL ( $\Psi_{md}$ ), AND LEAF AREA INDEX (LAI).

Taxa	Effects	An	gs	Ci	Tr	$\Psi_{md}$	LAI
<i>E. globulus</i>	SI	<b>&lt; 0.001</b>	<b>&lt; 0.001</b>	0.066	<b>&lt; 0.001</b>	<b>0.020</b>	<b>&lt; 0.001</b>
	P	0.901	0.595	0.921	0.653	-	-
	G	0.372	<b>0.008</b>	<b>0.005</b>	0.059	0.218	<b>&lt; 0.001</b>
	SI $\times$ P	<b>&lt; 0.001</b>	0.065	0.041	<b>0.040</b>	-	-
	SI $\times$ G	0.554	0.812	0.216	0.775	0.806	<b>&lt; 0.001</b>
	P $\times$ G	0.764	0.155	0.101	0.690	-	-
	SI $\times$ P $\times$ G	0.588	0.470	0.475	0.675	-	-
<i>E. nitens</i>	SI	<b>0.011</b>	<b>0.005</b>	0.215	<b>&lt; 0.001</b>	0.351	<b>0.006</b>
	P	0.725	<b>0.005</b>	0.054	0.213	-	-
	G	<b>0.004</b>	<b>0.002</b>	0.479	<b>0.007</b>	0.730	0.150
	SI $\times$ P	<b>0.022</b>	0.609	0.242	0.147	-	-
	SI $\times$ G	0.949	0.231	0.114	0.305	0.222	0.072
	P $\times$ G	0.596	0.517	0.661	0.466	-	-
	SI $\times$ P $\times$ G	0.739	0.585	0.854	0.824	-	-
<i>E. gloni</i>	SI	<b>&lt; 0.001</b>	<b>&lt; 0.001</b>	<b>&lt; 0.001</b>	<b>&lt; 0.001</b>	0.367	<b>&lt; 0.001</b>
	P	<b>0.003</b>	0.333	0.691	0.488	-	-
	G	<b>0.021</b>	<b>0.001</b>	<b>0.021</b>	<b>0.005</b>	0.174	<b>&lt; 0.001</b>
	SI $\times$ P	<b>0.003</b>	0.146	<b>0.006</b>	0.135	-	-
	SI $\times$ G	0.201	<b>0.005</b>	0.245	<b>0.023</b>	0.194	0.058
	P $\times$ G	0.258	<b>0.042</b>	0.744	0.091	-	-
	SI $\times$ P $\times$ G	0.459	<b>0.005</b>	0.924	<b>0.034</b>	-	-

Source: The author (2021).

Across all genotypes and measurement period, the decrease in soil water between sampling instances reduced average physiology performance by 20% for An, 34% for gs, 4% for Ci, 37% for Tr, and 5% for  $\Psi_{md}$ , excepted for LAI which presented an increment of 40%. Considering individual taxa, *E. gloni* showed the greatest reduction in gas-exchange variables with 23% for An, 43% for gs, 5% for Ci, and 42% for Tr, and could be considered the most sensible taxa in the survey of physiological changes, and *E. nitens* presented the lowest reduction with 11% for An, 22% for gs, 2% for Ci, and 28% for Tr. *E. globulus* presented the greatest reduction in  $\Psi_{md}$  (10%) and *E. nitens* genotypes were capable to increase average  $\Psi_{md}$  in 5% with decrease in soil water, showing very contrasting behaviors. LAI increased for all taxa, being *E. gloni* which invested more in LAI (43%), followed by *E. nitens* (38%), and *E. globulus* (37%) (TABLE 6).

TABLE 6 – DESCRIPTIVE STATISTICS FOR PHOTOSYNTHESIS ( $A_n$  -  $\mu\text{mol CO}_2 \text{ m}^{-2} \text{ s}^{-1}$ ), STOMATAL CONDUCTANCE ( $g_s$  -  $\text{mol H}_2\text{O m}^{-2} \text{ s}^{-1}$ ), INTERCELLULAR CARBON ( $C_i$  -  $\mu\text{mol CO}_2 \text{ mol air}^{-1}$ ), TRANSPIRATION ( $Tr$  -  $\text{mmol H}_2\text{O m}^{-2} \text{ s}^{-1}$ ), MIDDAY WATER POTENTIAL ( $\Psi_{md}$  - MPa), AND LEAF AREA INDEX (LAI -  $\text{m}^2 \text{ m}^{-2}$ ) FOR EUCALYPTUS TAXA DURING SAMPLING INSTANCES<sup>1</sup>.

Taxa	Desc.	An		gs		Ci		Tr		$\Psi_{md}$		LAI	
		M <sub>0</sub>	M <sub>final</sub>	M <sub>0</sub>	M <sub>final</sub>	M <sub>0</sub>	M <sub>final</sub>	M <sub>0</sub>	M <sub>final</sub>	M <sub>0</sub>	M <sub>final</sub>	M <sub>0</sub>	M <sub>final</sub>
<i>E. globulus</i>	Mean	18.74	15.25	0.47	0.34	293.8	284.4	5.52	3.58	-1.21	-1.32	3.64	5.01
	Min.	6.34	6.71	0.08	0.12	225.5	192.3	1.49	1.73	-0.72	-0.35	1.78	2.95
	Max.	26.14	23.99	0.83	0.84	353.0	344.4	9.06	7.31	-1.78	-1.78	6.04	8.42
	Sd.	3.94	3.89	0.15	0.15	44.46	32.16	1.32	1.11	0.23	0.29	0.95	1.48
<i>E. nitens</i>	Mean	20.04	17.76	0.64	0.50	304.1	298.0	6.32	4.54	-1.40	-1.32	4.09	5.66
	Min.	13.25	10.27	0.32	0.22	273.0	248.6	4.06	2.53	-0.88	-0.90	1.80	4.26
	Max.	25.16	24.44	0.89	1.39	326.4	334.9	9.13	8.56	-1.74	-1.82	6.83	7.41
	Sd.	3.16	3.82	0.16	0.25	13.61	22.02	1.20	1.51	0.21	0.26	0.94	1.29
<i>E. gloni</i>	Mean	20.00	15.45	0.62	0.35	302.4	287.1	6.35	3.68	-1.32	-1.36	3.49	5.01
	Min.	11.18	6.60	0.19	0.08	271.8	211.1	3.39	1.18	-0.72	-0.75	1.80	2.14
	Max.	27.60	26.31	1.03	1.06	338.8	338.4	9.20	7.90	-1.70	-1.75	6.75	6.54
	Sd.	4.24	4.03	0.17	0.16	17.32	25.70	0.97	1.20	0.24	0.26	0.98	0.94

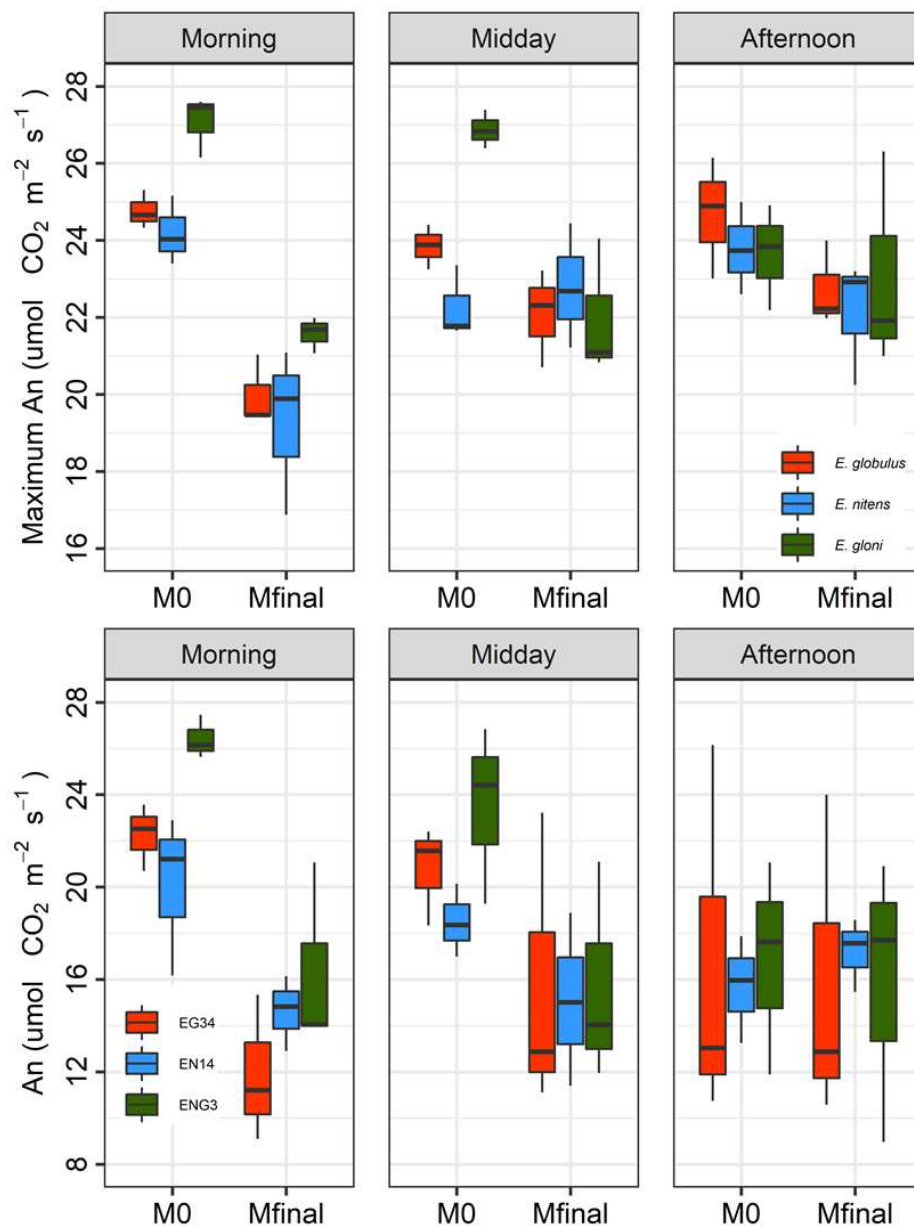
Source: The author (2021).

<sup>1</sup> Desc: Descriptive; Min: Minimum; Max: Maximum; and Sd: Standard deviation.

We graphically analyzed the average maximum daily value of An for each taxon and for key genotypes (EG34 (*E. globulus*), EN14 (*E. nitens*), ENG3 (*E. gloni*)) that showed a different relationship between IncVol and WSI behavior (FIGURE 17). In fact, greatest reductions were observed for morning An for all taxa between M<sub>0</sub> and M<sub>final</sub> (20% for *E. globulus*, *E. nitens*, and *E. gloni*). At midday, only *E. gloni* presented a significative decrease in An (20%), and small changes (< 10%) were observed in the afternoon An for all taxa.

The key genotypes showed similar  $A_n$  behavior as the individual taxa. Regardless of productivity and accumulated water stress, morning and midday  $A_n$  were the first to respond to changes in soil water availability. For ENG3, which showed larger accumulated water stress and higher growth than other genotypes, we observed a greater reduction in morning (40%) and midday (33%)  $A_n$  when compared to other genotypes (EG34 and EN14). During afternoon, there were no great changes in  $A_n$ , and genotypes like EN14 also improved  $A_n$  during this period.

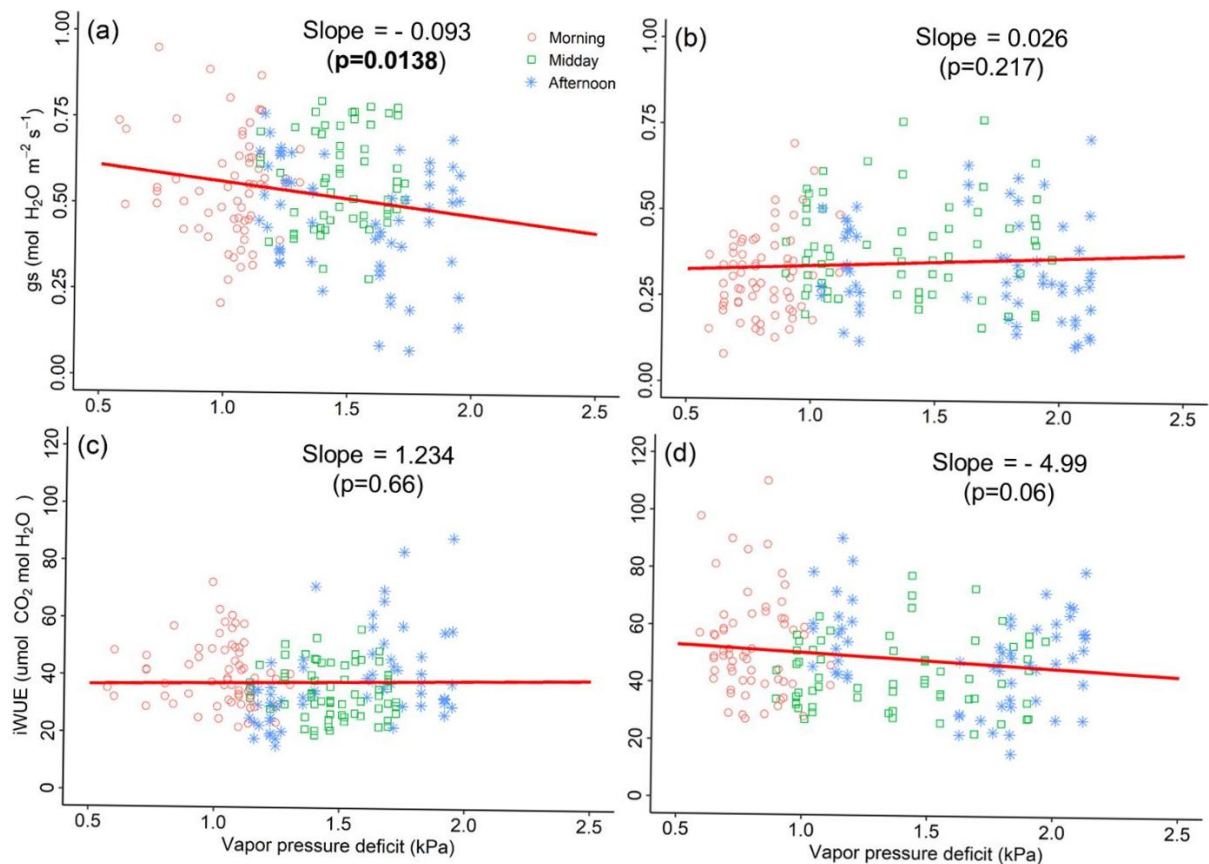
FIGURE 17 – MAXIMUM DAILY PHOTOSYNTHESIS FOR EACH TAXON (UPPER) AND DAILY PHOTOSYNTHESIS FOR EG34, EN14, AND ENG3 (BOTTOM).



Source: The author (2021).

Pearson correlation between  $A_n$  and  $g_s$  was 0.31 ( $p=0.01$ ) at  $M_0$  and 0.68 ( $p<0.001$ ) at  $M_{final}$ . These positive and significant relationship between  $A_n$  and  $g_s$  during sampling instances suggesting that  $A_n$  was affected by changes in  $g_s$ , and consequently intrinsic water use efficiency (iWUE). Regard of significance, at  $M_0$  we observed that  $g_s$  smoothly decreased with VPD increment along the day, on the other hand, at  $M_{final}$  occurred reduction in the  $g_s$  during all periods and this significative relationship was not observed. Average iWUE increased 27% between  $M_0$  and  $M_{final}$ , and the greatest increment was observed in afternoon (33%), followed by morning (27%), and midday (21%). However, we do not observe a significant relationship with VPD changes along the day in  $M_0$  and  $M_{final}$  (FIGURE 18). Also, we observed an increase in iWUE under soil water changes for all taxa, the highest average increment was observed for *E. gloni* (45%), followed by *E. nitens* (21%), and *E. globulus* (16%).

FIGURE 18 – RELATIONSHIP BETWEEN STOMATAL CONDUCTANCE AND VAPOR PRESSURE DEFICIT IN  $M_0$  (a) AND  $M_{final}$  (b), AND BETWEEN INTRINSIC WATER USE EFFICIENCY AND VAPOR PRESSURE DEFICIT IN  $M_0$  (c) AND  $M_{final}$  (d).<sup>1</sup>



Source: The author (2021).

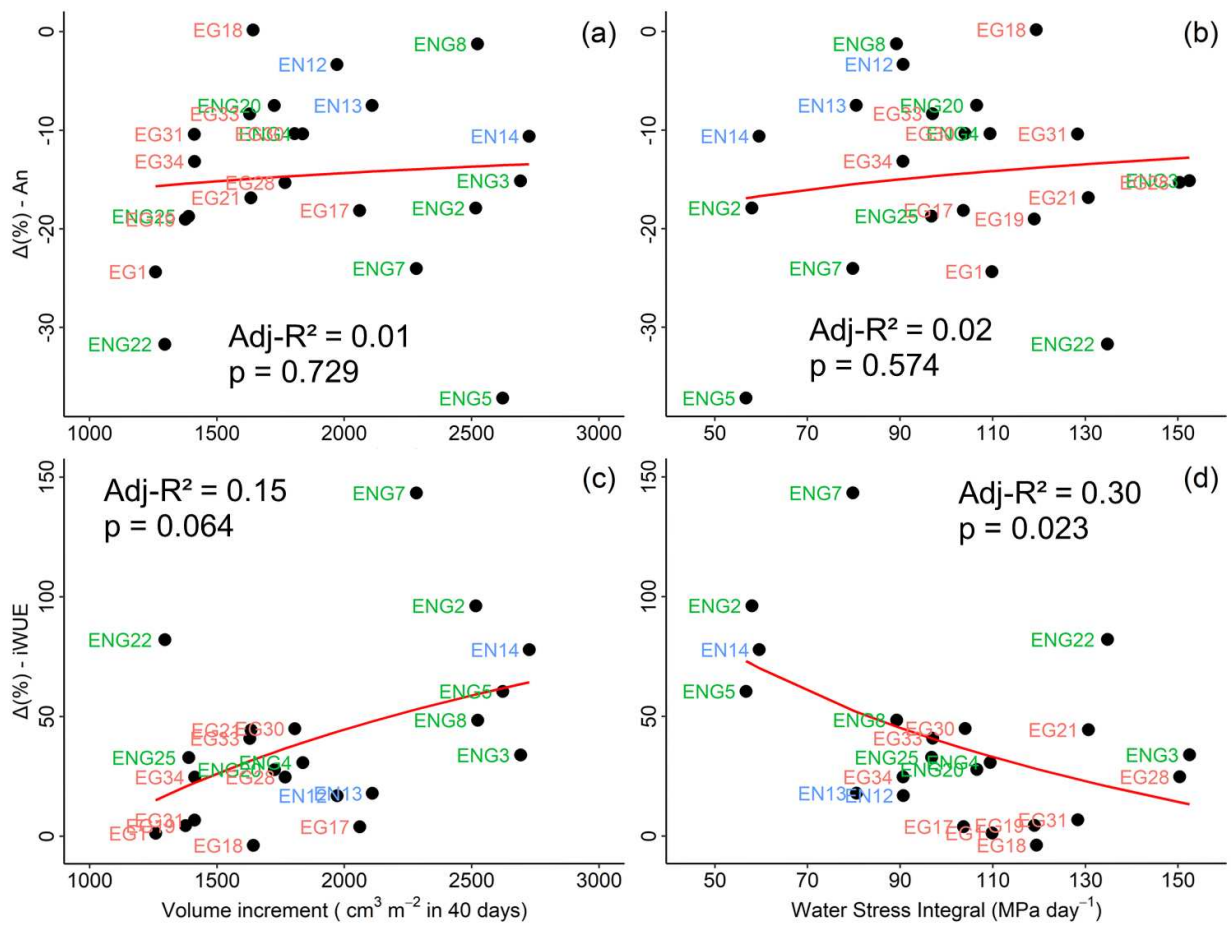
<sup>1</sup> Red lines are the linear models represented by the expression  $g_s$  or iWUE =  $\beta_0 + \beta_1 \cdot \text{VPD}$ .

Non-significative relationships were observed for IncVol and WSI to changes in  $A_n$ , (FIGURE 19 a, b). Regardless of growth and cumulative water stress,  $A_n$  decreased for all genotypes. However, with the same average IncVol and WSI, we observed a large  $A_n$  range in response to the decrease in soil water. *E. nitens* genotypes reduced  $A_n$  between 5 and 10%, while almost all *E. gloni* genotypes presented an average  $A_n$  reductions above 20%.

Tree growth was not correlated with changes in iWUE (Figure 19 c). Unlike  $A_n$ , iWUE showed a significative relationship with WSI (FIGURE 19 d). Genotypes with lower WSI improved their water use efficiency at individual leaves, mainly because of stomatal closure under reduced soil water availability. Genotypes with distinct behavior in IncVol and WSI relationship, e.g. ENG3, presented iWUE range similar to genotypes with higher accumulated stress, e.g. EG21 and EG28, indicated that WSI possible influenced more physiology changes of individual leaves than growth. However, ENG3 was very productive, and we could conclude that this genotype seems to be highly efficient in partitioning carbon to stem growth.



FIGURE 19 – VARIATION IN PHOTOSYNTHETIS (a AND b) AND INTRINSIC WATER USE EFFICIENCY (c AND d) BETWEEN  $M_0$  AND  $M_{final}$ , AND ITS RELATIONSHIP WITH GROWTH (a AND c) AND WATER STRESS INTEGRAL (b AND d) FOR *EUCALYPTUS* GENOTYPES.<sup>1</sup>

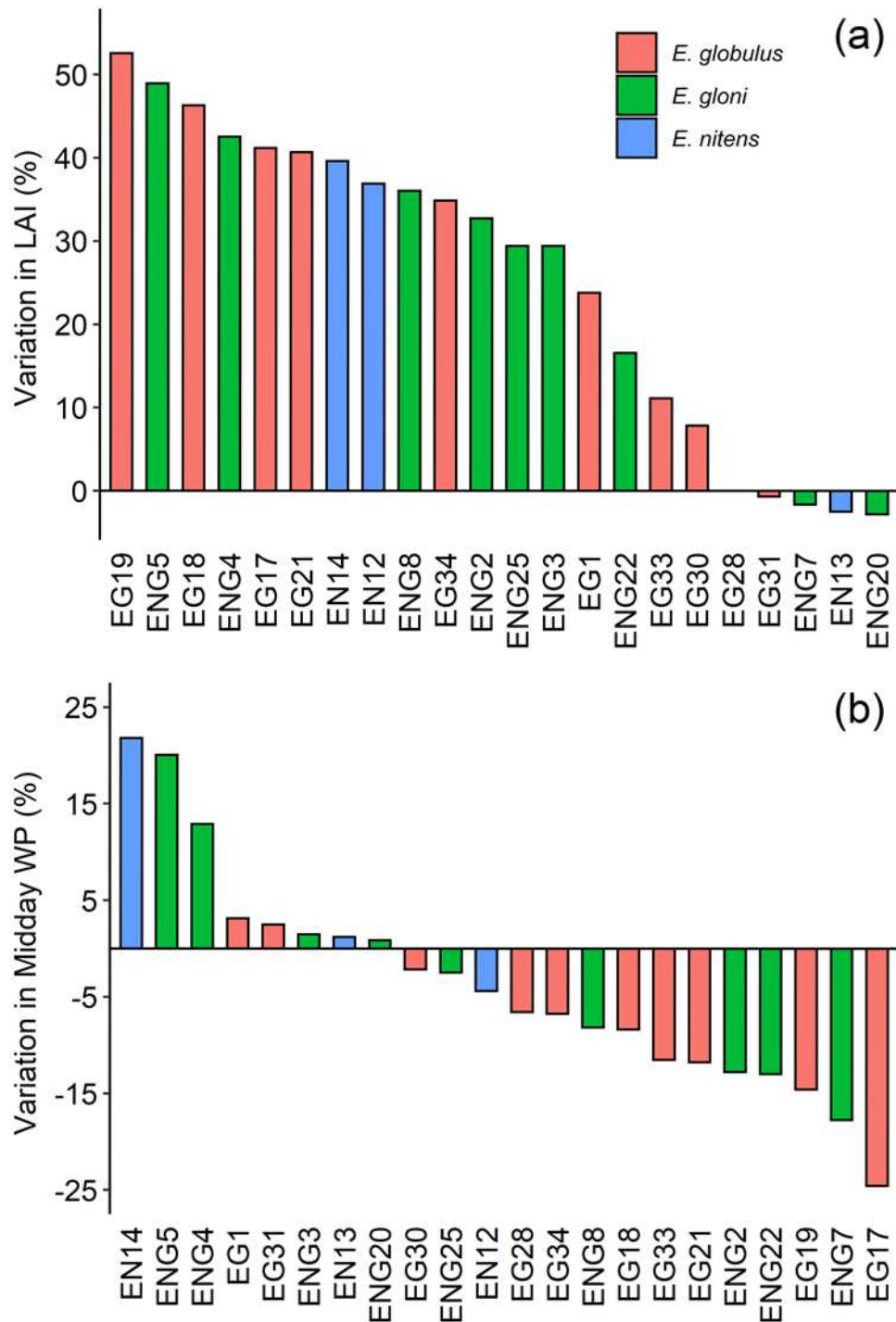


Source: The author (2021).

<sup>1</sup> Regressions models are represented by expression  $\Delta(\%) = \beta_0 + \beta_1 * \log(Y)$ .

Almost all genotypes (78%) increased their LAI between  $M_0$  and  $M_{final}$  (FIGURE 20 a). This LAI increments occurred regardless WSI, since genotypes with high absolute WSI (e.g. EG21, ENG3, and ENG22) and low absolute WSI (e.g. EN14, ENG2, and ENG5) showed similar LAI increments.  $\Psi_{md}$  presented a small reduction between  $M_0$  and  $M_{final}$  from -1.29 to -1.34 MPa (-4.3%). We observed that, even with decreased soil water availability, eucalyptus genotypes did not present great changes in  $\Psi_{md}$  values. That is the reason of decrease stomata conductance as the first response to changes in soil water availability (FIGURE 20 b). In general, genotypes with low absolute WSI, such as *E. nitens*, were capable to maintained  $\Psi_{md}$  values, however, genotypes with high absolute WSI, such as almost *E. globulus*, decreased their  $\Psi_{md}$  values with decrease soil water availability.

FIGURE 20 – CHANGES IN (a) LEAF AREA INDEX AND (b) MIDDAY WATER POTENTIAL BETWEEN  $M_0$  AND  $M_{final}$ <sup>1</sup>.



Source: The author (2021).

<sup>1</sup> Genotypes were ordered from the maximum to minimum change between  $M_0$  and  $M_{final}$ .

#### 4.4 DISCUSSION

Before irrigation was turned off, we observed a large range in WSI indicating that trees faced different water stress levels through the 1.5-year and these negatively influenced growth in the period of decreased soil water (Waghorn et al., 2015). However, Myers (1988), who developed the concept of WSI, observed that the WSI was not only determined by soil water deficits. At the site of this experiment, we observed higher values of summer VPD and temperature, and this increased plant water stress because of a higher atmospheric demand (Lim et al., 2020).

Before and after the period of decreased soil water ( $M_0$  and  $M_{final}$ ), there was a large change in the IncVol of eucalyptus genotypes. Increment in wood production from *Eucalyptus* genotypes were also reported by other studies at the same site (Rubilar et al., 2020). The genotypes that grew the most were *E. gloni* which reached values of WSI ranging between -60 to -168 MPa day<sup>-1</sup>. Interestingly, ENG3 showed higher IncVol (2692 cm<sup>3</sup> m<sup>-2</sup> in 40 days) between  $M_0$  and  $M_{final}$ , but lower values of WSI (-152. MPa day<sup>-1</sup>), indicated that even with higher accumulated water stress this genotype was very productive during decrease soil water availability. In contrast, EG34 presented lower growth during the same period (1412 cm<sup>3</sup> m<sup>-2</sup> in days) and higher values of WSI (-90 MPa day<sup>-1</sup>). This indicated that even with lower accumulated water stress this genotype was not able to improve its growth as soil water decrease.

Despite of the different responses of some *Eucalyptus* genotypes, we observed that WSI was a useful tool for assessing the effect of water availability on tree growth (Gonzalez-Benecke and Dinger, 2018). Hakamada et al. (2017) highlighted that eucalypt genotypes changes in leaf water potential could be a predictor of plant water status in forest development. In our study, genotypes that had lower predawn water potential showed lower WSI, mainly because the genotypes were more stressed during the survey. Changes in leaf water potential is a response of plants when soil water decreases and water stress starts (Silva et al., 2017). However, between  $M_0$  and  $M_{final}$ , we observed small average changes in midday water potential, indicated that genotypes were very conservative and did not change their water status even if soil water decrease, showing an isohydric behavior.

In our study,  $A_n$  and  $g_s$  showed no consistent trend between *Eucalyptus* genotypes. In general, average  $A_n$  and  $g_s$  reduced for almost all genotypes in midday

and increase in afternoon, as expected for *Eucalyptus* with decrease soil water (Mokotedi et al., 2010). The same authors observed that osmotic adjusted helped *Eucalyptus* species in maintained photosynthetic capacity during periods of lower soil water availability which makes plant growth possible when soil water decreased. Interestingly, that genotypes decreased their physiology and increase leaf area under soil water changes, suggesting that maybe small reduction in  $A_n$  would be compensated increase number and/or size of leaves, regardless accumulated water stress.

Previous studies showed that stomatal closure is the first event occurring in response to decreasing soil water and it limits photosynthetic rate (Flexas, et al., 2004) and this is the way to avoid water losses (Tafur et al., 2017; Taiz et al., 2017). *Eucalyptus* closes their stomata for long periods or at different hours of the day to avoid water losses during drought and because of high atmospheric demand (Silva et al., 2016; Gonçalves et al., 2017). However, eucalyptus show a high variation in physiological responses even in genotypes of the same taxon, as reported in this study. Stomatal closure improves iWUE (Saadaoui et al., 2017) and this could be used as a tool to select genotypes that are tolerant of water stress (Navarrete-Campos et al., 2013). *E. gloni* genotypes showed the highest average increment in iWUE as soil water decreased, from 33.84 to 49.34  $\mu\text{mol CO}_2 \text{ mol H}_2\text{O}$ , and *E. nitens* showed the lowest response, from 33.01 to 40.27  $\mu\text{mol CO}_2 \text{ mol H}_2\text{O}$ .

Changes in daily values of leaf gas exchanges in *Eucalyptus* were reported by Battie-Laclau et al. (2016), and also observed in this study (TABLE 5; FIGURE 11). When irrigation was turned on, average  $A_n$  was higher in the morning for all taxa, decreasing throughout the day. For *E. gloni* higher values of  $A_n$  were observed in the morning and midday, decreasing  $A_n$  in the afternoon. However,  $A_n$  did not ever reach maximum values at midday, even in the well-irrigated period ( $M_0$ ) and decreased on average for all taxa with decreasing soil water. Sometimes, midday depression in  $A_n$  arises because of the negative association with weather conditions (Borišev et al., 2015), while  $A_n$  increases at other periods of the day, such as morning or afternoon (Baldocchi, 1997).

These patterns may reflect stomatal closure during the day, reducing the uptake of  $\text{CO}_2$  in the leaves, decreasing intercellular  $\text{CO}_2$ . After 40 days of decreased soil water (between  $M_0$  and  $M_{\text{final}}$ ), there were no specific patterns among *Eucalyptus*

genotypes and there was high variability in the response of  $A_n$ . During the dry season, Battie-Laclau et al. (2016) observed that *E. grandis* clones responded to a water deficit, increasing their midday values of  $iWUE$ , mainly because at noon there was a higher atmospheric demand (VPD).

Higher increments in  $iWUE$  were observed for higher productive genotypes and with lower accumulate water stress (WSI), suggesting that these genotypes were very coordinated in stomatal closure. This occurred because, during a decrease in soil water, most plants reduced their metabolism at midday. Some ecological studies observed that above 35 °C (midday) there was a significant reduction in plant metabolism (George et al., 2018). Other studies reported that changes in physiology did not explain changes in growth for *E. tereticornis* Sm seedlings, mainly because non-photosynthetic parameters, such as leaf water potential and shoot: root relationships, were kept constant (Campany et al., 2017), like we observed in our study.

However, the link between physiology and productivity is not clear. This is mainly because stem growth is not just the result of photosynthesis measurements of individuals leaves and consequently intrinsic water use efficiency, since *Eucalyptus* genotypes presented a large crown with leaves of different conditions of radiation and atmospheric demand along the day (Battie-Laclau et al., 2016), and sometimes, tree growth and  $A_n$  or  $iWUE$  are not well correlated (Farquhar et al., 1989; Lévesque et al., 2014), like we observed on this study. Contrary to  $iWUE$ , water use efficiency for stem growth is influenced by many non photosynthetic factors, such as carbon loss from respiration, allocation to turnover and litter, and water loss independently from photosynthesis (Farquhar et al., 1989; Battie-Laclau et al., 2016). However, our results indicate the most productive genotypes generally maintained less negative water potential (WSI) along early development, suggesting a correlation between growth and plant water status in the first year. Also, genotypes with less negative WSI along early development, could smoothly improve their  $iWUE$  during soil water decrease, indicating that water potential could be a key parameters to connected physiology, growth, and plant water demand in early forest management.

#### 4.5 CONCLUSIONS

Genotypes with higher absolute WSI after 1.5 years of development also present the lowest IncVol, indicating that accumulated water stress affected growth performance. Photosynthesis ( $A_n$ ), stomatal conductance ( $g_s$ ), and midday water potential ( $\Psi_{md}$ ) reduce under soil water decrease, resulting in increment of intrinsic water use efficiency (iWUE) being most pronounced by *E. gloni* genotypes. Regardless WSI, all *Eucalyptus* genotypes in this study invest in leaf area during small changes in soil water. In general, leaf water potential is a key parameter to connect productivity, physiology and water use in young *Eucalyptus* plantations, and differences responses in water potential among *Eucalyptus* genotypes on the same environment still show the possibility of progress in our understanding drought risks in forest management.

## 5 CHAPTER 3 TEMPERATURE EFFECTS ON EARLY GROWTH OF *EUCALYPTUS* GENOTYPES OF THREE TAXA

### ABSTRACT

Temperature is a crucial factor that affect tree physiology and consequently growth. Understanding temperatures range (cardinal) for optimal growth are necessary for *Eucalyptus* genotypes production during different phenological stages. Our experiment evaluated monthly stem biomass growth ( $\text{kg m}^{-2}$ ) in 1.3-year-old of development of 22 eucalyptus genotypes of *E. globulus*, *E. nitens* and *E. nitens* x *E. globulus* hybrid. We used a model that match mean daily air temperature and early daily growth to estimated genotype cardinal temperatures. The model showed a small root mean square error (RSME) ranging from 0.01 to 0.09  $\text{kg m}^{-2}$ , and correlation between observed and predicted values was above 0.97. Average optimum temperature was 21.4 °C and considering stem biomass growth, high productivity genotypes showed optimum temperature closer to mean air temperature at this site (14 °C). Interestingly, some genotypes exhibited a large range between base minimum ( $T_{\text{min}_g}$ ) and base maximum ( $T_{\text{max}_g}$ ) temperatures, which allowed them to growth during almost all seasons. These results support the idea that some eucalyptus genotypes should be planted in different sites to increase early growth. Cardinal temperatures provide an insight of genotypes growth at different sites and are useful for produced maps that describe species growth along the years.

Keywords: Eucalyptus growth, cardinal temperatures, growth models.

### 5.1 INTRODUCTION

Climate drives forest development and the incorporation of climate variables in growth modeling must increase our understands in forest ecology and management. Among climate, the most important variable is temperature (Went, 1953; Ryan, 2010; Binkley et al., 2017), since prediction of future climates average temperatures are projected to increase 0.2 °C, arriving at an increase of up to 3 °C in the worst scenarios and increase the number of extreme events connected with temperatures, such as frost and heat (IPCC, 2014).

Temperature is the main factor affecting tree metabolism, such as plant biochemistry and photosynthesis, and varies dramatically across seasons in subtropical areas (Aspinwall et al., 2019). Way and Oren (2010) observed that increased temperatures increase tree growth in subtropical forests, however this response was not simply because plant growth showed a maximum temperature that growth could occurred (Watt et al., 2014). Growth rate depend of the cardinal

temperatures, represented by minimum, maximum and optimum temperature for plant development (Hatfield and Prueger, 2015).

The estimation of cardinal temperatures among plant development is very useful, since temperature is an important driver in process-based models to describe the influence of weather conditions on plant growth, such as 3-PG (Landsberg and Waring, 1997), CABALA (Battaglia et al., 2004), and BIOMASS (McMurtrie et al., 1990). The incorporation of temperature effects in plant growth is done by modifiers that vary between 0 and 1 among a temperature range, out of this range the modifier is equal to 0 and growth stops (Yin et al., 1995). The models that use this modifier information are more precise than empirical plant growth models, however they are more complex because the number of parameters to be estimated, requiring restrictions and calibrations (Kimberley and Richardson, 2004).

Using a model to estimate responses of *Eucalyptus* early growth to temperature changes will allow for planning species/genotypes allocation at different production areas, ensuring the maintenance of forest production over the years (Binkley et al., 2017). The study aimed to identify the cardinal air temperature effects on early growth over 1.3 years of development of different *Eucalyptus* genotypes. We tested the hypothesis that the most productive *Eucalyptus* genotypes maintain optimum temperature close to mean site air temperature and average cardinal temperatures for *E. nitens* are lower than *E. gloni* and *E. globulus*.

## 5.2 MATERIAL AND METHODS

### 5.2.1 Tree measurements

Measurements were made in the four central trees in each plot, considering monthly root collar diameter (rcd) in centimeters and total height (h) in centimeters. The measurements occurred between mid-summer on January 2018 to mid-summer on February 2019.

For growth models in this chapter, we used stem biomass data ( $w_{\text{stem}}$ ). Destructive sampling of trees for stem biomass were performed at May 2019 in all genotypes. Sampled trees were distributed among blocks and selected to encompass the rcd range in inventories, using four trees per genotype. After felling the tree, h and rcd was measured and all branches were cut from the stem. After removing all



branches, stem was sectioned into three or four sections. Individual tree stem biomass was estimated with a balance accurate to 0.05 kg. A sample disc of 8 cm thick was cut from stem at 10 cm groundline to determine moisture content with analytical balance accurate to 0.01 g. Dry weights of the discs were measured after samples were dried at 65°C to constant weight. Then individual stem biomass was calculated based on the ratio of dry weight to fresh weight. Nonlinear models for each genotype were used to estimate stem biomass using as independent variable  $rcd^2h$ :

$$w_{\text{stem}} = \beta_0 * (rcd^2h)^{\beta_1} \quad (5.1)$$

where,  $w_{\text{stem}}$  is the individual stem biomass (kg),  $rdc$  is the root collar diameter measured at 0.1-m height (cm),  $h$  is the total tree height (cm), and  $\beta$  is the model coefficients.

Coefficient  $\beta_0$  ranged between 0.0003 to 0.2474 and  $\beta_1$  ranged between 0.4525 to 1.6778. Mean  $R^2$  was  $0.93 \pm 0.08$  and mean RMSE was  $0.23 \pm 0.16$  kg (TABLE 7). In this chapter, we did not use *E. globulus* genotypes EG28 and EG31, because their biomass models did not show significant adjustment.

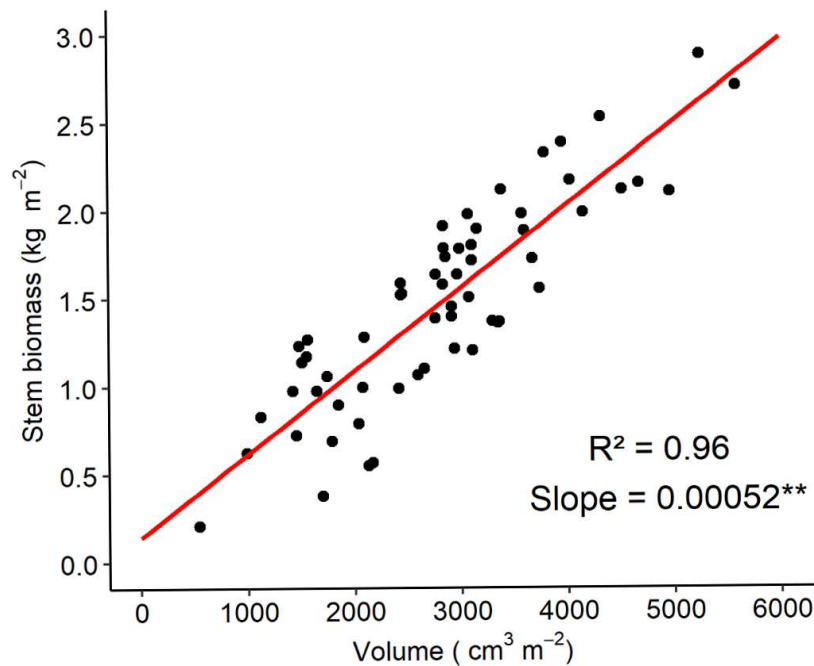
Biomass models were used to estimate  $w_{\text{stem}}$  in the previous dates using measurements of  $rdc$  and  $h$  along the survey. Stem biomass was scaled up to square meter ( $W_{\text{stem}}$  - kg m<sup>-2</sup>) by summing  $w_{\text{stem}}$  in measurement plots and divided by measurement plot area (6 m<sup>2</sup>). Using stem biomass did not interfere in our main conclusions because we observed a strong and significant correlation between stem biomass and wood volume calculated in previous chapters during February 2019 (FIGURE 21).

TABLE 7 – ADJUSTED COEFFICIENTS,  $R^2$ , AND ROOT MEAN SQUARE ERROR (RMSE) IN STEM BIOMASS MODEL FOR EACH GENOTYPE.

Specie	Genotype	$\hat{\beta}_0$	$\hat{\beta}_1$	$R^2$	RMSE
<i>E. globulus</i>	EG1	0.0554	0.7368	0.99	0.05
	EG17	0.0982	0.6677	0.70	0.55
	EG18	0.0188	0.9192	0.94	0.41
	EG19	0.0681	0.6961	0.99	0.41
	EG21	0.0533	0.7760	0.95	0.07
	EG30	0.0685	0.7085	0.91	0.20
	EG33	0.0395	0.7813	0.99	0.13
	EG34	0.2474	0.4525	0.99	0.01
<i>E. nitens</i>	EN12	0.0618	0.6950	0.88	0.23
	EN13	0.1433	0.5745	0.86	0.20
	EN14	0.0549	0.7293	0.98	0.23
<i>E. glioni</i>	ENG2	0.1287	0.5895	0.96	0.21
	ENG3	0.0576	0.7603	0.76	0.46
	ENG4	0.0098	1.0175	0.99	0.13
	ENG5	0.0757	0.6891	0.83	0.59
	ENG7	0.0085	1.0459	0.97	0.22
	ENG8	0.0124	0.9691	0.95	0.29
	ENG20	0.0096	1.0082	0.99	0.07
	ENG22	0.0003	1.6778	0.92	0.29
ENG25	0.0194	0.9071	0.99	0.01	

Source: The author (2021).

FIGURE 21 – RELATIONSHIP BETWEEN VOLUME ( $\text{cm}^3 \text{m}^{-2}$ ) AND STEM BIOMASS ( $\text{kg m}^{-2}$ ) ON FEBRUARY 2019.<sup>1</sup>



Source: The author (2021).

<sup>1</sup> Red line represent the linear model:  $Y = aX$ ; \*\* =  $p < 0.001$ .

### 5.2.2 Growth Model and data analyses

Under optimal environmental conditions growth (e.g. diameter, height, volume or biomass) could be describe by large number of functions according to Kimberley and Richardson (2004). For this study, we tested three models to described growth as a function of time (t) (TABLE 8):

TABLE 8 – GROWTH FUNCTION, INVERSE AND DERIVATIVES FOR GROWTH (f(t)) IN FUNCTION OF TIME (t) WHERE a, b AND c ARE MODEL PARAMETERS.

Model	Growth Function (f(t))	Inverse f <sup>-1</sup> (t)	Derivative (f'(t))
Power	$at^b$	$\left(\frac{y}{a}\right)^{\frac{1}{b}}$	$abt^{b-1}$
Schumacher	$ce^{-at^{-b}}$	$\left[-\frac{1}{a}\ln\left(\frac{y}{c}\right)\right]^{\frac{1}{b}}$	$abct^{-(1+b)}e^{-at^{-b}}$
Exponential	$ce^{at}$	$\left[\frac{1}{a}\ln\left(\frac{y}{c}\right)\right]$	$ce^{at}a$

Source: The author (2021).

Stem biomass growth during the 1.3-year (January 2018 to February 2019) was modeled using block-level measurements. The model parameters (a, b, and c) from the functions in TABLE 8 were estimated using PROC NLIN in SAS®Studio ([https://www.sas.com/en\\_us/software/studio.html](https://www.sas.com/en_us/software/studio.html)). Iterative convergence to minimize the residual sum of squares was the Marquardt method. Modeling performance was assessed by bias (B; Eq. 5.2), mean absolute error (MAE; Eq. 5.3), root mean square error (RMSE; Eq. 5.4) and correlation coefficient (R).

$$B = \frac{1}{n} \sum_{i=1}^n (O_i - E_i) \quad (5.2)$$

$$MAE = \frac{1}{n} \sum_{i=1}^n |O_i - E_i| \quad (5.3)$$

$$RMSE = \sqrt{\frac{1}{n} \sum_{i=1}^n (O_i - E_i)^2} \quad (5.4)$$

where, B is bias, n is the number of observations,  $O_i$  is the  $i$ th observed value,  $E_i$  is the  $i$ th estimated value, MAE is the mean absolute error, and RMSE is the root mean square error.

For adding temperature effects on growth, we used the approach described by Kimberley and Richardson (2004) and Watt et al. (2014). According to these authors, growth can be expressed by the differential equation considering an interval  $t$  to  $t + \Delta t$ :

$$y_{t+\Delta t} = y_t + [f(f^{-1}(y_t) + \Delta t) - y_t] \quad (5.5)$$

Where,  $y_t$  is the growth function,  $f^{-1}(y_t)$  is the inverse of growth function, and  $\Delta t$  is the interval of time.

Considering that model explained growth under optimal conditions, we need to add a modifier ( $m$ ), which varies between 0 to 1, and reduce growth under suboptimal conditions (e.g., air temperature, soil water content, radiation):

$$y_{t+\Delta t} = y_t + [f(f^{-1}(y_t) + \Delta t) - y_t] \cdot m \quad (5.6)$$

Where,  $y_t$  is the growth function,  $f^{-1}(y_t)$  is the inverse of growth function,  $\Delta t$  is the interval of time and  $m$  is modifier describing the impacts of environmental conditions on growth.

The growth data used in this study is from a period of the experiment was irrigated, so the modifier only requires to account for air temperature responses, because we assumed that plant optimal soil water availability was maintained during

irrigation period. The three specific parameters that characterized growth modifier with temperature called cardinal temperatures are the base minimum ( $T_{\min_g}$ ), optimum ( $T_{\text{opt}_g}$ ) and base maximum ( $T_{\max_g}$ ) temperatures of growth (Landsberg and Sands, 2011). The temperature modifier approaches to the shape of normal distribution with maximum growth rate ( $m=1$ ) in  $T_{\text{opt}_g}$  and a reduction in growth rate with decrease and increase in air temperatures. Following Watt et al. (2014) we used a modifier ( $m$ ) developed by Yin et al. (1995) based of beta distribution, that described growth responses to air temperature (Eq. 5.7):

$$m = \left[ \left( \frac{T - T_{\min_g}}{T_{\text{opt}_g} - T_{\min_g}} \right) \left( \frac{T_{\max_g} - T}{T_{\max_g} - T_{\text{opt}_g}} \right) \left( \frac{T_{\max_g} - T_{\text{opt}_g}}{T_{\text{opt}_g} - T_{\min_g}} \right) \right]^c \quad (5.7)$$

where,  $T$  is the air temperature ( $^{\circ}\text{C}$ ),  $T_{\min_g}$  is the base minimum temperature of growth ( $^{\circ}\text{C}$ ),  $T_{\text{opt}_g}$  is the optimum temperature of growth ( $^{\circ}\text{C}$ ),  $T_{\max_g}$  is the base maximum temperature of growth ( $^{\circ}\text{C}$ ), and  $c$  is the shape parameter of beta distribution.

All parameters except  $c$  are biologically meaningful, so we simplified the equation by setting  $c$  equal to 1 (Yan and Hunt, 1999). Since the model is quite complex with five or six parameters ( $a, b, c, T_{\min_g}, T_{\text{opt}_g}, T_{\max_g}$ ) to adjust, we use non-linear Generalized Reduced Gradient (GRG) solver in Microsoft Excel<sup>®</sup>. The model was adjusted to minimize root mean square error (RSME) by changing the values of the model parameters. One-way analysis of variance was fitted using PROC MIXED procedure in SAS to test genotypes or taxon significant differences ( $p < 0.05$ ) in model parameters.

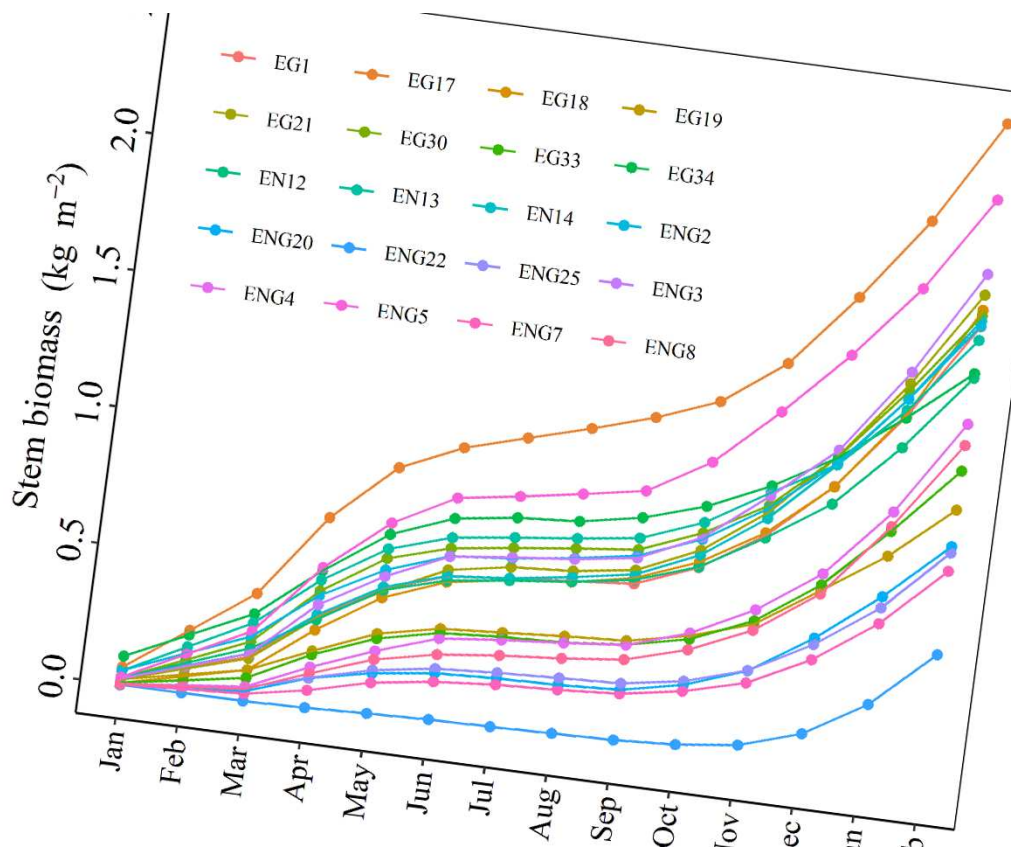
## 5.3 RESULTS

### 5.3.1 Tree growth

Significant genotypes differences were observed by the end of the evaluation period (468 days after planting) for  $h$  ( $p=0.020$ ),  $rcd$  ( $p=0.014$ ) and  $W_{\text{stem}}$  ( $p<0.001$ ). Changes in  $W_{\text{stem}}$  growth exhibited an exponential increase after October 2018

(FIGURE 22). Genotypes cumulative growth at the end of the study ranged from 3.9 to 5.4 m for h, 4.5 to 6.6 cm for rcd, and from 0.49 to 2.44 kg m<sup>-2</sup> for  $W_{stem}$ . Among taxa, genotypes EN14 (*E. nitens*), ENG5 (*E. gloni*), and EG17 (*E. globulus*) showed the highest average cumulative  $W_{stem}$  at the end of the measurements. For our three models, the coefficient of correlation between predicted and observed values was significant and always above 0.97. In general, the Power and Schumacher models underestimated growth and the Exponential model overestimated growth along the survey (TABLE 9).

FIGURE 22 – CHANGES IN STEM BIOMASS ( $W_{stem}$ ) OVER THE SURVEY FOR *EUCALYPTUS* GENOTYPES.<sup>1</sup>



Source: The author (2021).

<sup>1</sup> Each value shown is the mean of three blocks.

TABLE 9 – CORRELATION (R), BIAS (B), MEAN ABSOLUTE ERROR (MAE), AND ROOT MEAN SQUARE ERROR (RMSE) FROM THE ADJUSTED GROWTH MODELS.

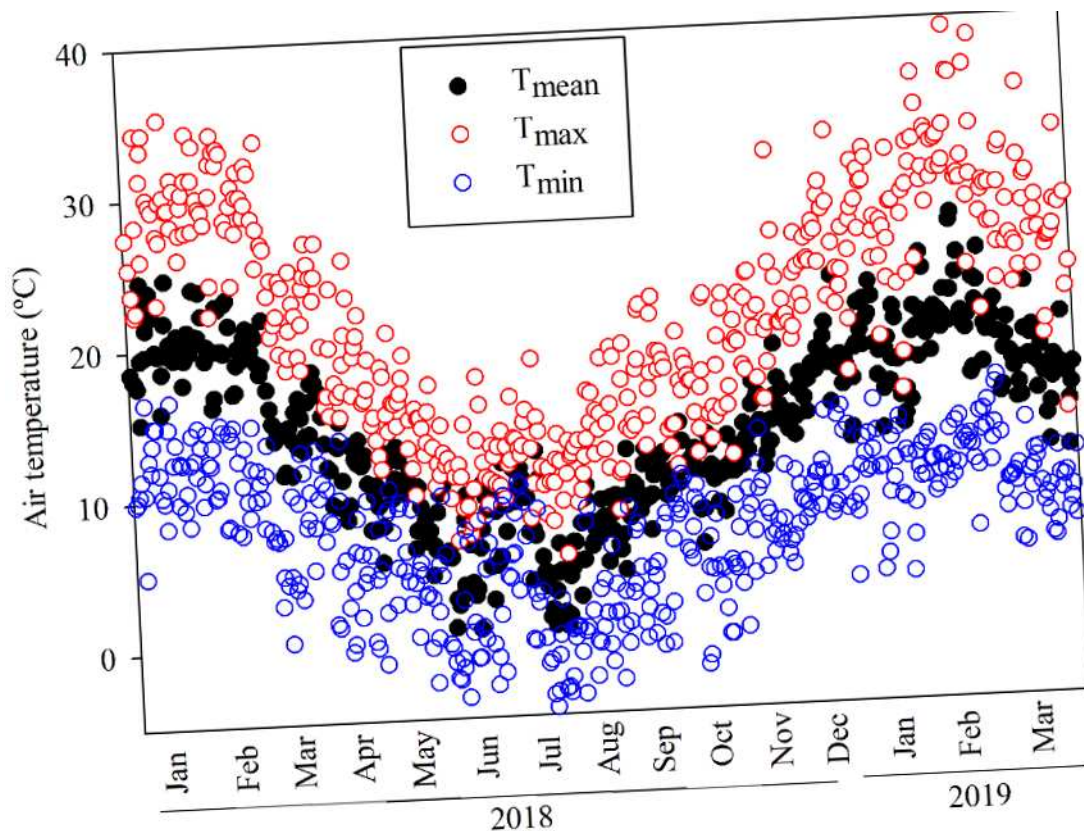
Model	R	B	MAE	RMSE
Power	0.97 ± 0.008	0.009 ± 0.006	0.07 ± 0.029	0.08 ± 0.035
Schumacher	0.97 ± 0.007	0.009 ± 0.006	0.07 ± 0.029	0.09 ± 0.035
Exponential	0.98 ± 0.008	-0.004 ± 0.005	0.06 ± 0.031	0.08 ± .040

Source: The author (2021).

### 5.3.2 Site range in air temperature

There was a higher seasonal range in air temperature at the site, with maximum temperature in summer (Jan-Mar) and minimum temperature in winter (Jun-Aug). Summer showed the highest temperature amplitude. During the study, the lowest temperature was  $-5.4\text{ }^{\circ}\text{C}$  on June 2018 and the highest temperature was  $41.2\text{ }^{\circ}\text{C}$  in February 2019. The mean temperature was  $14\text{ }^{\circ}\text{C}$  and ranged between  $0.79\text{ }^{\circ}\text{C}$  to  $26.9\text{ }^{\circ}\text{C}$  ( $\text{FIGURE 23}$ ).

**FIGURE 23 – CHANGES IN MINIMUM, MEAN, AND MAXIMUM TEMPERATURES FOR THE STUDY SITE DURING JANUARY 2018 TO MARCH 2019.**



Source: The author (2021).

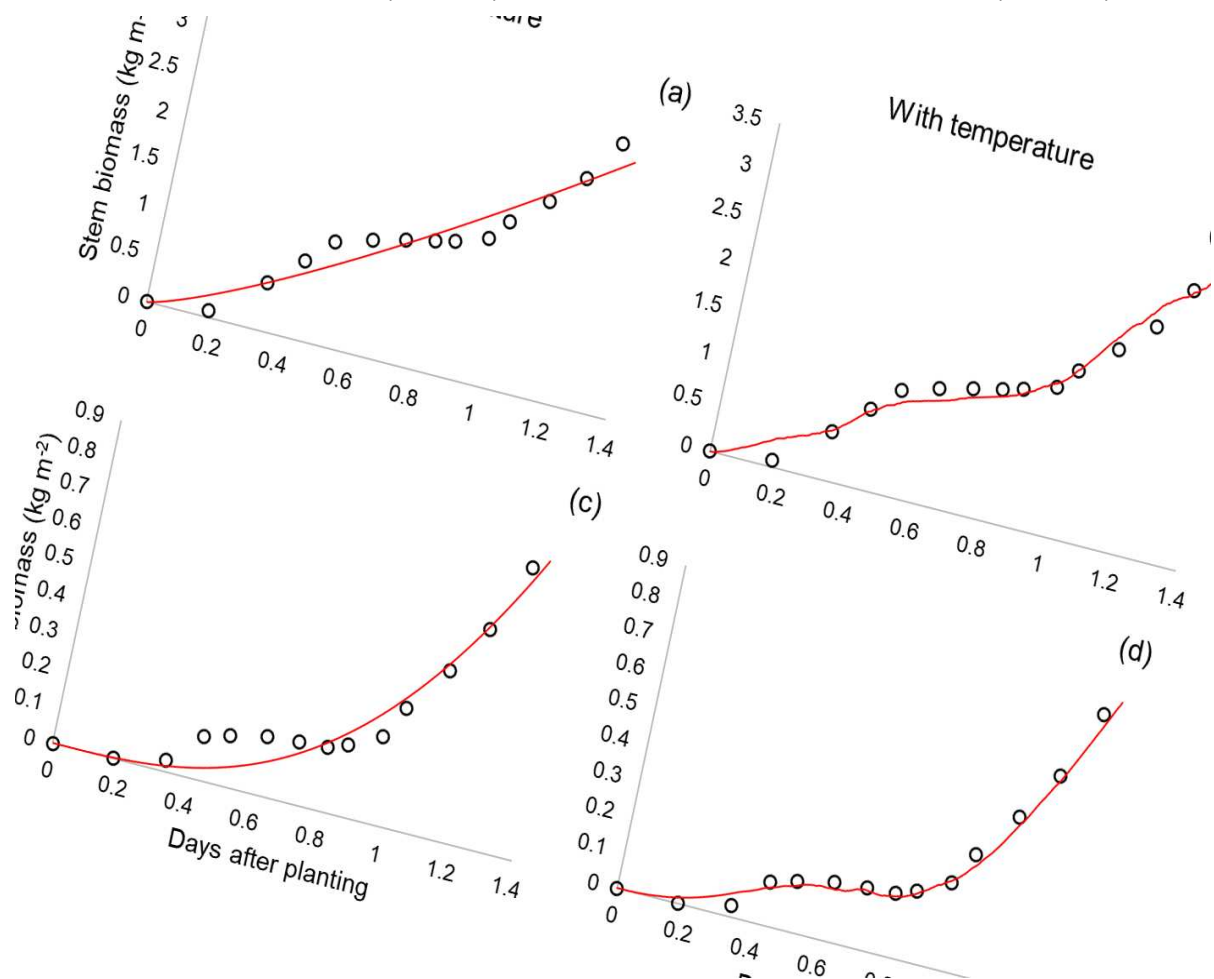
### 5.3.3 Temperature model parameters and air temperature modifier

We used the temperature modifier with the Power, Schumacher and Exponential models. The Exponential and Schumacher models showed worse RMSE

values and did not showed convergence for some genotypes. Only the Power functions showed convergence with more realistic values for cardinal temperatures.

The temperature modifier corresponded well to early growth data, with a decreasing average RMSE values from  $0.08 \text{ kg m}^{-2}$  to  $0.05 \text{ kg m}^{-2}$  (40%) in our models, regardless of genotype productivity. For example, we observed good temperature responses for two genotypes with different  $W_{\text{stem}}$  at the end of the trial (FIGURE 24). This suggested that all genotypes were influenced by the temperature range during early growth. Statistically, significance difference ( $p > 0.05$ ) was observed among eucalyptus genotypes for a, b,  $T_{\text{min}_g}$ ,  $T_{\text{opt}_g}$ ,  $T_{\text{max}_g}$ , m, and temperature amplitude ( $T_{\text{max}_g} - T_{\text{min}_g}$ ) (TABLE 10).

FIGURE 24 – VARIATION IN MEASUREMENT (SYMBOLS) AND MODELLED (LINE) STEM BIOMASS FOR EG17 (ABOVE FIGURES) AND FOR ENG20 (BELOW FIGURES) OVER THE COURSE OF THE TRIAL FOR TREES WITHOUT (a AND c) AND WITH TEMPERATURE MODIFIER (b AND d).



Source: The author (2021).



TABLE 10 – MEAN, STANDARD DEVIATION (SD), COEFFICIENT OF VARIATION (CV%), F-VALUES OF ANALYSIS OF VARIANCE BY THE p-CATEGORY <sup>1</sup>, MODEL PARAMETERS (a, b, c, T<sub>min<sub>g</sub></sub>, T<sub>opt<sub>g</sub></sub>, T<sub>max<sub>g</sub></sub>), ROOT MEAN SQUARE ERROR (RMSE) FOR *EUCALYPTUS* GENOTYPES.

Taxa	Genotype	a	b	RMSE	T <sub>min<sub>g</sub></sub>	T <sub>opt<sub>g</sub></sub>	T <sub>max<sub>g</sub></sub>	(T <sub>max<sub>g</sub></sub> – T <sub>min<sub>g</sub></sub> )	m	W <sub>stem</sub>
<i>E. globulus</i>	EG1	2.000	1.723	0.06	9.7	21.4	23.5	13.8	0.452	1.70
	EG17	2.013	1.421	0.09	10.3	15.6	21.3	11.0	0.410	2.44
	EG18	2.803	1.793	0.08	11.5	16.9	19.4	7.9	0.267	1.76
	EG19	0.722	1.664	0.03	9.1	22.2	27.7	18.7	0.511	1.02
	EG21	1.301	1.719	0.04	8.9	18.9	24.6	15.4	0.553	1.82
	EG30	1.146	1.618	0.05	7.6	19.7	22.8	15.1	0.554	1.74
	EG33	1.215	1.696	0.03	9.1	23.7	27.8	18.7	0.465	1.17
	EG34	1.005	1.235	0.05	5.7	23.4	28.0	22.4	0.567	1.53
<i>E. nitens</i>	EN12	1.109	1.581	0.05	8.2	19.7	24.4	16.2	0.570	1.51
	EN13	1.677	1.501	0.08	10.0	22.3	23.6	13.6	0.412	1.65
	EN14	0.950	1.675	0.04	6.9	18.2	25.9	19.0	0.656	1.72
<i>E gloni</i>	ENG2	1.171	1.628	0.05	8.4	20.4	26.3	17.9	0.559	1.70
	ENG3	1.426	1.711	0.08	9.3	18.9	25.0	15.7	0.554	1.89
	ENG4	2.614	1.806	0.04	10.9	25.6	26.5	15.5	0.316	1.34
	ENG5	1.378	1.523	0.07	7.7	15.6	25.4	17.6	0.548	2.16
	ENG7	1.527	1.748	0.01	10.5	27.0	28.9	18.4	0.310	0.80
	ENG8	2.523	1.771	0.04	10.6	23.7	24.6	13.9	0.329	1.26
	ENG20	0.949	1.666	0.02	7.5	22.1	29.7	22.2	0.554	0.89
	ENG22	0.079	7.80	0.02	9.4	27.6	28.3	18.9	0.312	0.49
	ENG25	1.673	1.752	0.02	10.7	25.0	28.3	17.6	0.363	0.87
Mean	1.464	1.952	0.05	9.1	21.4	25.6	16.5	0.464	1.47	
Sd	0.67	1.38	0.02	1.51	3.51	2.68	3.46	0.11	0.48	
CV%	45.78	70.89	43.29	16.58	16.40	10.50	21.03	24.72	33.00	
F-stat	3.96*	64.6**	-	1.94*	9.02**	5.94**	4.60**	4.52**	7.71**	

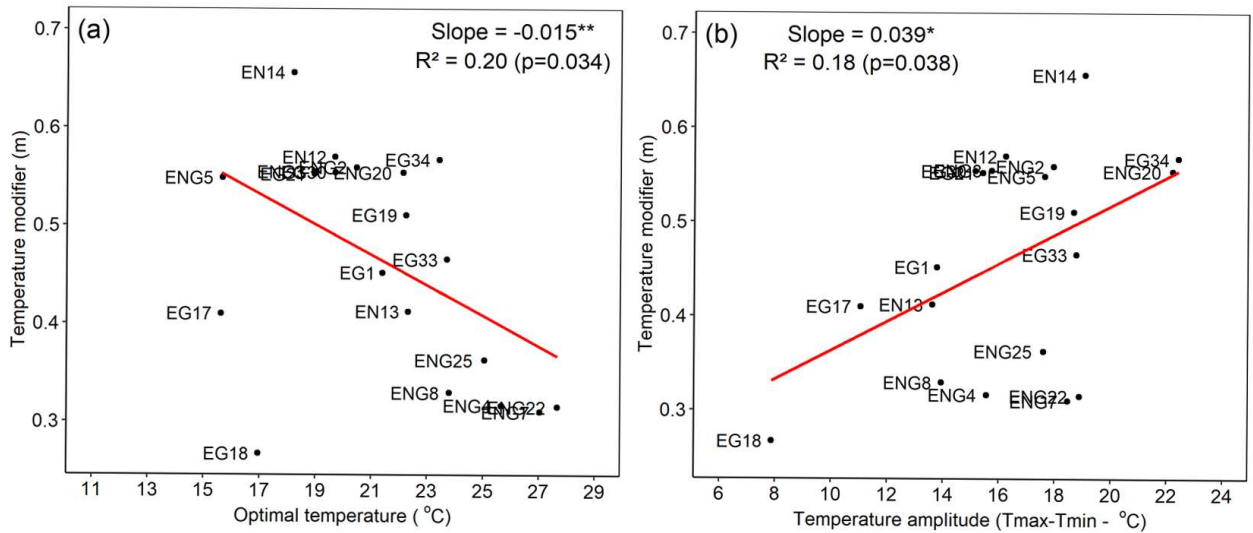
Source: The author (2021).

<sup>1</sup> \* - significant at  $p = 0.05$ ; ns – not significant at  $p = 0.05$ .

Average T<sub>opt<sub>g</sub></sub> was 21.4 °C, and ranged between 15.6 and 27.6 °C. Almost all low productivity genotypes (EG19, EG33, ENG4, ENG7, ENG20, ENG22, and ENG25) presented higher T<sub>opt<sub>g</sub></sub> (> 22 °C) than the average temperature of the experiment site (14 °C), which suggest that these genotypes were not able to achieve their full potential early growth and temperature was a limiting factor. Differently of high productivity genotypes (EG17, EN14, ENG3, and ENG5) which presented average T<sub>opt<sub>g</sub></sub> (17 °C) close to average temperature of the experiment site.

Average  $T_{min_g}$  and  $T_{max_g}$  was 9.1 °C and 25.6 °C, respectively, and they were significant different among *Eucalyptus* genotypes. The temperature modifier (m) ranged from 0.26 to 0.65, being sub-optimal for genotypes EG18 (0.26) and ENG22 (0.31), and optimal for genotypes EN12 (0.57) and EN14 (0.65). Interestingly, higher m values were not only observed for genotypes that present  $T_{opt_g}$  close to the average site air temperature but also for genotypes that presented higher cardinal temperature amplitude ( $T_{max_g} - T_{min_g}$ ) (FIGURE 25).

FIGURE 25 - RELATIONSHIP BETWEEN TEMPERATURE MODIFIER (m) WITH OPTIMAL TEMPERATURE (a), AND WITH CARDINAL TEMPERATURE AMPLITUDE ( $T_{max_g} - T_{min_g}$ ) (b).



Source: The author (2021).

At taxa level, it was only observed significant differences for  $T_{opt_g}$ ,  $T_{max_g}$  and  $W_{stem}$ . *E. nitens* presented the lowest  $T_{min_g}$  (8.4 °C),  $T_{opt_g}$  (20.1 °C) and a median cardinal temperature amplitude (16.3 °C) than other taxa, therefore higher m (0.55) was observed. *E. gloni* presented the lowest average modifier (0.42) and highest  $T_{opt_g}$  (22.9 °C) among taxa, consequently presented the lowest average  $W_{stem}$  growth (1.27 kg m<sup>-2</sup>) (TABLE 11).

TABLE 11 - MEAN, STANDARD DEVIATION (SD), COEFFICIENT OF VARIATION (CV%), F-VALUES OF ANALYSIS OF VARIANCE BY THE p-CATEGORY <sup>1</sup>, AND MODEL PARAMETERS (a, b, c, T<sub>min<sub>g</sub></sub>, T<sub>opt<sub>g</sub></sub>, T<sub>max<sub>g</sub></sub>) AT TAXA LEVEL.

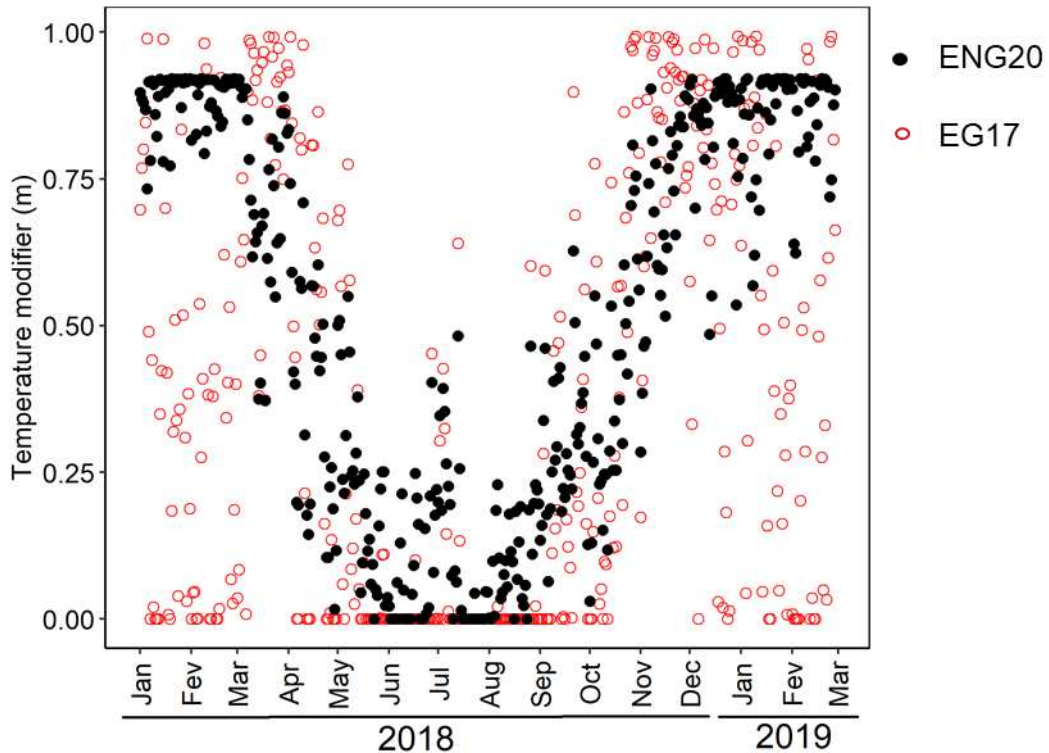
<b>Taxa</b>	<b>a</b>	<b>b</b>	<b>T<sub>min<sub>g</sub></sub></b>	<b>T<sub>opt<sub>g</sub></sub></b>	<b>T<sub>max<sub>g</sub></sub></b>	<b>(T<sub>max<sub>g</sub></sub> – T<sub>min<sub>g</sub></sub>)</b>	<b>m</b>	<b>W<sub>stem</sub></b>
<i>E. globulus</i>	1.526	1.609	9.0	20.2	24.4	15.4	0.472	1.64
<i>E. nitens</i>	1.245	1.586	8.4	20.1	24.7	16.3	0.546	1.62
<i>E. gloni</i>	1.483	2.379	9.5	22.9	27.0	17.5	0.428	1.27
Mean	1.418	1.858	8.9	21.1	25.4	16.4	0.482	1.51
Sd	0.15	0.45	0.53	1.60	1.45	1.09	0.06	0.21
CV(%)	10.64	24.28	6.03	7.63	5.72	6.62	12.38	14.00
F-stat	0.39 <sup>ns</sup>	2.46 <sup>ns</sup>	0.92 <sup>ns</sup>	4.13 <sup>*</sup>	6.14 <sup>*</sup>	1.18 <sup>ns</sup>	2.73 <sup>ns</sup>	3.78 <sup>*</sup>

Source: The author (2021).

<sup>1</sup> \* - significant at  $p = 0.05$ ; ns – not significant at  $p = 0.05$ .

As we observed in FIGURE 22, almost all genotypes presented a peak in growth during late spring (Nov-Dec), as a result, a higher air temperature modifier was observed in warmer months due to average T<sub>opt<sub>g</sub></sub> was close to 21 °C. For instance, we observed different temperature responses for two genotypes with different growth along the trial (FIGURE 26). For ENG20 (*E. gloni*), we observed a higher seasonal change in temperature modifier (m), with increment in spring and summer periods (Oct-Feb), reaching its maximum on January. In winter, we observed a higher decrease in early growth rate since T<sub>opt<sub>g</sub></sub> was 22.1 °C for this genotype. Interestingly, EG17 (*E. globulus*) did not presented the same pattern, since for this genotype T<sub>opt<sub>g</sub></sub> was 15.6 °C which is close to average air temperature for this site (14 °C). However, the smallest cardinal temperature amplitude for EG17 (11 °C), not allowed this genotype to maintain the same range of temperature responses in growth rate during seasons.

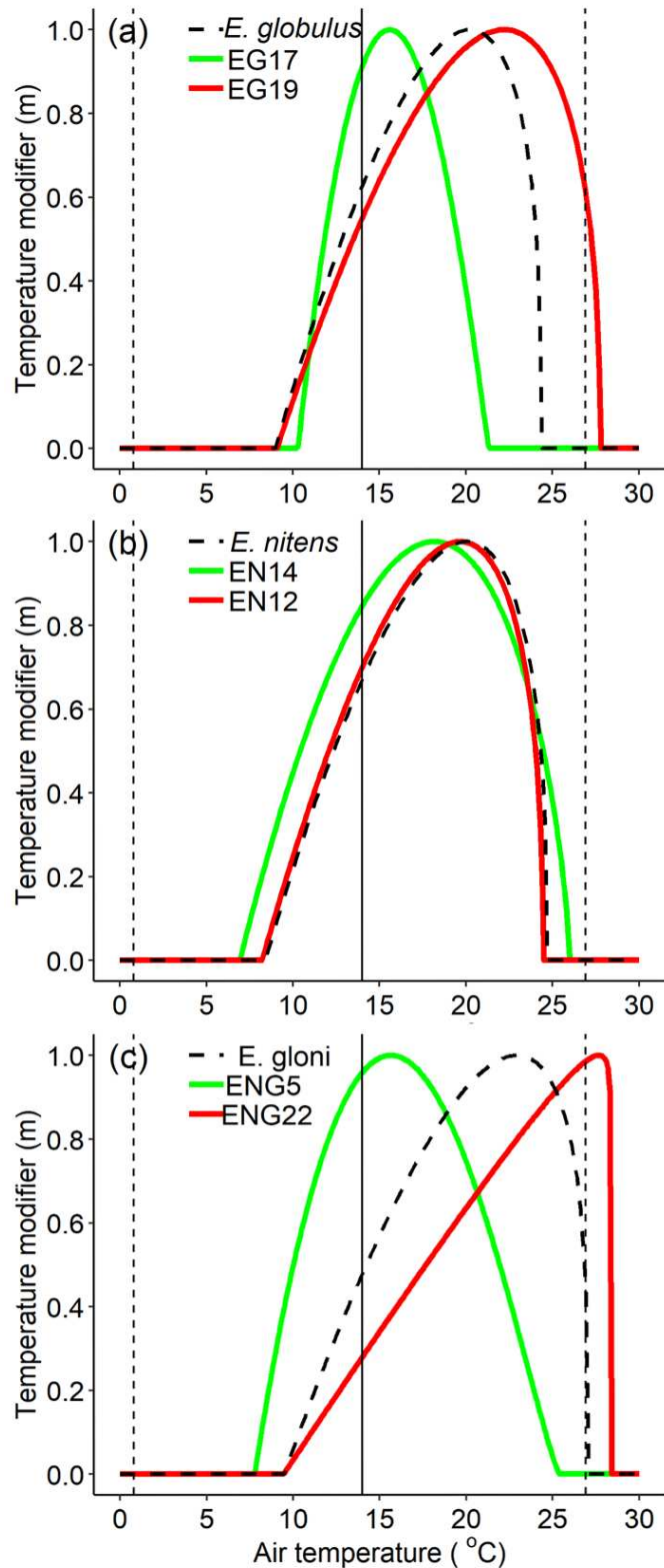
FIGURE 26 – TEMPERATURE MODIFIER OVER THE COURSE OF THE TRIAL FOR EG17 AND ENG20.



Source: The author (2021).

The temperature modifier varied markedly among *E. gloni* genotypes compared to *E. globulus* and *E. nitens* genotypes (FIGURE 27). High productivity genotypes always showed  $T_{opt_g}$  close to the mean air temperature, regardless of taxa. During early development, large differences in temperature modifier behavior were observed for *E. gloni* genotypes, since ENG22 (low productivity) presented  $T_{opt_g}$  (27.6 °C) higher than daily maximum mean air temperature (26.9 °C) for this site, differently from ENG5 (high productivity), with  $T_{opt_g}$  closer to mean air temperature of the site (15.6 vs. 14 °C). Regardless of productivity, smoothly differences were observed among *E. nitens* genotypes and their temperature amplitude were always between daily minimum and maximum mean air temperature of the site.

FIGURE 27 – AVERAGE TEMPERATURE MODIFIER (DOTTED LINE) FOR *E. globulus* (a), *E. nitens* (b), AND *E. gloni* (c) AND CONSIDERING THE HIGHEST (GREEN LINE) AND THE LOWEST (RED LINE) PRODUCTIVITY GENOTYPE FOR EACH TAXA.<sup>1</sup>



Source: The author (2021).

<sup>1</sup> Dotted lines represent the minimum (0.79 °C) and maximum (26.9 °C) mean air temperature and solid line represent the mean (14 °C) air temperature for the site.

## 5.4 DISCUSSION

The model used in study increase the precision of estimated growth along the early development with inclusion of daily mean air temperature. Since, the inclusion of environmental variables, such as temperature, in forest growth models increase the understanding of forest development in physiological point of view (Watt et al., 2010). Temperatures changes are key parameter to control photosynthetic and respiration rate, which result in forest growth (Battaglia et al., 1996), and therefore differences in carbon allocation among genotypes.

The method used in this study estimated higher average optimal temperatures (21 °C) than other studies with *E. globulus* and *E. nitens*, such as Booth and Pryor (1991) with optimal mean annual air temperatures ranging from 9-18 °C, and Watt et al. (2014), with optimal mean temperature ranging from 14-18 °C. Despite of this differences, Booth and Pryor (1991) estimated mean temperatures from the hottest months for *E. globulus* and *E. nitens* development between 20-28 °C, which is on the range of average optimal temperature estimated by our models (15-27 °C). However, when we considered optimal temperatures of high productivity genotypes among taxa (EG17, EG18, EN14, ENG3, and ENG5), average optimal temperatures were closer than mean air temperature of the site (17° vs. 14 °C).

The optimal temperature development was always above mean site air temperature (14 °C), this indicated that increase temperatures could favor stem biomass growth for some genotypes, as was observed in Coops et al. (2010) using ecophysiological model 3-PG for Douglas-Fir plantations and Way and Oren (2010) using growth temperatures in different forest biomes. On the other hand, it was observed differences in basal minimum temperature required for *Eucalyptus* genotypes grow and  $T_{min_g}$  ranged between 5.6 to 11.5 °C, with almost genotypes began to growth at 9.0 °C. Low temperature is common in subtropical regions (Watt et al., 2014; Queiroz et al., 2020) and that is the reason in winter there was a reduction in tree growth for all genotypes, because the average temperature on this period was 6.6 °C (0.8 – 10 °C). The same was observed for  $T_{max_g}$ , with average of 25.6 °C. Some genotypes, such as, EG18 (*E. globulus*) stopped growing around 19.4 °C and ENG20 (*E. gloni*) stopped growing around 29.7 °C, which is very advantageous in summer when there were warmer periods.

Temperatures above or below cardinal temperatures for plant development induced heat and chilling stress, and can impact crop productivity due changes in physiological traits. Under temperatures stress there is a reduced in chlorophyll (Chl) biosynthesis and enzyme activities, resulting in a damage of plant metabolism, growth and adaptation (Raza et al., 2021). Taking into account, large differences were also observed for amplitude of cardinal temperatures ( $T_{\max_g} - T_{\min_g}$ ), ranged between 7.8 ° and 22.4 °C. Higher amplitude of cardinal temperatures allowed genotypes maintain growth during seasonal temperature changes, and is an indication of genotypes adaptability of different environmental conditions, such as changes in annual mean air temperature (Martínez-Villegas et al., 2021), resulting in a high competitive ability against other genotypes that have lower cardinal temperature amplitude.

Our results also indicated that the best matching in *Eucalyptus* genotypes with particular site result in increase or decrease forest production (Watt et al., 2014). Nowadays, forest breeding programs result in higher specific genotypes for particular sites (Gonçalves et al., 2013) which they will respond to specific range in air temperature for optimal development (Binkley et al., 2017). Different sites could also present large range estimated cardinal temperatures and this is more important considering intra-specific genotypes (Queiroz et al., 2020). Since we observed a large difference in stem growth and temperature parameters for genotypes at the same taxa, since average taxa value was not significative and result in similar temperature responses regardless of differences in growth.

The cardinal temperatures are the inputs to process based models in forest development using a temperature modifier that reduced tree growth, such as, Sands and Landsberg (2002) which defined minimum, optimum and maximum temperatures for net photosynthesis of *E. globulus* were 7.5, 15 and 35 °C, respectively, and Pérez-Cruzado et al. (2011) for *E. nitens* were 2, 15, and 32 °C. These temperatures range were similar what was observed in our models (16.4 °C). As we observed, each genotype presented different temperature ranged for growth, and this knowledge is quite important for accurate estimated in ecophysiological models.

Overall, it has remained clear the relationship between early tree growth and cardinal temperatures, since genotypes with different accumulated stem biomass at the end of the trail showed different values of  $T_{\min_g}$ ,  $T_{\text{opt}_g}$ , and  $T_{\max_g}$ . Maybe for this particular experiment on early growth, temperature influences were not similar for all

genotypes and early stem biomass growth could not respond unique to temperature, but its interaction with other parameters could be affecting tree development, such as, genotypes photosynthetic rates, litter fall, root turnover, and carbon partitioning (Landsberg and Sands, 2011). Despite of higher model precision, there were limitations of our study that should be take into account. Dataset was in short period of time, in juvenile trees growing in higher density plots ( $\sim 6000$  tree  $\text{ha}^{-1}$ ) and one site. However, we observed a robust estimated cardinal temperature and its relation with stem growth which could be used for forest companies, considering model applicability and parameter understanding. For calibration and validation of the cardinal temperatures, we recommended add more measurements along forest development and different sites with distinct mean temperature ranges.

## 5.5 CONCLUSION

The range of favorable temperature of *Eucalyptus* early growth on this site was 5.6 to 29.7 °C, with average optimal temperature of 21.4 °C. High productivity eucalyptus genotypes (EG17, EN14, ENG3, and ENG5) maintained optimal temperatures close to mean site air temperature. On the other hand, high cardinal temperature amplitude for some *Eucalyptus* genotypes is connected to adaptation and competitive ability against other genotypes that have lower cardinal temperature amplitude, which makes them more tolerant to temperature changes along the year. Average base minimum, optimal, and base maximum temperature for *E. nitens* is similar to *E. globulus* and *E. gloni*. Cardinal temperatures results supporting the recommendation of specific genotypes in different sites, help forest plantation faced temperature increments under climate changes scenario, and are useful to produce maps of genotypes early growth along the year.



## 6 FINAL CONCLUSIONS AND CONSIDERATIONS

Climate change, mainly related to the increase in water deficit areas and extreme temperatures, is a huge threat to forest, as it causes stresses that lead to decrease in forest productivity. Therefore, the link between the three chapters of this study is genotypes differences in stem carbon allocation face of seasonal changes in temperature and the accumulation of water stress during the early development. So, we have a greater interest in increasing the planting area of tolerant and avoidance species or genotypes (White et al., 2009; Luo, 2010).

Our thesis aimed to evaluate the response of *Eucalyptus* early growth and physiology to genetic and environmental changes along the 1.5 years old of development. We divided the thesis in three chapters and some hypotheses were corroborated, partial corroborated, and not corroborated. Among different early growth rates, *Eucalyptus* has a wide variety of physiological responses to environmental conditions, being characterized as an isohydric behavior. The isohydric behavior indicates that the first response to decrease soil water is stomatal closure, consequently decreasing the photosynthetic rate, and no significative changes in midday leaf water potential (Silva et al., 2017).

In the first chapter, we observed that growth efficiency was higher during season with higher growth rate, such as fall, spring and second summer, however in second summer we observed genotype effect in the relationship of early growth and leaf area index, where for some genotypes an increment in leaf area index did not follow higher growth rate (low growth efficiency). Otherwise, this could be an advantage when we observed *E. nitens* and *E. gloni* genotypes with higher productivity did not increase leaf area index, consequently, diminish water loss by transpiration.

For early growth we observed changing in ranking of the best genotypes on each season, however these was not observed for leaf area index that presented a similar behavior during 1.5 years of development, indicating genotypes differences in stem carbon allocation face of climate changes throughout the year. Also, annual growth efficiency was not related with seasonal growth efficiency, however we observed one *E. gloni* genotype (ENG5) that was capable to maintaining higher growth efficiency along the early development, with higher growth rate and lower leaf area index.

In the second chapter, we discuss changes in physiology at leaf level during decreased soil water among *Eucalyptus* genotypes with different growth rates and accumulated water stress integral. Average photosynthesis decreased for all genotypes during soil water changes, however there was no significant relationship with growth rate and water stress integral. Interestingly that for all genotypes, leaf area index increased during soil water changes, and a possible explanation was to compensate the decrease in the photosynthetic rate. A significant relationship with accumulated water stress integral was observed only with intrinsic water use efficiency, since we observed a higher reduction in stomatal conductance and transpiration during soil water decrease (isohydric behavior).

We observed that *Eucalyptus* genotypes, mainly *E. globulus*, with higher absolute accumulated water stress integral presented lower growth rate during soil water decrease, and like season in previous chapter, water stress affected genotypes carbon allocation during soil water changes. Genotypes with higher accumulate water stress, such as *E. globulus*, were less efficient in use water at leaf level, however we observed a single *E. gloni* (ENG3) which were capable to improve growth with higher accumulate water stress and presented small changes in intrinsic water use efficiency, being less sensitive to soil water changes. However, these results should be treated carefully, since studies like Battie-Laclau et al. (2016) observed that physiological variables at leaf level did not necessarily related at tree level (growth), mainly due to different microclimatic conditions, e.g. light and temperature, of the leaves in the crown.

In third chapter, we discuss the cardinal temperature effects in early growth among *Eucalyptus* genotypes. We observed that temperature effects on early growth was high significant, since genotypes with different final stem biomass presented different cardinal air temperatures. In general, the temperature increase will be advantageous for early growth for almost all eucalyptus genotypes, because average optimal temperature was 21 °C and average air temperature was 14 °C. Also, despite of *E. nitens* has its origin in colder regions than *E. globulus* in Australia, we observed similar average values for optimal temperatures considering the taxa.

However, high productivity genotypes such as EG17, ENG3, and ENG5 presented optimal temperature closer to mean site air temperature (16 vs. 14 °C) what allowed them partitioning more carbon to stem than low productivity genotypes such as ENG20, ENG22, and ENG25 (25 vs. 14 °C) and we observed that higher amplitude

of cardinal temperatures will be an advantage for genotypes growth face air temperature changes along early development in different sites.

Finally, we observed that the same silvicultural practices and the same climate led to different growth patterns which have implied interaction between genotype and environmental and influenced carbon partitioning in *Eucalyptus*. Also, we observed that water and temperature stress operate in the same manner for early growth, since lower absolute accumulated water stress was observed for genotypes that have optimal temperatures for growth close to mean air temperature, and consequently had higher growth over 1.5 years. We conclude that this study opens the way for forest companies and research institutes to evaluate ecophysiology against forest planning, in situations of beginning of stresses in the initial development of plantations.

## REFERENCES

- ADAMS, H.D.; ZEPPEL, M.J.B.; ANDEREGG, W.R.L.; HARTMANN, H.; LANDHÄUSSER, S. M.; TISSUE, D.T.; ... MCDOWELL, N.G. A multi-species synthesis of physiological mechanisms in drought-induced tree mortality. **Nature Ecology and Evolution**, v. 1, n. 9, p. 1285–1291, 2017. Available in: <https://doi.org/10.1038/s41559-017-0248-x>. Access in: 5 July 2020.
- ALBAUGH, J.; DYE, P. J.; KING, K. *Eucalyptus* and water use in South Africa. **International Journal of Forest Research**, v. 2013, p. 1-11, 2013. Available in: <https://doi.org/10.1155/2013/852540>. Access in: 10 April 2020.
- ALLEN, C.D.; BRESHEARS, D.D.; MCDOWELL, N.G. On underestimation of global vulnerability to tree mortality and forest die-off from hotter drought in the Anthropocene. **Ecosphere**, v. 6, n. 8, p. 1–55, 2015. Available in: <https://doi.org/10.1890/ES15-00203.1>. Access in: 10 July 2020.
- ALLEN, C.D.; MACALADY, A.K.; CHENCHOUNI, H.; BACHELET, D.; MCDOWELL, N.; VENNETIER, M.; ... COBB, N. A global overview of drought and heat-induced tree mortality reveals emerging climate change risks for forests. **Forest Ecology and Management**, v. 259, n. 4, p. 660–684, 2010. Available in: <https://doi.org/10.1016/j.foreco.2009.09.001>. Access in: 6 July 2020.
- ALLEN, R.G.; JENSEN, M.E.; WRIGHT, J.L.; BURMAN, R.D. Operational estimates of reference evapotranspiration. **Agronomy Journal**, v. 81, p. 650–662, 1989. Available in: <https://doi.org/10.2134/agronj1989.00021962008100040019x>. Access in: 5 July 2020.
- ASPINWALL, M.J.; PFAUTSCH, S.; TJOELKER, M.G.; VARHAMMAR, A.; POSSELL, M.; DRAKE, J.E.; REICH, P.B.; TISSUE, D.T.; ATKIN, O.K.; RYMER, P.D.; DENNISON, S.; SLUYTER, S.C.V. Range size and growth temperature influence *Eucalyptus* species responses to an experimental heatwave. **Global Change Biology**, v. 25, p. 1665-1684, 2019. Available in: DOI: 10.1111/gcb.14590. Access in: 20 July 2020.
- BALDOCCHI, D. Measuring and modelling carbon dioxide and water vapour exchange over a temperate broad-leaved forest during the 1995 summer drought. **Plant, Cell and Environment**, v. 20, n. 9, p. 1108–1122, 1997. Available in: <https://doi.org/10.1046/j.1365-3040.1997.d01-147.x>. Access in: 20 May 2020.
- BATTAGLIA, M.; BEADLE, C.; LOUGHHEAD, S. Photosynthetic temperature responses of *Eucalyptus globulus* and *Eucalyptus nitens*. **Tree Physiology**, v. 16, p. 81–89, 1996.
- BATTAGLIA, M.; CHERRY, M.L.; BEADLE, C.L.; SANDS, P.J.; HINGSTON, A. Prediction of leaf area index in eucalypt plantations: effects of water stress and temperature. **Tree Physiology**, v. 18, p. 521–528, 1998.

BATTAGLIA, M.; SANDS, P.; WHITE, D.; MUMMERY, D. CABALA: a linked carbon, water and nitrogen model of forest growth for silvicultural decision support. **Forest Ecology and Management**, v. 193, n. 1-2, p. 251-282, 2004. Available in: <https://doi.org/10.1016/j.foreco.2004.01.033>. Access in: 25 July 2020.

BATTIE-LACLAU, P.; DELGADO-ROJAS, J.S.; CHRISTINA, M.; NOUVELLON, Y.; BOUILLET, J.P.; PICCOLO, M. de C.; MOREIRA, M. Z.; GONÇALVES, J. L. M.; ROUPSARD, O.; LACLAU, J. P. Potassium fertilization increases water-use efficiency for stem biomass production without affecting intrinsic water-use efficiency in *Eucalyptus grandis* plantations. **Forest Ecology and Management**, v. 364, p. 77-89, 2016. Available in: <https://doi.org/10.1016/j.foreco.2016.01.004>. Access in: 20 May 2020.

BINKLEY, D.; CAMPOE, O.C.; ALVARES, C.; CARNEIRO, R.L.; CEGATTA, Í.; STAPE, J.L. The interactions of climate, spacing and genetics on clonal *Eucalyptus* plantations across Brazil and Uruguay. **Forest Ecology and Management**, v. 405, p. 271-283, 2017. Available in: <https://doi.org/10.1016/j.foreco.2017.09.050>. Access in: 20 May 2020.

BINKLEY, D.; STAPE, J.L. Sustainable management of *Eucalyptus* plantations in a changing world. In: BORRALHO, N.; PEREIRA, J.S.; MARQUES, C.; COUTINHO, J.; MADEIRA, M.; TOME, M. (Ed) **Proceedings of the IUFRO Conference of Eucalyptus in a Changing World**. Aveiro, Portugal, 2004, p. 11-17.

BINKLEY, D.; STAPE, J.L.; RYAN, M.G. Thinking about efficiency of resource use in forests. **Forest Ecology and Management**, v. 193, p. 5-16, 2004. Available in: <https://doi.org/10.1016/j.foreco.2004.01.019>. Access in: 20 May 2020.

BOOTH, T.H. Eucalypt plantations and climate change. **Forest Ecology and Management**, v. 301, p. 28-34, 2013. Available in: <https://doi.org/10.1016/j.foreco.2012.04.004>. Access in: 22 May 2020.

BOOTH, T.H.; PRYOR, L.D. Climatic requirements of some commercially important eucalypt species. **Forest Ecology and Management**, v. 43, p. 47-60, 1991. Available in: 10.1016/0378-1127(91)90075-7. Access in: 15 June 2020.

BOREHAM G.R.; PALLETT, R.N. The influence of tree improvement and cultural practices on the productivity of *Eucalyptus* plantations in temperate South Africa. **South Forests**, v. 71, p. 85-93, 2009. Available in: DOI: 10.2989/SF.2009.71.2.1.816. Access in: 20 May 2020.

BORIŠEV, M.; HORAK, R.; PAJEVIĆ, S.; ORLOVIĆ, S.; NIKOLIĆ, N.; ŽUPUNSKI, M.; PILIPOVIĆ, A. Daily dynamics of photosynthetic parameters in beech population under periodical drought conditions. **Open Life Sciences**, v. 10, n. 1, p. 201-210, 2015. Available in: <https://doi.org/10.1515/biol-2015-0022>. Access in: 25 May 2020.

CAMPBELL, G.S. Extinction coefficients for radiation in plant canopies calculated using an ellipsoidal inclination angle distribution. **Agricultural and Forest Meteorology**, v. 36, p. 317-21, 1986. Available in: [https://doi.org/10.1016/0168-1923\(86\)90010-9](https://doi.org/10.1016/0168-1923(86)90010-9). Access in: 15 June 2020.

CAMPANY, C.E.; MEDLYN, B.E.; DUURSMA, R. A. Reduced growth due to belowground sink limitation is not fully explained by reduced photosynthesis. **Tree Physiology**, v. 37, n. 8, p. 1042–1054, 2017. Available in: <https://doi.org/10.1093/treephys/tpx038>. Access in: 10 June 2020.

CHAVES, M.M.; MAROCO, J.P.; PEREIRA, J.S. Understanding plant responses to drought - From genes to the whole plant. **Functional Plant Biology**, v. 30, n. 3, p. 239–264, 2003. Available in: <https://doi.org/10.1071/FP02076>. Access in: 10 June 2020.

CORREIA, B.; PINTÓ-MARIJUAN, M.; NEVES, L.; BROSSA, R.; DIAS, M.C.; COSTA, A.; ... PINTO, G. Water stress and recovery in the performance of two *Eucalyptus globulus* clones: Physiological and biochemical profiles. **Physiologia Plantarum**, v. 150, n. 4, p. 580–592, 2014. Available in: <https://doi.org/10.1111/ppl.12110>. Access in: 1 June 2020.

COOPS, N.C.; HEMBER, R.A.; WARING, R.H. Assessing the impact of current and projected climates on Douglas-Fir productivity in British Columbia, Canada, using a process-based model (3-PG). **Canadian Journal of Forestry Research**, v. 40, p. 511–524, 2010. Available in: doi:10.1139/X09-201. Access in: 1 June 2020.

DRAKE P.L.; MENDHAM, D.S.; WHITE, D. A.; OGDEN, G.N. A comparison of growth, photosynthetic capacity and water stress in *Eucalyptus globulus* coppice regrowth and seedlings during early development. **Tree Physiology**, v. 29, p. 663–674, 2009. Available in: doi:10.1093/treephys/tpp006. Access in: 20 May 2020.

DU TOIT, B.; DOVEY, S.B. Effect of site management on leaf area, early biomass development, and stand growth efficiency of a *Eucalyptus grandis* plantation in South Africa. **Canadian Journal of Forestry Research**, v. 35, p. 891–900, 2005. Available in: DOI: 10.1139/X04-205. Access in: 20 May 2020.

ELIAS, P.; BOUCHER, D. **Planting for the Future: How Demand for Wood Products Could be Friendly to Tropical Forests**. Union of Concerned Scientists. 29 p. 2014.

ELLI, E. F.; SENTELHAS, P. C.; BENDER, F. D.; Impacts and uncertainties of climate change projections on *Eucalyptus* plantations productivity across Brazil. **Forest Ecology and Management**, v. 474, p. 118365, 2020. Available in: <https://doi.org/10.1016/j.foreco.2020.118365>. Access in: 20 August 2020.

FAROOQ, M.; WAHID, A.; KOBAYASHI, N.; FUJITA, D.; BASRA, S.M.A. Plant drought stress: effects , mechanisms and management. **Agronomy for Sustainable Development**, v. 29, n. 1, p. 185–212, 2009. Available in: <https://doi.org/10.1051/agro:2008021>. Access in: 20 May 2020.

FARQUHAR, G.D.; EHLERINGER, J.R.; HUBICK, T. Carbon isotope discrimination and photosynthesis. **Annual Review of Plant Physiology and Plant Molecular Biology**, v. 40, p. 503–537, 1989. Available in: <https://doi.org/10.1146/annurev.pp.40.060189.002443>. Access in: 21 May 2020.

FLEXAS, J.; BOTA, J.; LORETO, F.; CORNIC, G.; SHARLEY, T.D. Diffuse and metabolic limitations to photosynthesis under drought and salinity in C3 plants. **Plant Biology**, v. 6, p. 269-279, 2004. Available in: <https://doi.org/10.1055/s-2004-820867>. Access in: 21 May 2020.

GALINDO, A.; CALÍN-SÁNCHEZ, Á.; GRIÑÁN, I.; RODRÍGUEZ, P.; CRUZ, Z.N.; GIRÓN, I.F.; CORELL, M.; MARTÍNEZ-FONT, R.; MORIANA, A.; CARBONELL-BARRACHINA, A.A.; TORRECILLAS, A.; HERNÁNDEZ, F. Water stress at the end of the pomegranate fruit ripening stage produces earlier harvest and improves fruits quality. **Scientia Horticulturae**, v. 226, p. 68-74, 2017. Available in: <http://dx.doi.org/10.1016/j.scienta.2017.08.029>. Access in: 25 May 2020.

GAUDRY, M.J.I.; DAGENAIS, M.G. Heteroscedasticity and the use of Box-Cox transformations. **Economics Letters**, v. 2, p. 225-229, 1979. Available in: [https://doi.org/10.1016/0165-1765\(79\)90026-0](https://doi.org/10.1016/0165-1765(79)90026-0). Access in: 26 June 2020.

GAUTHIER, M. M.; JACOBS, D. F. Ecophysiological drivers of hardwood plantation diameter growth under non-limiting light conditions. **Forest Ecology and Management**, v. 419–420, p. 220–226, 2018. Available in: <https://doi.org/10.1016/j.foreco.2018.03.036>. Access in: 5 May 2020.

GEORGE, R.; GULLSTRÖM, M.; MANGORA, M. M.; MTOLERA, M. S. P.; BJÖRK, M. High midday temperature stress has stronger effects on biomass than on photosynthesis: A mesocosm experiment on four tropical seagrass species. **Ecology and Evolution**, v. 8, n. 9, p. 4508–4517, 2018. Available in: <https://doi.org/10.1002/ece3.3952>. Access in: 12 May 2020.

GONÇALVES, J.L.M.; ALVARES, C.A.; HIGA, A.R.; SILVA, L.D.; ALFENAS, A.C.; STAHL, J.; FERRAZ, S.F.B.; LIMA, W.P.; BRANCALION, P.H.S.; HUBNER, A.; BOUILLET, J.P.; LACLAU, J.P.; NOUVELLON, Y.; EPRON, D. Integrating genetic and silvicultural strategies to minimize abiotic and biotic constraints in Brazilian eucalypt plantations. **Forest Ecology and Management**, v. 301, p. 6-27, 2013. Available in: <http://dx.doi.org/10.1016/j.foreco.2012.12.030>. Access in: 5 May 2020.

GONÇALVES, J. L. M.; ALVARES, C. A.; ROCHA, J. H. T.; BRANDANI, C. B.; HAKAMADA, R. Eucalypt plantation management in regions with water stress. **Southern Forests**, v. 79, n. 3, p. 169–183, 2017. Available in: <https://doi.org/10.2989/20702620.2016.1255415>. Access in: 5 May 2020.

GONZALEZ-BENECKE, C. A.; DINGER, E. J. Use of water stress integral to evaluate relationships between soil moisture, plant water stress and stand productivity in young Douglas-fir trees. **New Forests**, v. 49, n. 6, p. 775–789, 2018. Available in: <https://doi.org/10.1007/s11056-018-9657-1>. Access in: 6 May 2020.

HAKAMADA, R.E.; HUBBARD, R.M.; STAPE, J.L.; LIMA, W.P.; MOREIRA, G.G.; FERRAZ, S.F.B. Stocking effects on seasonal tree transpiration and ecosystem water balance in a fast-growing *Eucalyptus* plantation in Brazil. **Forest Ecology and Management**, v. 466, 118149, 2020a. Available in: <https://doi.org/10.1016/j.foreco.2020.118149>. Access in: 6 May 2020.

HAKAMADA, R.E.; HUBBARD, R.M.; MOREIRA, G.G.; STAPE, J.L.; CAMPOE, O.; FERRAZ, S.F.B. Influence of stand density on growth and water use efficiency in *Eucalyptus* clones. **Forest Ecology and Management**, v. 466, 118125, 2020b. Available in: <https://doi.org/10.1016/j.foreco.2020.118125>. Access in: 15 May 2020.

HAKAMADA, R.; HUBBARD, R. M.; FERRAZ, S.; STAPE, J.L.; LEMOS, C. Biomass production and potential water stress increase with planting density in four highly productive clonal *Eucalyptus* genotypes. **Southern Forests**, v. 79, n. 3, p. 251–257, 2017. Available in: <https://doi.org/10.2989/20702620.2016.1256041>. Access in: 6 May 2020.

HARRAND L.; VARGAS HERNÁNDEZ, J.J.; LÓPEZ UPTON, J.; RAMIREZ VALVERDE, G. Genetic parameters of growth traits and wood density in *Eucalyptus grandis* progenies planted in Argentina. **Silvae Genetica**, v. 58, p. 11–19, 2009. Available in: DOI:10.1515/sg-2009-0002. Access in: 5 May 2020.

HATFIELD, J.L.; PRUEGER, J.H. Temperature extremes: effects on plant growth and development. **Weather and Climate Extremes**, v. 10, p. 4-10, 2015. Available in: <http://dx.doi.org/10.1016/j.wace.2015.08.001>. Access in: 5 May 2020.

HÉROULT, A.; LIN, Y.S.; BOURNE, A.; MEDLYN, B.E.; ELLSWORTH, D.S. Optimal stomatal conductance in relation to photosynthesis in climatically contrasting *Eucalyptus* species under drought. **Plant, Cell and Environment**, v. 36, n. 2, p. 262–274, 2013. Available in: <https://doi.org/10.1111/j.1365-3040.2012.02570.x>. Access in: 5 May 2020.

INSTITUTO FORESTAL (INFLOR). **Anuario Forestal: Chilean Statistical Yearbook of Forestry**. Santiago, Chile, n. 174, 274 p. 2020.

INSTITUTO DE INVESTIGACIONES AGROPECUARIAS (INIA). **Mapa Agroecológico de Chile**, 1989.

IPCC. **Climate Change 2014 Synthesis Report. Contribution of Working Groups I, II and III to the Fifth Assessment Report of the Intergovernmental Panel on Climate Change** (L. . Team, Core Writing, Pachauri, R.K., Meyer, ed.). Geneva, 2014.

KHOURY, S.; COOMES, D.A.; Resilience of Spanish forests to recent drought and climate change. **Global Change Biology**, v. 26, p. 7079-7098, 2020. Available in: 10.1111/gcb.15268. Access in: 15 May 2020.

KIMBERLEY, M.O.; RICHARDSON, B. Importance of seasonal growth patterns in modelling interactions between radiata pine and some common weed species. **Canadian Journal of Forest Research**, v. 34, n. 1, p. 184–194, 2004. Available in: doi: 10.1139/X03-201. Access in: 1 May 2020.

KOLB, T. E.; STONE, J. E. Differences in leaf gas exchange and water relations among species and tree sizes in an Arizona pine-oak forest. **Tree Physiology**, v. 20, n. 1, p. 1–12, 2000. Available in: <https://doi.org/10.1093/treephys/20.1.1>. Access in: 10 May 2020.



LACLAU, J.P.; ALMEIDA, J.C.R.; GONÇALVES, J.L.M.; SAINT-ANDRÉ, L.; VENTURA, M.; RANGER, J.; MOREIRA, R.M.; NOUVELLON, Y. Influence of nitrogen and potassium fertilization on leaf lifespan and allocation of above-ground growth in *Eucalyptus* plantations. **Tree Physiology**, v. 29, p. 111–124, 2008. Available in: doi:10.1093/treephys/tpn010. Access in: 8 June 2020.

LANDSBERG, J.J.; SANDS, P.J. **Physiological ecology of forest production: principles, processes and models**. Amsterdam, the Netherlands: Elsevier/Academic Press, 2011.

LANDSBERG, J.; WARING, R. Water relations in tree physiology: Where to from here? **Tree Physiology**, v. 37, n. 1, p. 18–32, 2017. Available in: <https://doi.org/10.1093/treephys/tpw102>. Access in: 11 June 2020.

LANDSBERG, J.J.; WARING, R.H. A Generalized Model of Forest Productivity Using Simplified Concepts of Radiation-Use Efficiency, Carbon Balance and Partitioning. **Forest Ecology and Management**, v. 95, n. 3, p. 209–228, 1997. Available in: [https://doi.org/10.1016/S0378-1127\(97\)00026-1](https://doi.org/10.1016/S0378-1127(97)00026-1). Access in: 11 May 2020.

LE MAIRE G.; GUILLEMOT, J.; CAMPOE, O.C.; STAPE, J.L.; LACLAU, J.P.; NOUVELLON, Y. Light absorption, light use efficiency and productivity of 16 contrasted genotypes of several *Eucalyptus* species along a 6-year rotation in Brazil. **Forest Ecology and Management**, v. 449, 117443, 2019. Available in: <https://doi.org/10.1016/j.foreco.2019.06.040>. Access in: 8 May 2020.

LÉVESQUE, M.; SAURER, M.; SIEGWOLF, R.; EILMANN, B.; BRANG, P.; BUGMANN, H.; RIGLING, A. Drought response of five conifer species under contrasting water availability suggests high vulnerability of Norway spruce and European larch. **Global Change Biology**, v. 19, n. 10, p. 3184–3199, 2013. Available in: <https://doi.org/10.1111/gcb.12268>. Access in: 15 May 2020.

LÉVESQUE, M.; SIEGWOLF, R.; SAURER, M.; EILMANN, B.; RIGLING, A. Increased water-use efficiency does not lead to enhanced tree growth under xeric and mesic conditions. **New Phytologist**, v. 203, n. 1, p. 94–109, 2014. Available in: <https://doi.org/10.1111/nph.12772>. Access in: 11 May 2020.

LIM, H.; ALVARES, C.A.; RYAN, M.G.; BINKLEY, D. Assessing the cross-site and within-site response of potential production to atmospheric demand for water in *Eucalyptus* plantations. **Forest Ecology and Management**, v. 464, 118068, 2020. Available in: <https://doi.org/10.1016/j.foreco.2020.118068>. Access in: 5 May 2020.

LUO, L.J. Breeding for water-saving and drought-resistance rice (WDR) in China. **Journal of Experimental Botany**, v. 61, n. 13, p. 3509–3517, 2010. Available in: <https://doi.org/10.1093/jxb/erq185>. Access in: 11 May 2020.

LUO J.; ZHOU, G.; WU, B.; CHEN, D.; CAO, J.; LU, W.; PEGG, R.E.; ARNOLD, R.J. Genetic variation and age-age correlations of *Eucalyptus grandis* at Dongmen Forest Farm in southern China. **Australian Forestry**, v. 73, p. 67–80, 2010. Available in: <http://dx.doi.org/10.1080/00049158.2010.10676312>. Access in: 11 May 2020.

MARTÍNEZ-VILLEGAS, J. A.; CASTILHO-ARGÜERO, S.; MÁRQUEZ-GUZMÁN, J.; OROZCO-SEGOVIA, A. The plasticity of the germinative response in the populations of two xeric species inhabiting two contrasting environments of central Mexico. **Plant Species Biology**, v. 36, n. 2, p. 295-307, 2021. Available in: <https://doi.org/10.1111/1442-1984.12313>. Access in: 8 June 2021.

MARTORELL, S.; DIAZ-ESPEJO, A.; MEDRANO, H.; BALL, M.C.; CHOAT, B. Rapid hydraulic recovery in *Eucalyptus pauciflora* after drought: Linkages between stem hydraulics and leaf gas exchange. **Plant, Cell and Environment**, v. 37, n. 3, p. 617–626, 2014. Available in: <https://doi.org/10.1111/pce.12182>. Access in: 10 May 2020.

MCMAHON, T.A.; PEEL, M.C.; LOWE L.; SRIKANTHAN, R.; MCVICAR, T.R. Estimating actual, potential, reference crop and pan evaporation using standard meteorological data: a pragmatic synthesis. **Hydrology and Earth System Sciences**, v. 17, p. 1331–1363, 2013. Available in: <https://doi.org/10.5194/hess-17-1331-2013>. Access in: 11 May 2020.

MCMURTRIE, R.E.; GHOLZ, H.L.; LINDER, S.; GOWER, T. Climatic factors controlling the productivity of pine stands: a model-based analysis. **Ecological Bulletins**, v. 43, p. 173–188, 1994.

MCMURTRIE, R.E.; ROOK, D.A.; KELLIHER, F.M. Modelling the Yield of *Pinus radiata* on a Site Limited by Water and Nitrogen. **Forest Ecology and Management**, v. 30, n. 1-4, p. 381-413, 1990. Available in: [https://doi.org/10.1016/0378-1127\(90\)90150-A](https://doi.org/10.1016/0378-1127(90)90150-A). Access in: 13 May 2020.

MERCHANT, A.; CALLISTER, A.; ARNDT, S.; TAUSZ, M.; ADAMS, M. Contrasting physiological responses of six *Eucalyptus* species to water deficit. **Annals of Botany**, v. 100, n. 7, p. 1507–1515, 2007. Available in: <https://doi.org/10.1093/aob/mcm234>. Access in: 12 May 2020.

MITCHELL, R.J.; ZUTTER, B.R.; GJERSTAD, D.H.; GLOVER, G.R.; WOOD, C.W. Competition among Secondary-Successional Pine Communities: A Field Study of Effects and Responses. **Ecology**, v. 80, n. 3, p. 857-872, 1999. Available in: <https://www.jstor.org/stable/177023>. Access in: 10 May 2020.

MOKOTEDI, M.E.O. Physiological responses of *Eucalyptus nitens x nitens* under experimentally imposed water stress. **Southern Forests**, v. 72, n. 2, p. 63-68, 2010. Available in: <https://doi.org/10.2989/20702620.2010.507017>. Access in: 8 May 2020.

MU, H.; JIANG, D.; WOLLENWEBER, B.; DAI, T.; JING, Q.; CAO, W. Long-term low radiation decreases leaf photosynthesis photochemical efficiency and grain yield in winter wheat. **Journal of Agronomy and Crop Science**, v. 196, p. 38–47, 2010. Available in: DOI:10.1111/j.1439-037X.2009.00394.x. Access in: 12 May 2020.

MYERS, B. J. Water stress integral. A link between short-term stress and long-term growth. **Tree Physiology**, v. 4, p. 315–323, 1988.

MYERS, B. J.; LANDSBERG, J. J. Water stress and seedling growth of two eucalypt species from contrasting habitats. **Tree Physiology**, v. 5, n .2, p. 207–218, 1989. Available in: <https://doi.org/10.1093/treephys/5.2.207>. Access in: 12 May 2020.

NAVARRETE-CAMPOS, D.; BRAVO, L.A.; RUBILAR, R.A.; EMHART, V.; SANHUEZA, R. Drought effects on water use efficiency, freezing tolerance and survival of *Eucalyptus globulus* and *Eucalyptus globulus* × *nitens* cuttings. **New Forests**, v. 44, n. 1, p. 119–134, 2013. Available in: <https://doi.org/10.1007/s11056-012-9305-0>. Access in: 12 May 2020.

NORMAN, J.M.; JARVIS, P.G. Photosynthesis in Sitka Spruce (*Picea sitchensis* (Bong.) Carr.) V. Radiation Penetration theory and a test case. **Journal of Applied Ecology**, v.12, p. 839-878, 1975. Available in: <https://doi.org/10.2307/2402094>. Access in: 8 June 2021.

OLIVEIRA, T.W.G.; PAULA, R.C.; MORAES, M.L.T.; ALVARES, C.A.; MIRANDA, A.C.; SILVA, P.H.M. Stability and adaptability for wood volume in the selection of *Eucalyptus saligna* in three environments. **Pesquisa Agropecuaria Brasileira**, v.53, p. 611–619, 2018. Available in: <https://doi.org/10.1590/S0100-204X2018000500010>. Access in: 16 May 2020.

PAYN, T.; CARNUS, J.M.; FREER-SMITH, P.; KIMBERLEY, M.; KOLLERT, W.; LIU, S.; ORAZIO C.; RODRIGUEZ, L.; SILVA, L.N.; WINGFIELD, M.J. Changes in planted forests and future global implications. **Forest Ecology and Management**, v. 352, p. 57–67, 2015. Available in: <https://doi.org/10.1016/j.foreco.2015.06.021>. Access in: 5 April 2020.

PEREZ-CRUZADO, C.; MUNOZ-SAEZ, F.; BASURCO, F.; RIESCO, G.; RODRIGUEZ-SOALLEIRO, R. Combining empirical models and the process-based model 3-PG to predict *Eucalyptus nitens* plantations growth in Spain. **Forest Ecology and Management**, v. 262, n. 6, p. 1067–1077, 2011. Available in: doi:10.1016/j.foreco.2011.05.045. Access in: 10 May 2020.

QUEIROZ, T.B.; CAMPOE, O.C.; MONTES, C.R.; ALVARES, C.A.; CUARTAS, M.Z.; GUERRINI, I.A. Temperature thresholds for *Eucalyptus* genotypes growth across tropical and subtropical ranges in South America. **Forest Ecology and Management**, v. 472, 118248, 2020. Available in: <https://doi.org/10.1016/j.foreco.2020.118248>. Access in: 8 May 2020.

R Core Development Team. **R: A Language and Environment for Statistical Computing**. R Foundation for Statistical Computing, Vienna, 2019. < <http://www.R-project.org> > Access in: 7 July 2020.

RAZA, A.; TABASSUM J.; KUDAPA, H.; VARSHNEY, R.K. Can omics deliver temperature resilient ready-to-grow crops? **Critical Reviews in Biotechnology**, p. 1-24, 2021. Available in: <https://doi.org/10.1080/07388551.2021.1898332>. Access in: 8 June 2021.

ROCKWOOD, D. L.; RUDIE, A. W.; RALPH, S. A.; ZHU, J. Y.; WINANDY, J. E. Energy product options for *Eucalyptus* species grown as short rotation woody crops.

**International Journal of Molecular Sciences**, v. 9, n. 8, p. 1361-1378, 2008. Access in: 8 April 2020.

RUBILAR, R.; HUBBARD, R.; EMHART, V.; MARDINES, O.; QUIROGA, J.J.; MEDINA, A.; VALENZUELA, H.; ESPINOZA, J.; BURGOS, Y.; BOZO, D. Climate and water availability impacts on early growth and growth efficiency of *Eucalyptus* genotypes: The importance of GxE interactions. **Forest Ecology and Management**, v. 458, 117763, 2020. Available in: <https://doi.org/10.1016/j.foreco.2019.117763>. Access in: 8 April 2020.

RYAN, M.G. Temperature and tree growth. **Tree Physiology**, v. 30, p. 667-668, 2010. Available in: doi:10.1093/treephys/tpq033. Access in: 8 June 2020.

RYAN, M.G.; STAPE, J.L.; BINKLEY, D.; FONSECA, S.; LOOS, R.A.; TAKAHASHI, E.N.; SILVA, R.C.; SILVA, S.R.; HAKAMADA, R.E.; FERREIRA, J.M.; LIMA, A.M.N.; GAVA, J.L.; LEITE, F.P.; ANDRADE, H.B.; ALVES, J.M.; SILVA, G.G.C. Factors controlling *Eucalyptus* productivity: How water availability and stand structure alter production and carbon allocation. **Forest Ecology and Management**, v. 259, p. 1695–1703, 2010. Available in: <https://doi.org/10.1016/j.foreco.2010.01.013>. Access in: 8 May 2020.

SAADAoui, E.; BEN YAHIA, K.; DHAHRI, S.; BEN JAMAA, M. L.; KHOUJA, M. L. An overview of adaptive responses to drought stress in *Eucalyptus* spp. **Forestry Studies**, v. 67, n. 1, p. 86–96, 2017. Available in: <https://doi.org/10.1515/fsmu-2017-0014>. Access in: 15 May 2020.

SANDS, P.J.; LANDSBERG, J.J. Parameterization of 3-PG for plantation grown *Eucalyptus globulus*. **Forest Ecology and Management**, v. 163, n. 1, p. 273–292, 2002.

SANTOS, R. K. A.; CAIRO, P.A.R.; BARBOSA, R. P.; LACERDA, J.de J.; NETO, C. da S. M.; MACEDO, T.H. de J. Physiological responses of eucalyptus urophylla young plants treated with biostimulant under water deficit. **Ciencia Florestal**, v. 29, n. 3, p. 1072–1081, 2019. Available in: <https://doi.org/10.5902/1980509826206>. Access in: 6 May 2020.

SARAVANAN, S.; Gas Exchange Characteristics and Water Use Efficiency in *Eucalyptus* Clones. **Journal of Stress Physiology & Biochemistry**, v. 14, n. 3, p. 49–58, 2018.

SARRICOLEA, P.; HERRERA-OSSANDON, M.; MESEGUER-RUIZ, O. Climatic regionalisation of continental Chile. **Journal of Maps**, v. 13, n. 2, p. 66-73, 2017. Available in: <https://doi.org/10.1080/17445647.2016.1259592>. Access in: 10 October 2020.

SILVA, M.; RUBILAR, R.; ESPINOZA, J.; YÁNEZ, M.; EMHART, V.; QUIROGA, J.J. Respuesta en parámetros de intercambio gaseoso y supervivencia en plantas jóvenes de genotipos comerciales de *Eucalyptus* spp sometidas a déficit hídrico. **Bosque**, v. 38, n. 1, p. 79–87, 2017. Available in: <https://doi.org/10.4067/S0717-92002017000100009>. Access in: 4 May 2020.

SILVA, P.H.M.; CAMPOE, O.C.; PAULA, R.C.; LEE, D.J. Seedling growth and physiological responses of sixteen eucalypt taxa under controlled water regime. **Forests**, v. 7, n. 6, p. 1–13, 2016. Available in: <https://doi.org/10.3390/f7060110>. Access in: 3 May 2020.

SMETHURST, P.; BAILLIE, C.; CHERRY, M.; HOLZ, G. Fertilizer effects on LAI and growth of four *Eucalyptus nitens* plantations. **Forest Ecology and Management**, v. 176, p. 531–542, 2003.

SOIL SURVEY STAFF. **Soil Taxonomy: A Basic System of Soil Classification for Making and Interpreting Soil Surveys**. United States Department of Agriculture, Natural Resources Conservation Service, 2nd edition, 1999, 886 p.

STAPE, J.L.; BINKLEY, D.; RYAN, M.G. *Eucalyptus* production and the supply, use and efficiency of use of water, light and nitrogen across a geographic gradient in Brazil. **Forest Ecology and Management**, v. 193, p. 17–31, 2004. Available in: <https://doi.org/10.1016/j.foreco.2004.01.020>. Access in: 2 May 2020.

STAPE, J.L.; BINKLEY, D.; RYAN, M.G. Production and carbon allocation in a clonal *Eucalyptus* plantation with water and nutrient manipulations. **Forest Ecology and Management**, v. 255, n. 3–4, p. 920–930, 2008. Available in: <https://doi.org/10.1016/j.foreco.2007.09.085>. Access in: 5 May 2020.

STAPE, J.L.; BINKLEY, D.; RYAN, M.G.; FONSECA, S.; LOOS, R.A.; TAKAHASHI, E.N.; SILVA, C.R.; SILVA, S.R.; HAKAMADA, R.E.; FERREIRA, J.M.A.; LIMA, A.M.N.; GAVA, J.L.; LEITE, F.P.; ANDRADE, H.B.; ALVES, J.M.; SILVA, G.G.C.; AZEVEDO, M.R. The Brazil *Eucalyptus* Potential Productivity Project: Influence of water, nutrients and stand uniformity on wood production. **Forest Ecology and Management**, v. 259, n. 9, p. 1684–1694, 2010. Available in: <https://doi.org/10.1016/j.foreco.2010.01.012>. Access in: 5 May 2020.

SZOTA, C.; FARRELL, C.; KOCH, J.M.; LAMBERS, H.; VENEKLAAS, E.J. Contrasting physiological responses of two co-occurring eucalypts to seasonal drought at restored bauxite mine sites. **Tree Physiology**, v. 31, n. 10, p. 1052–1066, 2011. Available in: <https://doi.org/10.1093/treephys/tpr085>. Access in: 15 May 2020.

TOMÉ, M.; TOMÉ, J.A.; ARAÚJO, M.C.; PEREIRA, J.S. Intraspecific competition in irrigated and fertilized eucalypt plantations. **Forest Ecology and Management**, v. 69, p. 211–218, 1994.

TAIZ, L.; ZEIGER, E.; MOLLER, I.; MURPHY, A. **Fisiologia e Desenvolvimento Vegetal** (6th edição; Artmed, ed.), 2017. Available in: [https://doi.org/10.1007/978-3-642-32304-1\\_19](https://doi.org/10.1007/978-3-642-32304-1_19). Access in: 1 May 2020.

TAFUR, M.S.M.; HERRERA, N.M.R.; MESA, J.B.U.; ESPINOSA, D.M.I.; DUQUE, C.M.Z. Effect of soil water availability on gas exchange in young trees of *Eucalyptus grandis* W. Hill ex Maiden. **Acta Agronómica**, v. 66, n. 4, p. 549–557, 2017. Available in: <https://doi.org/10.15446/acag.v66n4.58194>. Access in: 5 May 2020.

VICENTE-SERRANO, S. M.; GOUVEIA, C.; CAMARERO, J. J.; BEGUERÍA, S.; TRIGO, R.; LÓPEZ-MORENO, J. I.; AZORÍN-MOLINA, C.; PASHO, E.; LORENZO-LACRUZ, J.; REVUELTO, J.; MORÁN-TEJEDA, E.; SANCHEZ-LORENZO, A. Response of vegetation to drought time-scales across global land biomes. **Proceedings of the National Academy of Sciences of the United States of America**, v. 110, n. 1, p. 52–57, 2013. Available in: <https://doi.org/10.1073/pnas.1207068110>. Access in: 7 May 2020.

WAGHORN, M. J.; WHITEHEAD, D.; WATT, M. S.; MASON, E. G.; HARRINGTON, J. J. Growth, biomass, leaf area and water-use efficiency of juvenile *Pinus radiata* in response to water deficits. **New Zealand Journal of Forestry Science**, v. 45, n. 1, 2015. Available in: <https://doi.org/10.1186/s40490-015-0034-y>. Access in: 18 May 2020.

WANG, Z.; DU, A.; XU, Y.; ZHU, W.; ZHANG, J. Factors Limiting the Growth of *Eucalyptus* and the Characteristics of Growth and Water Use under Water and Fertilizer Management in the Dry Season of Leizhou Peninsula, China. **Agronomy**, v. 9, 2019. Available in: <https://doi.org/10.3390/agronomy9100590>. Access in: 8 May 2020.

WANG, Z.; GRANT, R. F.; ARAIN, M. A.; BERNIER, P. Y.; CHEN, B.; CHEN, J. M.; GOVIND, A.; GUINDON, L.; KURZ, W. A.; PENG, C.; PRICE, D. T.; STINSON, G.; SUN, J.; TROFYMOWE, J. A.; YELURIPATI, J. Incorporating weather sensitivity in inventory-based estimates of boreal forest productivity: A meta-analysis of process model results. **Ecological Modelling**, v. 260, p. 25–35, 2013. Available in: doi:10.1016/j.ecolmodel.2013.03.016. Access in: 7 March 2020.

WARING, R. H.; LANDSBERG, J. J. Generalizing plant-water relations to landscapes. **Journal of Plant Ecology**, v. 4, n. 1–2, p. 101–113, 2011. Available in: <https://doi.org/10.1093/jpe/rtq041>. Access in: 18 June 2020.

WARING, R.; LANDSBERG, J.; LINDER, S. Tamm Review: Insights gained from light use and leaf growth efficiency indices. **Forest Ecology and Management**, v. 379, p. 232–242, 2016. Available in: <https://doi.org/10.1016/j.foreco.2016.08.023>. Access in: 10 May 2020.

WARING, R.H.; THIES, W.G.; MUSCATO, D. Stem growth per unit of leaf area: A measure of tree vigor. **Forest Science**, v. 26, p. 112–117, 1980.

WATT, M.; PALMER, D.J.; KIMBERLEY, M.O.; HOCK, B.K.; PAYN, T.W.; LOWE, D.J. Development of models to predict *Pinus radiata* productivity throughout New Zealand. **Canadian Journal of Forest Research**, v. 40, p. 488–499, 2010. Available in: doi:10.1139/X09-207. Access in: 18 May 2020.

WATT, M.S.; RUBILAR, R.; KIMBERLEY, M.O.; KRITICOS, D.J.; EMHART, V.; MARDONES, O.; ACEVEDO, M.; PINCHEIRO, M.; STAPE, J.; FOX, T. Using seasonal measurements to inform ecophysiology: extracting cardinal growth temperatures for process-based growth models of five *Eucalyptus* species/crosses from simple field trials. **New Zealand Journal of Forest Science**, v. 44, 2014. Available in: <https://doi.org/10.1186/s40490-014-0009-4>. Access in: 20 April 2020.

WAY, D.A.; OREN, R. Differential responses to changes in growth temperature between trees from different functional groups and biomes: a review and synthesis of data. **Tree Physiology**, p. 1-20, 2010. Available in: doi:10.1093/treephys/tpq015. Access in: 15 May 2020.

WENT, F. W. The effect of temperature on plant growth. **Annual Review of Plant Physiology**, v. 4, n. 1, p. 347-362, 1953.

WHITE, D.A.; BEADLE, C.L.; WORLEDGE, D. Leaf water relations of *Eucalyptus globulus* ssp. *globulus* and *E. nitens*: seasonal, drought and species effects. **Tree Physiology**, v. 16, p. 469-476, 1996. Available in: <https://doi.org/10.1093/treephys/16.5.469>. Access in: 30 April 2020.

WHITE, D.A.; CROMBIE, D.S.; KINAL, J.; BATTAGLIA, M.; MCGRATH, J.F.; MENDHAM, D.S.; WALKER, S.N. Managing productivity and drought risk in *Eucalyptus globulus* plantations in south-western Australia. **Forest Ecology and Management**, v. 259, p. 33-44, 2009. Available in: <https://doi.org/10.1016/j.foreco.2009.09.039>. Access in: 2 May 2020.

WHITE, D.A.; TURNER, N.C.; GALBRAITH, J.H. Leaf water relations and stomatal behavior of four allopatric *Eucalyptus* species planted in Mediterranean southwestern Australia. **Tree Physiology**, v. 20, n. 17, p. 1157-1165, 2000. Available in: <https://doi.org/10.1093/treephys/20.17.1157>. Access in: 3 May 2020.

WHITEHEAD, D.; BEADLE, C.L. Physiological regulation of productivity and water use in *Eucalyptus*: a review. **Forest Ecology and Management**, v.193, p. 113-140, 2004. Available in: <https://doi.org/10.1016/j.foreco.2004.01.026>. Access in: 2 May 2020.

WICKHAM, H.; CHANG, W.; HENRY, L.; PEDERSEN, T.L.; TAKAHASHI, K.; WILKE, C.; WOO, K.; YUTUANU, H.; DUNNINGTON, D. ggplot2: create elegant data visualizations using the grammar of graphics. **R package version 3.3.2.**, 2020, 284 p. Available in: <https://cran.r-project.org/web/packages/ggplot2/index.html>. Access in: 18 May 2020.

WORLD WILDLIFE FUND. **Living planet report 2012: biodiversity, biocapacity and better choice**. Gland, 164 p., 2012.

YAN, W.; HUNT, L.A. An equation for modelling the temperature responses of plants using only the cardinal temperatures. **Annals of Botany**, v. 84, p. 607-614, 1999.

YIN, X.; KROPFF, M.J.; MCLAREN, G.; VISPERAS, R.M. A Nonlinear Model for Crop Development as a Function of Temperature. **Agriculture and Forest Meteorology**, v. 77, n.1-2, p. 1-16, 1995. Available in: [https://doi.org/10.1016/0168-1923\(95\)02236-Q](https://doi.org/10.1016/0168-1923(95)02236-Q). Access in: 18 June 2020.